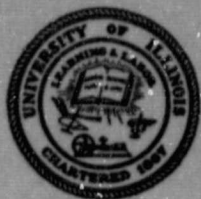


## **General Disclaimer**

### **One or more of the Following Statements may affect this Document**

- This document has been reproduced from the best copy furnished by the organizational source. It is being released in the interest of making available as much information as possible.
- This document may contain data, which exceeds the sheet parameters. It was furnished in this condition by the organizational source and is the best copy available.
- This document may contain tone-on-tone or color graphs, charts and/or pictures, which have been reproduced in black and white.
- This document is paginated as submitted by the original source.
- Portions of this document are not fully legible due to the historical nature of some of the material. However, it is the best reproduction available from the original submission.

DRA



UNIVERSITY OF ILLINOIS  
URBANA

# AERONOMY REPORT NO. 109

## PHASE MODULATING THE URBANA RADAR

(NASA-CR-172993) PHASE MODULATING THE URBANA RADAR (Illinois Univ.) 170 p  
HC A08/MF A01 CSCI 171

N83-33015

Unclass  
G3/32 15051

by  
L. J. Herrington, Jr.  
S. A. Bowhill

March 1, 1983



Library of Congress ISSN 0568-0581

Supported by  
National Aeronautics and Space Administration

Aeronomy Laboratory  
Department of Electrical Engineering  
University of Illinois  
Urbana, Illinois

A E R O N O M Y R E P O R T

N O. 109

PHASE MODULATING THE URBANA RADAR

by

L. J. Herrington, Jr.  
S. A. Bowhill

March 1, 1983

Supported by  
National Aeronautics  
and Space Administration  
Grant NSG 7506

Aeronomy Laboratory  
Department of Electrical Engineering  
University of Illinois  
Urbana, Illinois

## ABSTRACT

The design and operation of a switched phase modulation system for the Urbana Radar System are discussed. The system is implemented and demonstrated using a simple procedure. The radar system and circuits are described and analyzed.

PRECEDING PAGE BLANK NOT FILMED

## TABLE OF CONTENTS

	Page
ABSTRACT . . . . .	iii
TABLE OF CONTENTS . . . . .	v
LIST OF TABLES . . . . .	viii
LIST OF FIGURES . . . . .	ix
1. INTRODUCTION . . . . .	1
1.1 The Mesosphere . . . . .	1
1.2 Thompson Scatter Radar . . . . .	2
1.3 Coherent Scatter Radar . . . . .	3
1.4 Meteor Radar . . . . .	4
1.5 Range Resolution and the Radar Equation . . . . .	4
1.6 Waveform Design . . . . .	7
1.7 Summary and Statement of the Problem . . . . .	8
2. PHASE CODING OF RADAR TRANSMITTERS . . . . .	9
2.1 The Purpose of Phase Coding . . . . .	9
2.2 Barker Coding . . . . .	10
2.3 Complementary Coding . . . . .	14
2.4 Maximal Length Sequences . . . . .	16
2.5 Summary . . . . .	17
3. THE URBANA RADAR: A DESCRIPTION . . . . .	20
3.1 Introduction . . . . .	20
3.2 The Phase Switch and Gated Amplifier . . . . .	20
3.3 The 814B Linear Amplifier . . . . .	27
3.4 The 4CX5000A Intermediate Power Amplifier . . . . .	33
3.5 Units 3 and 4: The Driver and PAs . . . . .	40
3.6 Driver Output Power Divider . . . . .	57

	Page
3.7 Final Output Combiner Networks . . . . .	60
3.8 TR-ATR Switch . . . . .	60
3.9 High Voltage and Bias Supplies . . . . .	62
3.10 The Modulator . . . . .	66
3.11 Timing and Control . . . . .	74
3.12 The Receiving System . . . . .	82
3.13 Suggestions for Improvements . . . . .	93
3.14 Summary . . . . .	97
4. DESIGN CONSIDERATIONS FOR THE URBANA RADAR . . . . .	98
4.1 Introduction . . . . .	98
4.2 Frequency Selection . . . . .	98
4.3 Bandwidth Criteria . . . . .	99
4.4 Pulse Length Considerations . . . . .	101
4.5 Code Selection . . . . .	102
4.6 Summary of Design . . . . .	103
5. RESULTS AND CONCLUSIONS . . . . .	105
5.1 Results . . . . .	105
5.2 Conclusions . . . . .	105
APPENDIX I WIDEBAND FERRITE TRANSFORMERS AND DEVICES . . . . .	108
I.1 Introduction . . . . .	108
I.2 Conventional Wideband Transformers . . . . .	108
I.3 Wideband Autotransformers . . . . .	115
I.4 Transmission Line Transformers . . . . .	115
I.5 RF Combiners and Dividers . . . . .	117
I.6 Summary . . . . .	120
APPENDIX II IMPEDANCE MATCHING OF NONLINEAR LOADS . . . . .	121

	Page
APPENDIX III RIGID COAXIAL CABLE . . . . .	126
APPENDIX IV PROGRAM LISTINGS AND DESCRIPTIONS . . . . .	134
REFERENCES . . . . .	154

## LIST OF TABLES

Table		Page
2.1	Sequences with small $\max_j  c_j $ . . . . .	12
2.2	Some features of binary sequences with best possible auto-correlation function . . . . .	13
2.3	Number of shift register stages versus length of generated sequence, number of possible sequences, and feedback stage connections . . . . .	19
3.1	Transmitter ratings . . . . .	22
3.2	Continental Electronics 814B specifications . . . . .	34
3.3	87 KVA plate supply taps . . . . .	65
3.4	Modulator specifications . . . . .	68
3.5	T618 output connections . . . . .	72
3.6	T617 internal connections . . . . .	73
3.7	Characteristics of the preamplifier in the Urbana Radar receiving system . . . . .	92
III.1	Production test voltage versus outer conductor diameter . .	129

## LIST OF FIGURES

Figure		Page
2.1	Seven-, eleven- and thirteen-bit Barker codes and their autocorrelation functions . . . . .	11
2.2	Demonstration of the effect of limited system bandwidth on a 13-bit Barker code . . . . .	15
2.3	Shift register method of generation of maximal length sequences. . . . .	18
3.1	Block diagram of the Urbana Radar System . . . . .	21
3.2	Block diagram of the phase switch and low level gated amplifier and the associated circuitry . . . . .	23
3.3	Phase switch circuit diagram . . . . .	24
3.4	Phase switch driver circuit diagram . . . . .	25
3.5	RF amplifier circuit diagram . . . . .	27
3.6	Gate amplifier circuit diagram . . . . .	28
3.7	Output detector diagram . . . . .	29
3.8	RF output power meter circuit diagram . . . . .	30
3.9	(a) RF amplifier shown mounted in equipment rack. The amplifier is the light gray unit on the bottom. The output, power meter is shown mounted just above the amplifier. The next panel (black) is the mount for the 814B output power meter discussed in Section 2 of this chapter . . . . .	31
	(b) Chassis layout of the RF amplifier of unit 1 . . . . .	31
	(c) Internal construction of the RF detector unit . . . . .	32
	(d) Component layout of the two circuit boards mounted in the unit 1 chassis . . . . .	32

Figure	Page
3.10 RF amplifier circuits of the Continental Electronics 814B VHF transmitter . . . . .	35
3.11 814B power supply block diagram . . . . .	36
3.12 814B power supply circuit diagram . . . . .	37
3.13 814B peak power meter and "RF on" detector circuit diagram . . . . .	38
3.14 4CX5000A (unit 2) RF amplifier schematic . . . . .	39
3.15 Unit 2 bias supply . . . . .	41
3.16 Unit 2 screen supply . . . . .	42
3.17 Picture of units 1, 2, and 3, showing unit 2 on the right, unit 1 in the center, and the 814B linear amplifier on the left . . . . .	43
3.18 Detail of the bias input portion of the 4CX5000A input matching network . . . . .	44
3.19 Simplified physical structure of the driver and power amplifiers . . . . .	45
3.20 Details of the input circuit of the driver and power amplifiers, showing the 20 $\Omega$ transmission line, irrathane "collar" capacitor C301 and the toroidal variable induc- tor L301 . . . . .	46
3.21 Simplified schematic of the input match network . . . . .	48
3.22 Model of the output match network . . . . .	49
3.23 Typical passband of the output match network of units 3 or 4, as generated by the program named PA BANDWIDTH . . . . .	51
3.24 Bias circuits of units 3 and 4 . . . . .	52

Figure	Page
3.25 Anode voltage rating versus outer grid to anode spacing from Doolittle (1964) . . . . .	53
3.26 Picture of the driver (unit 3). Each of the four power amplifiers has an identical appearance . . . . .	56
3.27 Driver output (and PA input) match network . . . . .	58
3.28 Bandpass of the asynchronous T-match network . . . . .	59
3.29 Final output combiner networks . . . . .	61
3.30 T/R switch diagram . . . . .	63
3.31 25-kV power supply block diagram . . . . .	64
3.32 25-kV power supply and bias supply for units 3 and 4 circuit diagrams . . . . .	67
3.33 Modulation simplified schematic . . . . .	69
3.34 Modulator power supplies (a) supply for V601; (b) supply for V602, V603, and bias for V604; (c) bias supply for V605, V606, and V607 . . . . .	70
3.35 Pulse shaper circuit diagram . . . . .	75
3.36 Picture of V604, V605, V606 and V607 . . . . .	76
3.37 Modulator chassis layout . . . . .	77
3.38 Radar timing diagram . . . . .	78
3.39 Apple radar director block diagram . . . . .	79
3.40 Interlock and high current adaptor circuit diagram . . . .	81
3.41 Logic and interlock module (a) transmitter output detector (b) "814 OUTPUT ON" amplifier (c) pulse length control, duty cycle exceeded tester, and TX output present tester circuits and (d) RF gate pulse control . . . . .	83

Figure	Page
3.42 Equivalent logic of Figure 3.41(c) . . . . .	87
3.43 Pictures of the interlock and high current adaptor. (a) front panel (b) chassis layout (c) logic board layout . .	88
3.44 Receive system block diagram . . . . .	89
3.45 PIN diode blanker . . . . .	90
3.46 Drive and control circuitry for the PIN diode blanker . .	91
3.47 Phase detectors used by the coherent-scatter radar and meteor radar . . . . .	94
3.48 (a) and (b) Two methods to improve modulator efficiency and rise time . . . . .	95
4.1 Mathematical model of the modulator in the Urbana Radar. .	100
5.1 Block diagram of the verification system . . . . .	106
5.2 (a) Picture of the coded RF pulse taken on a 100 MHz oscilloscope connected to a dipole antenna. The effects of phase coding are clearly visible on the envelope. Taken at 5 $\mu$ sec/cm . . . . .	107
(b) Coherently detected RF pulse with no phase coding applied. Taken at 10 $\mu$ sec/cm . . . . .	107
(c) Coherently detected RF pulse phase modulated with a 7-bit Barker code. Taken at 10 $\mu$ sec/cm. The effects of limited system bandwidth are plainly visible . . . . .	107
I.1 Schematic representations of the three types of wideband ferrite transformers . . . . .	109
I.2 Diagram of a commonly used model of a conventional wide- band transformer . . . . .	110

Figure	Page
I.3 Typical transmission loss versus frequency chart of a wideband transformer . . . . .	110
I.4 Typical magnetic flux path in a BALUN type ferrite core. .	111
I.5 Core shapes, sizes, and form factors for Fair-Rite Products Corp. cores . . . . .	113
I.6 Two approaches to wideband hybrid combiners/splitters . .	118
I.7 A conventional wideband hybrid combiner/splitter . . . . .	119
I.8 (a) method whereby two 180° transistor outputs may be combined (b) method for winding a transmission line transformer which permits upright mounting . . . . .	119
II.1 Applied voltage versus current waveforms for a nonlinear load of the piecewise continuous type . . . . .	122
II.2 Nonlinear load bypassed with a high Q tank circuit . . . . .	123
II.3 Measurement method for input and output impedances measured at high power . . . . .	125
III.1 Average power limitations versus frequency for the currently used types of rigid transmission lines . . . . .	127
III.2 Derating factor vs. frequency for rigid transmission line . . . . .	128
III.3 Variation of permissible average power vs. temperature for rigid coaxial transmission line . . . . .	128
III.4 Peak power limits vs. internal pressure for SF <sub>6</sub> and dry air or nitrogen . . . . .	130
III.5 Attenuation vs. frequency for rigid coaxial transmission line . . . . .	130

Figure	Page
III.6 Attenuation vs. VSWR for rigid coaxial transmission	
line . . . . .	131
III.7 Attenuation vs. temperature for rigid coaxial transmission	
line . . . . .	151
III.8 Inner conductor v%, outer conductor temperature rise . . .	133

## 1. INTRODUCTION

### 1.1 The Mesosphere

The Earth's mesosphere is the region from about 50 to 85 km altitude; its composition and dynamics are currently the subject of a wide range of observational techniques, both direct and indirect. The composition of this region is known to be homogeneous and similar to the stratosphere below, differing only in having reduced density and pressure rather than the stratified composition of the thermosphere above. Eddy diffusion (turbulence) is the mechanism maintaining the homogeneity which extends to the turbopause. The region is heated primarily by ozone absorption of solar radiation; indeed the region was initially defined by its thermal properties: it is the region above the stratosphere which exhibits decreasing temperature with altitude.

The D region or mesosphere is lightly ionized when compared to the E and F layers. The primary ion source is photoionization of neutral molecules; the higher density leads to higher collision and recombination rates, thus fewer ions. One feature of the mesosphere is the steep decrease in ion density with altitude called the D-region ledge. Another is the rapid decrease in D-region ionization after sunset. Furthermore, due to the high collision rate all charged and neutral species in the mesosphere have nearly the same temperature.

The mesosphere's large-scale dynamics may be investigated using a plasma model. This plasma is perturbed by a variety of sources, e.g., tides, gravity waves etc.; in addition, thermal processes produce ion-acoustic waves. The scale limit of the latter process is the Debye length ( $D$ ) which varies from less than 1 cm below 1000 km to 6 cm at 2000 km. It is not

possible to excite thermal irregularities in a plasma on a scale smaller than D.

A coherent wave motion on any length or time scale which becomes unstable generates turbulence, whereby the wave energy is ultimately converted to heat; occurring only below the turbopause, it is an inherently nonlinear dissipative process. The smallest scale of motion it contains is termed the "inner scale" of the turbulence.

Investigations into the mesosphere have traditionally proceeded by a variety of methods. Direct measurements through balloon-borne instrument packages have provided good data on pressure, temperature, and composition in the lower regions. Rocket-probe devices have provided additional data, though for short periods at relatively high cost; other methods used have been to "stain" the region with explosive devices or chemicals, or through the use of natural explosions like volcanic eruptions. Radar based examination, however, is probably the most cost-effective method for long-term, low-cost research.

## 1.2 Thompson Scatter Radar

The Thompson scatter principle as described by Evans (1968) was originally based on a medium which is quiescent, homogeneous, plasma having an effective radar cross section per unit volume of

$$\sigma = N \sigma_e \quad (1.1)$$

where N is the electron density per unit volume and  $\sigma_e$  is the effective cross section of a single electron:

$$\sigma_e = 4\pi(r_e \sin\chi)^2 \approx 10^{-28} \sin^2\chi \text{ m}^2 \quad (1.2)$$

Because the assumption of a quiescent medium is not accurate, Thompson scatter experiments as first noted by Bowles do not always produce the expected results. A more useful model envisions the medium as a plasma in

ORIGINAL PAGE IS  
OF POOR QUALITY

which density fluctuations are brought about by longitudinal oscillations.

Based on these assumptions the effective radar cross section per unit volume becomes

$$\sigma = \left| \frac{\Delta \epsilon_0}{\epsilon_0} \right|^2 \frac{4}{\lambda_0} \frac{3}{4} \sin^2 \chi P(\bar{K}_2 - \bar{K}_1) \quad (1.3)$$

where  $\sigma$  = the effective cross section/unit volume

$\epsilon_0$  = the permittivity of free space

$\Delta \epsilon_0$  = the variations in  $\epsilon_0$

$\lambda_0$  = the wavelength of the exploring frequency used

$\bar{K}_1$  = the propagation vector of the incident wave

$\bar{K}_2$  = the propagation vector of the reflected wave

$P(K)$  = the three dimensional wave number spectrum of the density variation

$\chi$  = the polarization angle; the angle between  $K_2$  and the incident electric field.

Within limits, though, the Thompson scatter technique has contributed a quantity of useful data concerning the mesosphere; ion density profiles, temperature, and composition have all been studied using Thompson scatter techniques and high powered radars.

### 1.3 Coherent Scatter Radar

Coherent scatter radar techniques make use of the turbulent mixing-in-gradient which gives rise to the rapid temporal variations in received power described by Rastogi and Bowhill (1976b) and by Countryman and Bowhill (1979). Eddies of different scales are generated by the gradual dissipation of large scale eddies driven by the overall global circulation and superimposed planetary waves, tides, and gravity waves. The energy in this process is dissipated in viscous damping in the small-scale eddies. Since

these processes may be viewed as variations in local permittivity, the radar cross section is the same as that given in Equation 1.3.

Since these processes in the mesosphere take place with a correlation time of approximately 1 second, coherent detection and pulse integration times of between 1/8 and 1/2 second provide data on the line-of-sight velocity, relative size, and relative altitude of different eddies. These in turn make it possible to investigate the internal coupling and energy dissipation mechanisms in the mesosphere, which occur in relatively small physical and temporal scales.

#### 1.4 Meteor Radar

Large numbers of meteors burn up in the atmosphere every day, each leaving an ionized trail in its wake. These ionized trails provide excellent radar targets; they may be thought of as passive probes in the upper mesosphere, usually in the 80 to 120 km range.

Below heights of about 100 km the whole of the Earth's atmosphere participates in the planet's rotation. This motion, pressure, and gravity generate the geostrophic wind system (prevailing wind system) which is continually perturbed by gravity waves, tides and solar heating, together with hurricanes and other atmospheric events. All these perturbations generate waves which can be observed as fluctuations in the zonal mean wind.

The meteor radar system, then, uses echoes from meteor trails to collect data on the altitude, structure, and velocity of the prevailing winds in the mesosphere. It can do this inexpensively and for long periods of time.

#### 1.5 Range Resolution and the Radar Equation

For a radar system employing coherent integration in the detection process the Radar Equation is, from Skolnik (1980):

$$R_{\max}^4 = \frac{P_{\text{av}} G A_e \Gamma n E_i(n)}{(4\pi)^2 K T_o F_n (B_n \tau) (S/N)_1 f_p} \quad (1.4)$$

- where
- $R_{\max}$  = the maximum range of the system
  - $G$  = the transmit antenna gain
  - $A_e$  = the effective area of the receiver antenna
  - $\Gamma$  = the target cross-sectional area
  - $n$  = the number of pulses integrated
  - $K$  = Boltzman's constant
  - $T_o$  = absolute temperature, 290K
  - $F_n$  = noise figures of the receiver system
  - $B_n$  = noise bandwidth of the receiver system
  - $\tau$  = pulse length
  - $f_p$  = pulse repetition rate
  - $(S/N)_1$  = signal-to-noise ratio required for a given probability of detection
  - $(S/N)_n$  = signal-to-noise ratio required to give the same probability of detection when  $n$  pulses are integrated

$$E_i(n) = \frac{(S/N)_1}{n(S/N)_n}$$

and

$E_i(n)$  = the integration improvement factor.

One of the primary considerations in the design of any radar system is the maximum range, given in 1.1 as an explicit function of average transmitted power. If the range is thus to be held constant, yet the resolution increased, the pulse length must be decreased and either the peak power or the pulse repetition rate increased. Both these approaches have difficulties associated with them, however, in many radars it is simply not

practical to increase the peak power. On the other hand, increasing the PRF can lead to aliasing problems. In addition, short pulses require greater bandwidth in both the transmitter and receiver, which may in itself present significant problems.

The Urbana Radar System is an excellent example of the application of eq. 1.1, and of the limits of the expression. Having both peak and average power limitations, plus a fixed maximum bandwidth, gain, and noise figure leaves only three variables which can easily be controlled over a wide range  $f_p$ ,  $\tau$ , and  $n$ ; and two over which only limited control is possible:  $B_n$  and  $P_{av}$ . As discussed in the previous paragraph, one cannot maintain the maximum range, yet increase resolution by decreasing  $\tau$  and increasing  $f_p$ ; aliasing results.

One of the techniques which has been developed to deal with this problem is that of return pulse integration, which can improve range resolution at the cost of increased processing. The echo received from any target can be thought of as consisting of signal plus noise. If the signal is coherent from pulse to pulse, it is consistently present in the returns at about the same magnitude and phase. Noise, on the other hand, is a random stationary process, and is incoherent from pulse to pulse. When the returns are summed over  $n$  pulses, then the signal adds coherently, while the noise adds incoherently. Hence the integrated signal return tends to rise above the noise floor, enhancing the range of the radar (i.e., enhancing the probability of detection of marginal targets). There is a limit to the rate at which pulses can be transmitted: namely, the point at which aliasing begins to be objectionable. Also, the number of pulses integrated must be kept below the correlation time of the returned signal.

### 1.6 Waveform Design

The radar equation of the preceding section is based on a transmitted waveform which consists of a single, repetitively transmitted pulse. This may not be an acceptable waveform for every application.

The output of any optimum receiver system is proportional to the cross correlation between the received signal,  $y(t) = s(t - T_0) + n(t)$  and a stored replica of the transmitted waveform  $s(t - T_R)$ :

$$c(\Delta T_R) = \int y(t) s(t - T_R) dt \quad (1.5)$$

where  $c(\Delta T_R)$   $\equiv$  the cross correlation between signals  
 $T_0$   $\equiv$  the travel time to the target and back  
 $T_R$   $\equiv$  the estimate of actual travel time  
 $\Delta T_R$   $\equiv T_0 - T_R =$  error in time delay

Please note that the above expression places no requirements in itself on the transmitted pulse waveform. The designer must, therefore, select a waveform which permits him to meet his objectives in terms of:

1. detection of the presence of targets
2. position and velocity measurements
3. reduced ambiguity
4. resolution - the ability to distinguish between closely spaced targets

Since the resolution of a rectangular transmitted pulse is  $c\tau/2$  where

$c \equiv$  velocity of light,  $3 \times 10^8$  m/sec

$\tau \equiv$  transmitted pulse length

one might surmise that an ideal waveform would be one which when autocorrelated would yield a single, very high, narrow pulse. This is indeed the case; as usual the requirements and available tradeoffs dictate waveform

selection.

In Chapter 2 different waveforms are discussed; however, the emphasis will be on binary phase coding techniques, several of which permit the waveform designer an excellent approximation to the ideal.

### 1.7 Summary and Statement of the Problem

The Urbana Radar System is a multipurpose instrument used in researching atmospheric phenomena over central Illinois. Having a choice of antennas, pulsewidths, PRF, and peak output power gives the system considerable versatility in its ability to perform M.T.I. scattering research using both coherent and incoherent processing techniques; in addition the device can function as a Meteor Radar.

Like any instrument 25 years in age, this device has a requirement for maintenance, adaption, and improvement to keep up with recent advances in technology and the science it serves. The several purposes of this project are, therefore:

1. to evaluate and document the present state of the radar transmitter
2. to provide phase modulation capabilities to the transmitter

Chapter 2 describes the types of phase coding and attempts to evaluate their relative merits to the Urbana Radar System.

Chapter 3 describes the Urbana Radar System at various levels down to the component. Detailed schematics and descriptions are given.

Chapter 4 details design considerations for the Urbana Radar transmitter.

Chapter 5 presents the results and conclusions.

## 2. PHASE CODING OF RADAR TRANSMITTERS

### 2.1 The Purpose of Phase Coding

As was pointed out in Section 1.6 the ideal waveform is one in which the autocorrelation of the transmitted pulse yields a single, high-amplitude, narrow pulse, which permit improved detection, position and velocity measurements, reduced ambiguity, and improved resolution. This chapter examines some of these methods with emphasis on the techniques achievable with a phase-switching approach.

Linear FM chirp radars employ a linear increase or decrease in frequency which may be demodulated with a matched filter to produce a waveform of the  $\sin(x)/x$  type. Originally patented by R. H. Dicke in 1945, this method of pulse compression has been used more than any other, in spite of its relatively poor peak-to-sidelobe ratio of 13.2 dB.

Other types of pulse compression methods are 1) Nonlinear FM method, in which the frequency is varied in a nonlinear manner to achieve both optimum sensitivity and noise figure using a matched filter. For symmetrical waveforms of this type the ambiguity function has a single peak rather than a ridge; 2) The discrete frequency shift method in which the transmit pulse is divided into subintervals and the carrier frequency varies inversely in proportion to the width of the subinterval. This method is good for large compression ratio and large time-bandwidth products; 3) Polyphase codes in which the phase is shifted over intervals smaller than  $\pi$ , yielding time sidelobes which are lower than those for binary-coded waveforms of similar length. Still other types of pulse compression are Barker coding, complementary coding, and maximal length sequence coding, each of which is practical for use in the Urbana Radar and which are each discussed in a

succeeding section.

## 2.2 Barker Coding

Barker coding is a method of pulse compression in which each transmitted pulse is phase-coded with codes chosen for the properties of their autocorrelation functions: each has a single sharp peak at zero lag and is a maximum of 1 elsewhere. The longest true Barker code known has a length of 13 bits. Diagrams of the codes and their autocorrelation functions for  $n = 7$ , 11, and 13 are given in Figure 2.1.

If one desires a greater compression ratio one can select similar but longer codes; each of these, however, has the failing that the peak sidelobe level is greater than 1; hence their ambiguity properties do not continue to improve in proportion to code length. Much work has been done in this area, though. Turyn (1968) lists all the desirable codes from  $n = 14$  to  $n = 34$ . These are presented in Table 2.1. Further, Lindner (1975) summarizes data on the codes with best possible autocorrelation functions up to  $n = 40$ . His results are presented in Table 2.2. Gray and Farley (1973) describe the theory of incoherent-scatter measurements using compressed pulses with consideration of both Barker codes and a longer 28-baud code with good autocorrelation properties. Ioannidis and Farley (1972) describe the actual use of compressed pulse techniques in observations at Arecibo.

In addition to selecting codes with low autocorrelation sidelobes investigations have taken place into various methods of processing the returned pulse to reduce the peak sidelobe levels. One typical example is the work of Key et al. (1959) in which a processing system consisting of weighted sums of a tapped delay line were used to decrease the sidelobes of a 13-bit Barker code. As in all these techniques, the resolution of the peak suffered, as well as a small loss in detection capability.

ORIGINAL PAGE IS  
OF POOR QUALITY

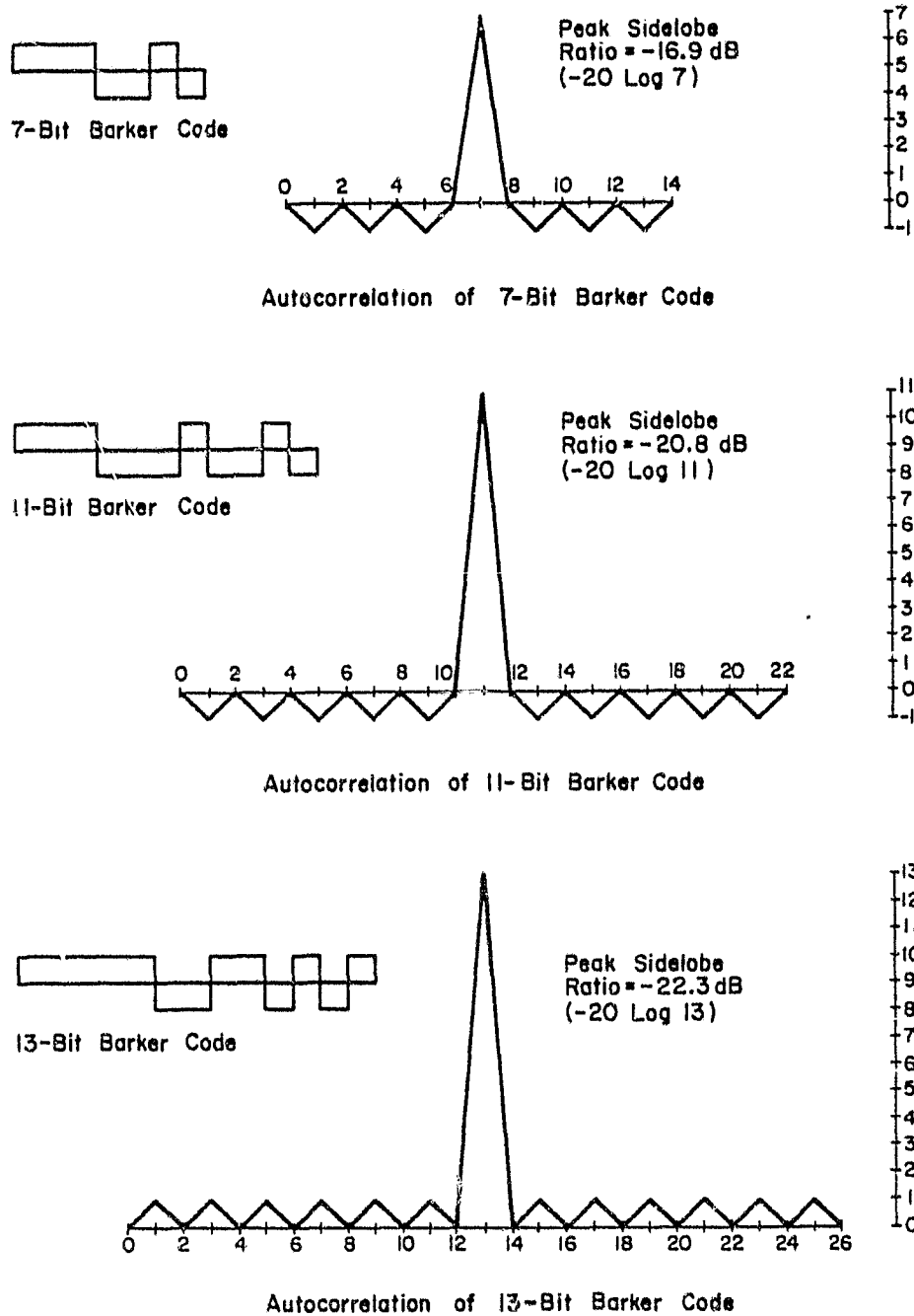


Figure 2.1 Seven-, eleven- and thirteen-bit Barker codes and their autocorrelation functions.

Table 2.1 Sequences with small  $\max_j |c_j|$ .

n	Sequence	$\max  c_j $
14	5 2 2 2 1 1 1	2
15	5 2 2 1 1 1 2 1	2
	6 2 2 1 1 1 2	2
16	3 1 3 4 1 1 2 1	2
	5 2 2 2 1 1 1 2	2
17	2 2 5 1 1 1 1 2 1 1	2
	4 2 2 1 2 1 1 1 1 2	2
18	5 1 1 2 1 1 3 2 2	2
19	4 3 3 1 3 1 2 1 1	2
20	5 1 3 3 1 1 2 1 1 2	2
21	6 1 1 3 1 1 2 3 2 1	2
	5 1 1 3 1 1 2 3 2 2	2
	3 5 1 3 1 2 1 1 1 2 1	2
22	8 3 2 1 2 2 1 1 1 1	3
23	1 2 2 2 2 1 1 1 5 4 1 1	3
24	8 3 2 1 1 1 1 2 2 1 2	3
25	3 2 3 6 1 1 1 1 1 2 1 2 1	2
26	8 2 1 1 2 2 1 1 1 1 1 2 3	3
27	2 1 2 1 1 2 1 3 1 3 1 3 4 2	3
28	2 1 2 1 1 2 1 3 1 3 1 3 4 3	2
	3 2 3 6 1 1 1 1 1 2 1 2 1 2 1	2
29	2 1 2 1 1 2 1 3 1 3 1 3 4 4	3
30	7 1 2 2 1 1 1 1 2 1 1 3 4 2 1	3
31	3 2 2 3 6 1 1 1 1 1 1 2 1 2 1 3	3
32	6 1 3 2 1 1 2 1 2 1 1 3 1 1 3 1	3
	6 1 3 2 1 3 3 1 1 2 1 2 1 1 3 1	3
33	6 3 1 2 3 2 1 1 3 2 1 1 2 2 1 1 1	3
	6 3 1 2 2 2 1 1 3 2 4 1 1 1 2	3
	6 3 1 2 1 1 1 2 1 2 2 3 1 1 1 3 1 1	3
34	7 4 2 1 1 2 1 1 2 2 2 2 1 1 1 1 1 1	3

ORIGINAL PAGE IS  
OF POOR QUALITY

Table 2.2 Some features of binary sequences with best possible autocorrelation function.

N	M	Number of sequence	Mean $M_1$	R.M.S. $M_2$	$M_3$	$M_4$
3	1	1	-0.50	0.71	1	2
4	1	2	0.00	0.82	2	1
5	1	1	0.50	0.71	2	2
6	2	7	-0.20	1.18	1	4
7	1	1	-0.50	0.71	3	2
8	2	16	-0.28	1.07	1	4
9	2	20	0.00	1.22	2	5
10	2	10	0.33	1.20	2	6
11	1	1	-0.50	0.71	5	2
12	2	32	0.18	0.95	1	6
13	1	1	0.50	0.71	6	2
14	2	18	0.08	1.21	3	8
15	2	26	-0.21	1.28	4	5
16	2	20	0.00	1.37	5	4
17	2	8	-0.25	1.41	6	1
18	2	4	-0.41	1.21	4	4
19	2	2	-0.28	1.43	7	1
20	2	6	-0.10	1.41	7	4
21	2	6	0.19	1.30	6	3
22	3	756	-0.14	1.36	1	19
23	3	1021	0.05	1.46	1	16
24	3	1716	-0.17	1.25	1	19
25	2	2	0.00	1.35	8	3
26	3	484	0.20	1.34	1	21
27	3	774	-0.04	1.19	2	20
28	2	4	-0.22	1.36	9	4
29	3	561	-0.07	1.49	2	16
30	3	172	0.10	1.43	2	15
31	3	502	-0.10	1.49	3	16
32	3	844	0.06	1.52	2	13
33	3	278	-0.12	1.41	2	24
34	3	102	0.03	1.40	2	13
35	3	222	-0.15	1.54	3	16
36	3	322	0.00	1.64	3	19
37	3	110	-0.17	1.65	4	10
38	3	34	-0.03	1.53	4	9
39	3	60	0.13	1.77	6	10
40	3	114	-0.05	1.66	6	17

As a point for consideration it was decided to look at the effects of normal transmission and reception distortion due to bandwidth limitations. As a first approximation the 13-bit Barker code was modified as depicted in Figure 2.2, with the square edges replaced by sine functions in appropriate locations. A computer program called CORRELATION (Program 7, Appendix IV) was written to provide the form of the autocorrelation function, also shown in Figure 2.2. As can be seen, this method generated a waveform with a peak-to-sidelobe ratio of about 20.4 dB, a loss of 1.9 dB when compared to the 13-bit Barker code shown in Figure 2.1.

### 2.3 Complementary Coding

Another coding scheme having excellent ambiguity functions is the "complementary series". This method requires more processing, but the results permit viable compression ratios in excess of 1000. Basically the idea is a simple one: two binary codes, known to be "complements" are transmitted alternately; each pulse is then autocorrelated and the results of the first pulse are then summed, point for point with the results of the second pulse cancelling all the sidelobes of both and leaving only a single peak. A typical example is given below.

Example 1. Given the pair of 4-bit complementary series 1 1 1 -1 and 1 1 -1 1 we first autocorrelate each which results in -1 0 1 4 1 0 -1 for the first and 1 0 -1 4 -1 0 1 for the second. These are then summed element by element to yield

$$\begin{array}{r}
 -1 \ 0 \ 1 \ 4 \ 1 \ 0 \ -1 \\
 1 \ 0 \ -1 \ 4 \ -1 \ 0 \ 1 \\
 \hline
 0 \ 0 \ 0 \ 8 \ 0 \ 0 \ 0
 \end{array}$$

an ambiguity function having a single central spike.

Golay (1961) summarized the properties of complementary series as they

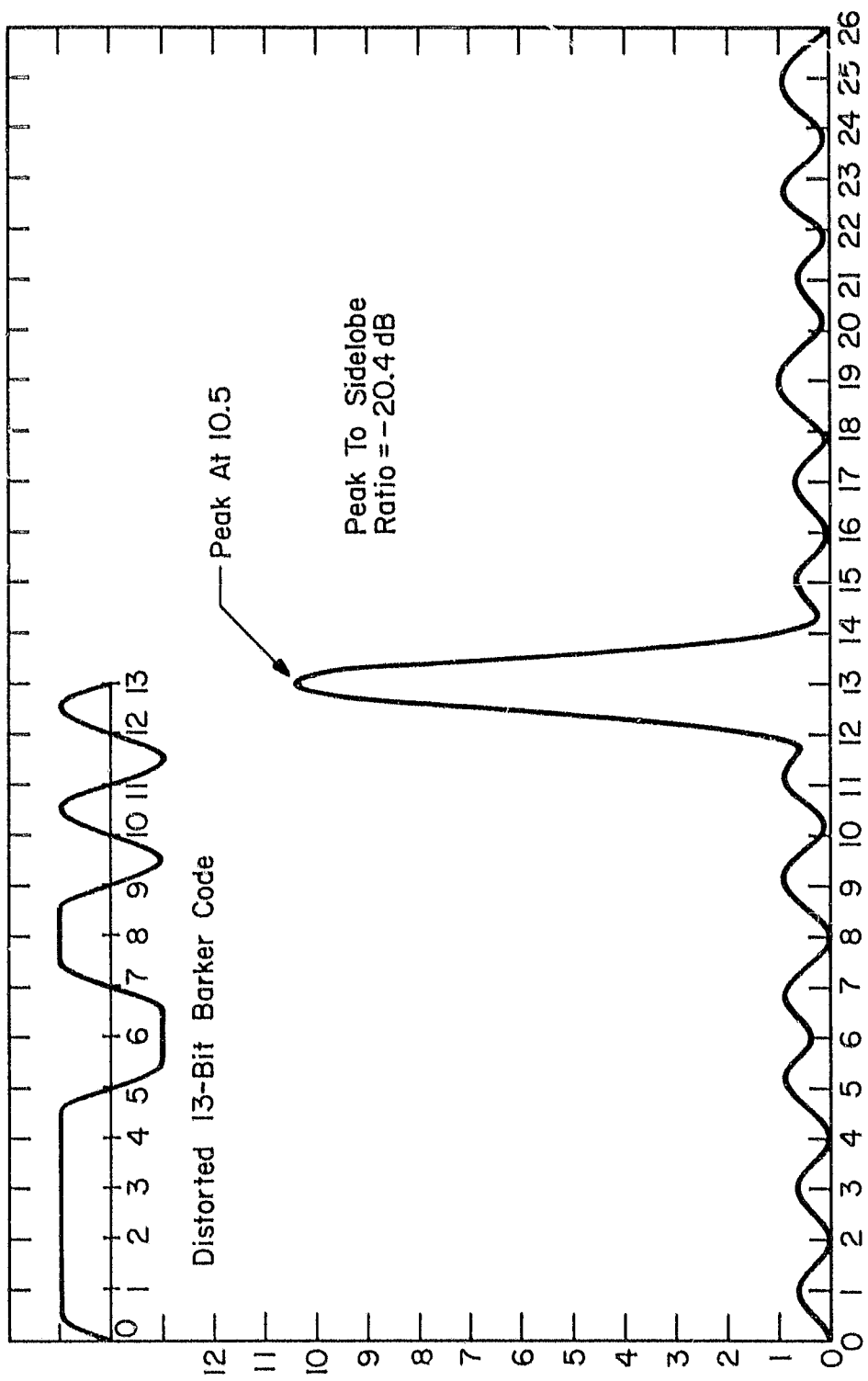


Figure 2.2 Demonstration of the effect of limited system bandwidth on a 13-bit Barker code.

were then known and delineated six rules for generating new codes and demonstrated the existence of codes whose elements number  $2^n$  and certain codes having  $n \neq 2^n$ .

The simplest complementary series are based on the kernel series pair 1 1 and 1 -1. Longer codes may be generated by the following algorithm:

1. Append the second code to the first. This creates the first element of the larger complementary pair.

2. Reverse the second code, then append it to the first. This generates the other series.

3. Repeat the above until the desired compression factor is reached. Note that any of Golay's six rules may be used to generate new codes from these at any point in the process.

Golay's work has been extended by several authors; however, Tseng and Liu (1971) have generalized these results by extending the concept of a complementary pair of sequences to a complementary set of sequences having the same properties as a complementary pair and permitting shorter codes for the same pulse compression ratio; but demanding of course that the correlation time of the reflecting body be greater than the period of the code cycle transmitted, and requiring still more processing before the data are accessible.

#### 2.4 Maximal Length Sequences

Another valid form of pulse compression which has seen use is maximal length sequence type. Used only in bistatic CW radars, this method has the benefit of completely cancelling all sidelobes while using only a single code. The received waveforms must flow continuously through an autocorrelator, the output of which consists of a single high peak occurring at the zero lag point of each cycle. The method has the disadvantages of CW

radar; since the transmitter is on all the time, separate transmit and receive antennas are required, and usually different transmit and receive sites as well.

One method used to continuously generate the maximal length sequence is shown in Figure 2.3. Which sequence is generated depends on the initial contents of the shift register and on the feedback connections chosen. Table 2.3 lists the data necessary to construct this generator.

## 2.5 Summary

Each type of pulse compression described has its own merits and weaknesses. All of them are capable of yielding more information than non-coded pulses, but they also require more processing to retrieve the information. In particular, all of the equipment necessary to the implementation of a phase switching technique are already present at the Urbana Radar site.

Barker coding is the simplest of these techniques; any of the Barker codes on the codes listed in Table 2.1 up to length 16 are easily within the capabilities of the Urbana transmitter; still, the Barker code of length 13 is the better choice from an ambiguity standpoint.

Requiring still more processing, the complementary sequence pairs and sets are another excellent approach, having only the additional limitation of cycle length time due to the correlation time of the mesosphere.

Maximal length sequence techniques require the reconfiguration of the radar for CW operation, and hence lower peak power, though the average power would only increase. This technique is more suited to real time processing and the bistatic arrangement would necessitate the operation of another site. Also, due to the extensive use of this technique elsewhere, the overall results would likely be unprofitable.

ORIGINAL PAGE IS  
OF POOR QUALITY

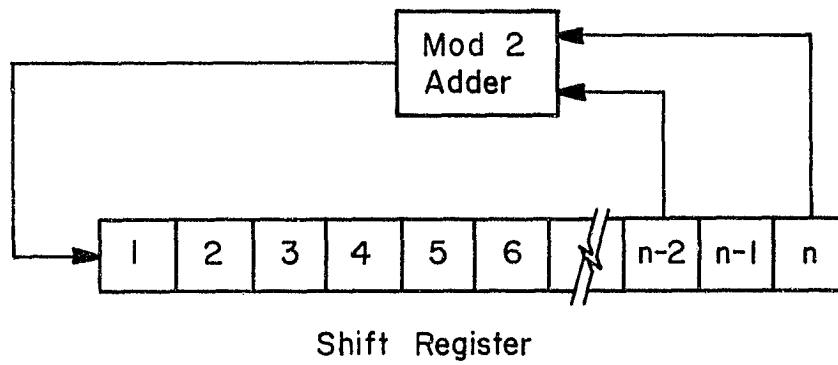


Figure 2.3 Shift register method of generation of maximal length sequences.

ORIGINAL PAGE IS  
OF POOR QUALITY

Table 2.3 Number of shift register stages versus length of generated sequence, number of possible sequences, and feedback stage connections.

Number of Stages	Length of Maximal Sequence Generated	Number of Sequences Possible	Feedback Stages Connected
2	3	1	2,1
3	7	2	3,2
4	15	2	4,3
5	31	6	5,3
6	63	6	6,5
7	127	18	7,6

### 3. THE URBANA RADAR: A DESCRIPTION

#### 3.1 Introduction

The Urbana Radar has been used as a research instrument for nearly twenty years, during which time it has been repeatedly modified. Unfortunately, not all the documentation recording these changes has survived, nor have the intentions of the various engineers and scientists who implemented them. This chapter is the result of an extensive analysis of the circuitry of the radar, and is intended as an explanation of the device and its idiosyncrasies, for the future users' information.

Figure 3.1 is a signal flow block diagram displaying signal paths between the major units of the radar, each of which will be described in the succeeding paragraphs. Table 3.1 shows the current transmitter ratings.

#### 3.2 The Phase Switch and Gated Amplifier

Stage 1 of the transmitter consists of a phase switch followed by a gated RF amplifier. The block diagram of the stage is shown in Figure 3.2. The RF signal path is through the phase switch, through the amplifier, then through the power meter detector. The phase switch is diagrammed in Figure 3.3. The transformers are trifilar wound stacked (73 material) ferrite balun cores wound for the widest possible bandwidth. Using a matched set of IN 914 diodes, this device is capable of changing phase in less than 30 nanoseconds.

The switch driver circuit shown in Figure 3.4 consists of a 7413 Schmitt trigger followed by an emitter follower and two differential amplifier stages. The outputs are buffered by VN66AK VMOS devices. The whole device is designed around the need for converting a single control signal into a balanced, fast switch drive to change the phase of the RF drive

ORIGINAL PAGE IS  
OF POOR QUALITY

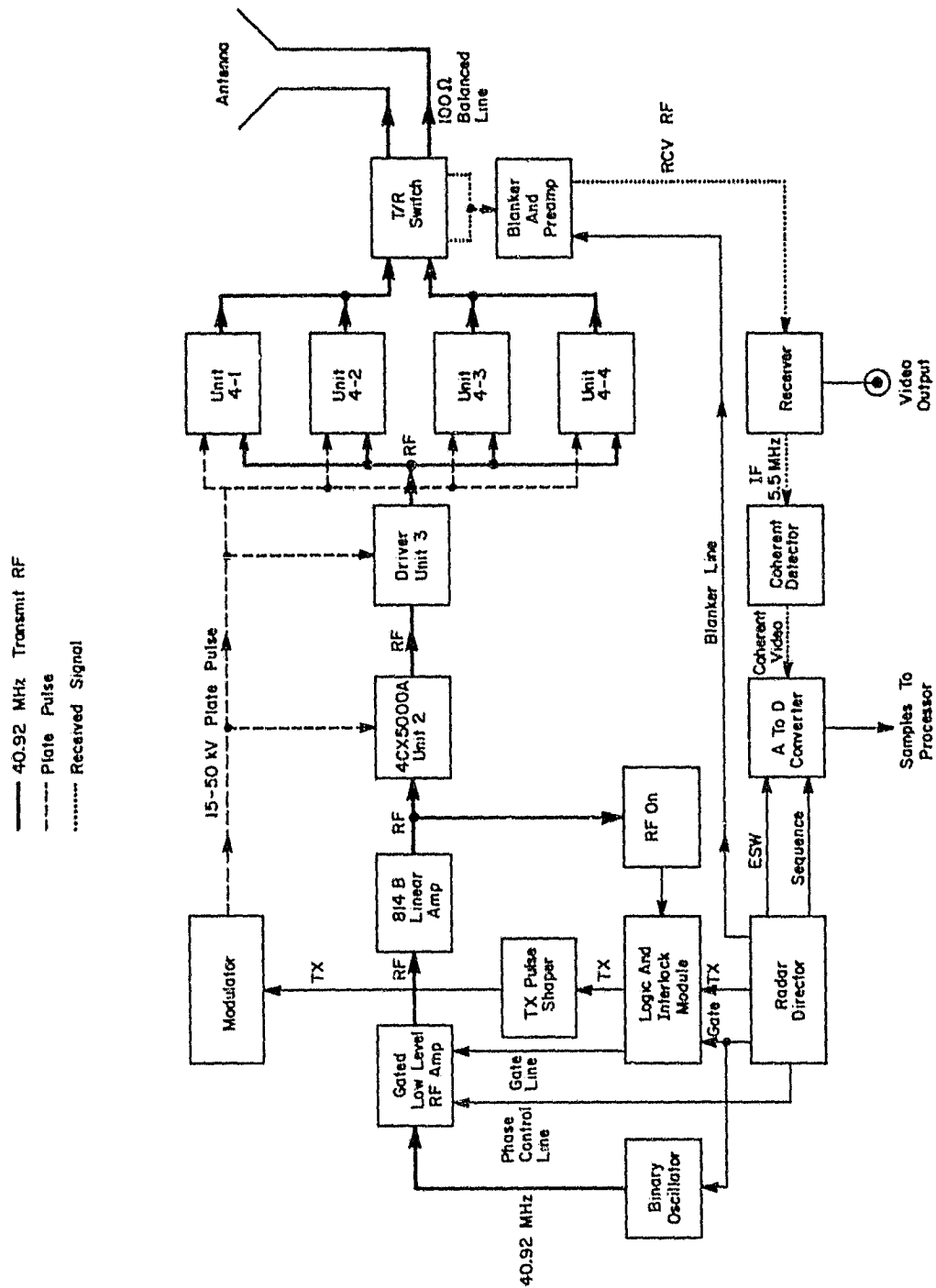


Figure 3.1 Block diagram of the Urbana Radar System.

Table 3.1 Transmitter ratings.

Output frequency	40.92 MHz
Peak power output	4 MW
Average power output	20 kW nominal 40 kW maximum
Duty cycle	.004 nominal
Pulsewidth	3 - 100 nominal
Power supply requirement	230V 3 phase
Power source capacity recommended	200 kVA
Types of emission	Pulsed CW or phase modulated pulses
Output impedance	100 $\Omega$ balanced
Bandwidth	1 MHz side-to-side

ORIGINAL PAGE IS  
OF POOR QUALITY

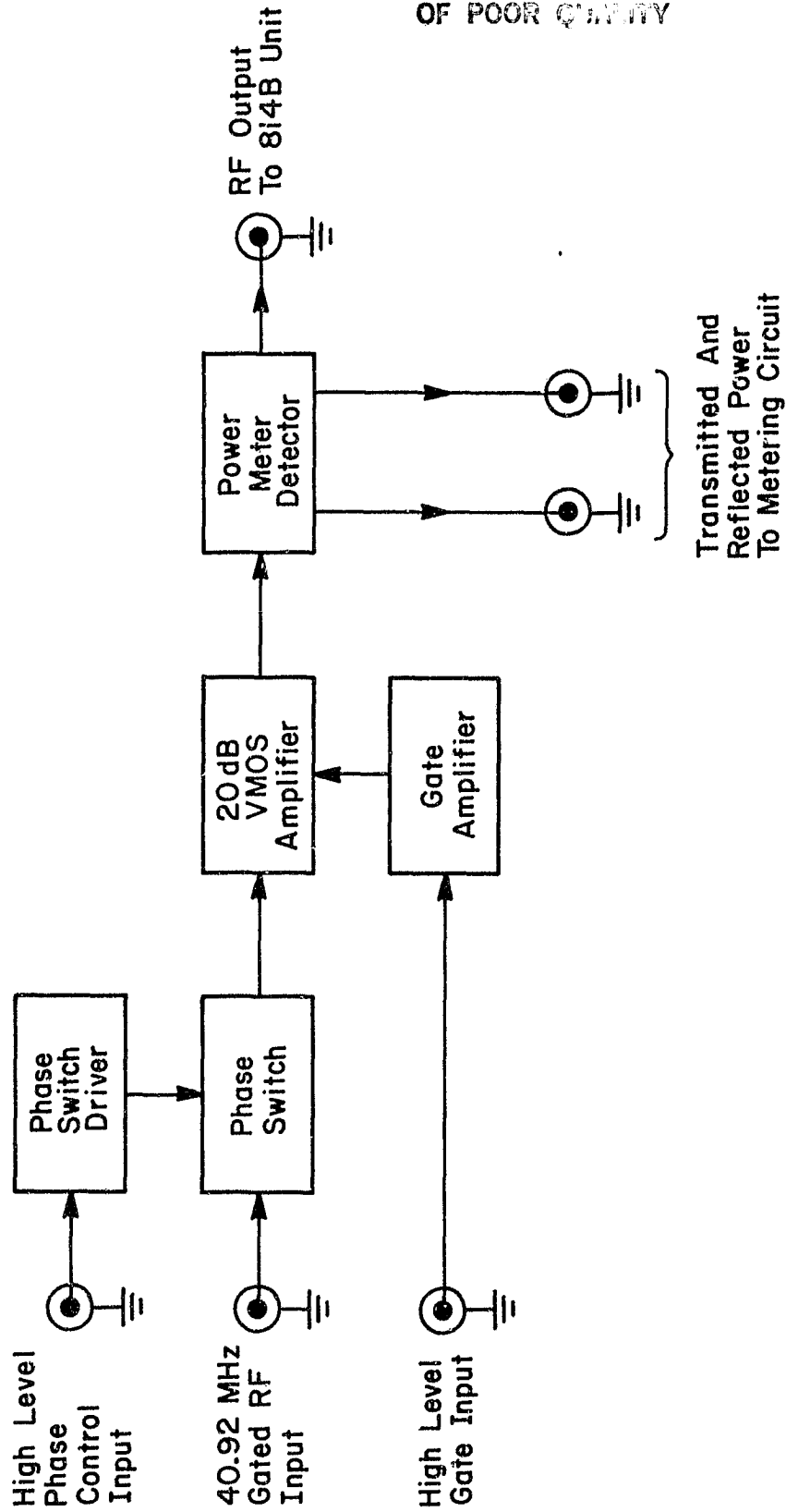


Figure 3.2 Block diagram of the phase switch and low level gated amplifier and the associated circuitry.

ORIGINAL PAGE IS  
OF POOR QUALITY

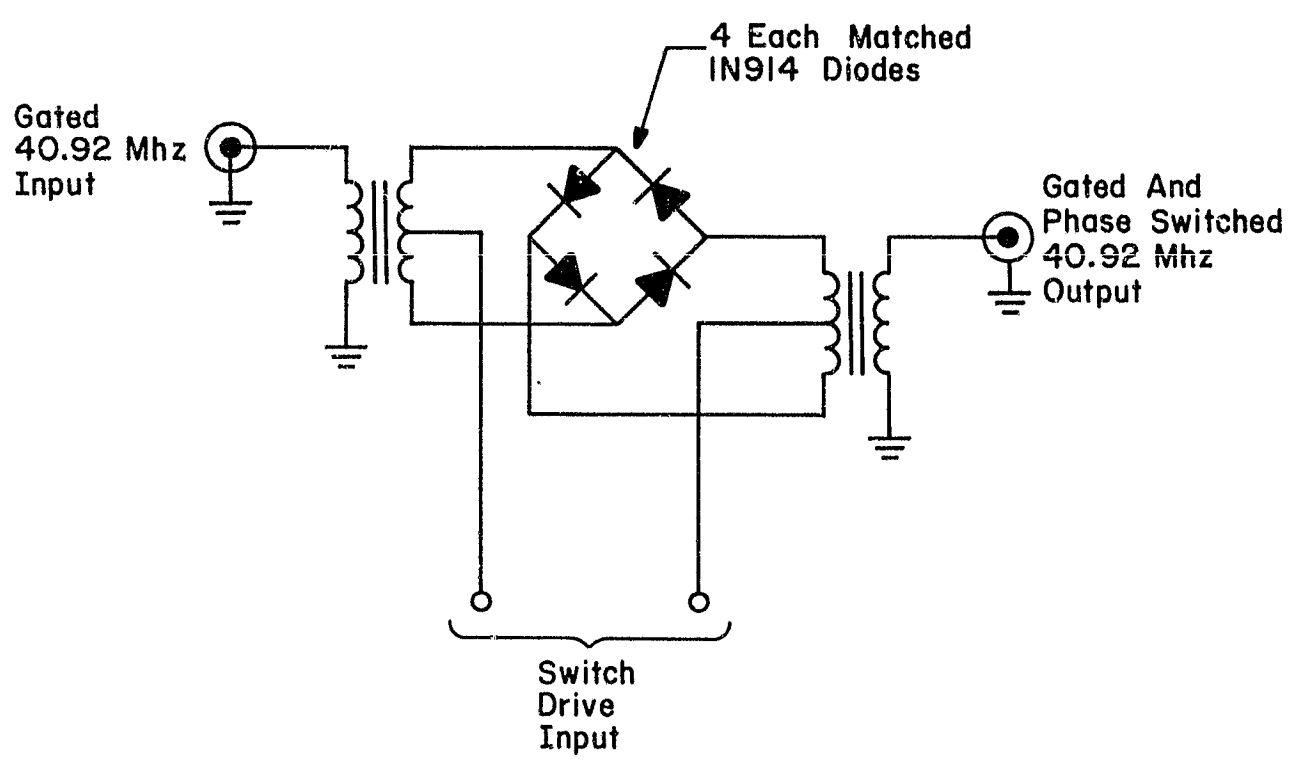
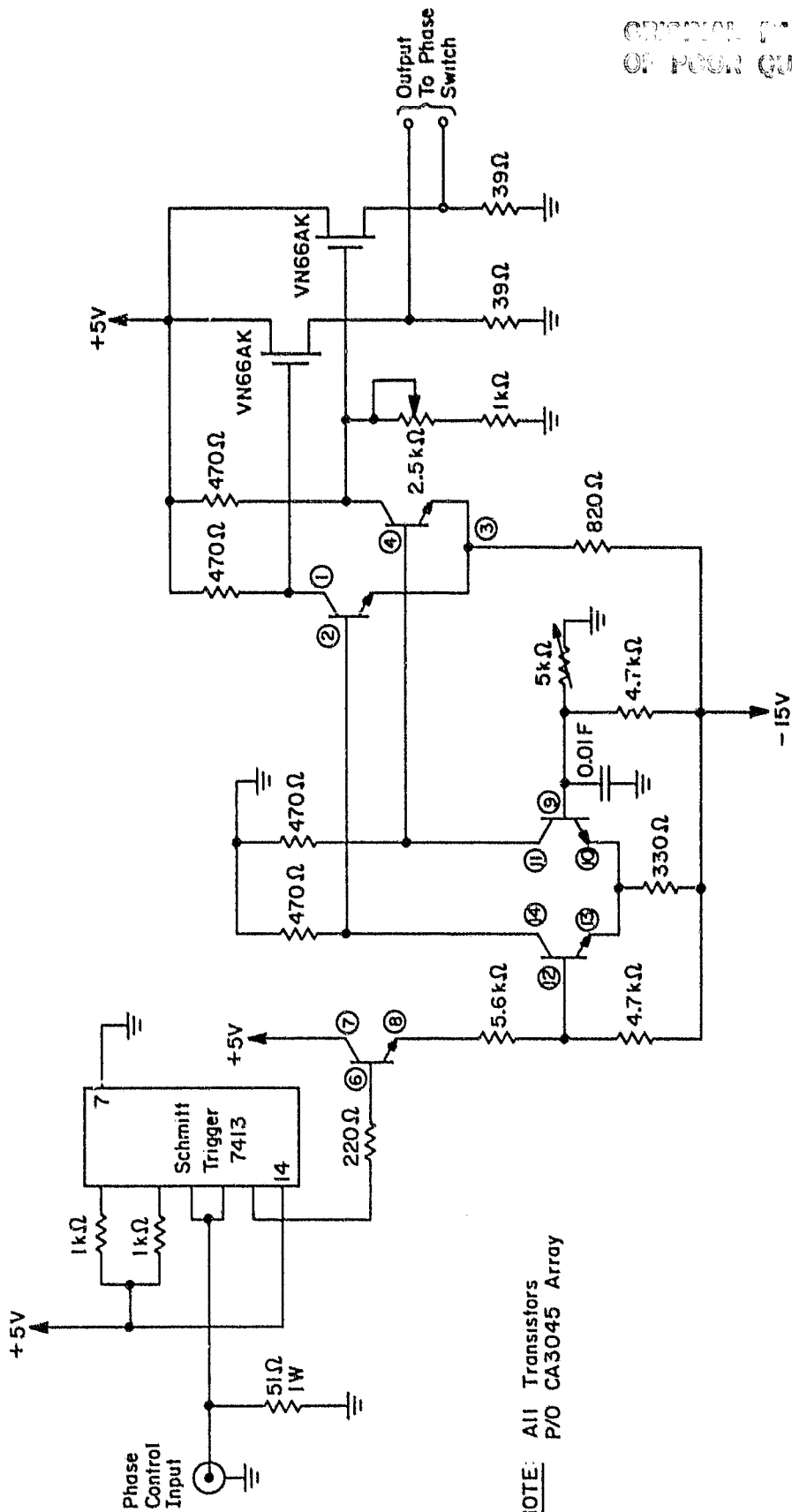


Figure 3.3 Phase switch circuit diagram.

ORIGINAL FILE IS  
OF POOR QUALITY



NOTE: All Transistors  
P/O CA3045 Array

Figure 3.4 Phase switch driver circuit diagram.

rapidly and cleanly.

The RF amplifier shown in Figure 3.5 consists of a pair of MOSFET DV2805W's operating class AB in push-pull. T1 and R1 together form a 180° hybrid power splitter, with R1 tending to maintain equal division regardless of moderately differing impedances presented by the MOSFETs. L1, C2, and L3 form one input matching network, with L2, C3, and L4 forming the other. C7, L5, and C5 match the output of one device; C8, L6, and C10 match the other. T2 and R5 comprise a hybrid output combiner.

This amplifier has worked quite well. The output power reaches 4 watts, with about a 5 MHz bandwidth and a 2  $\mu$ sec turn on time.

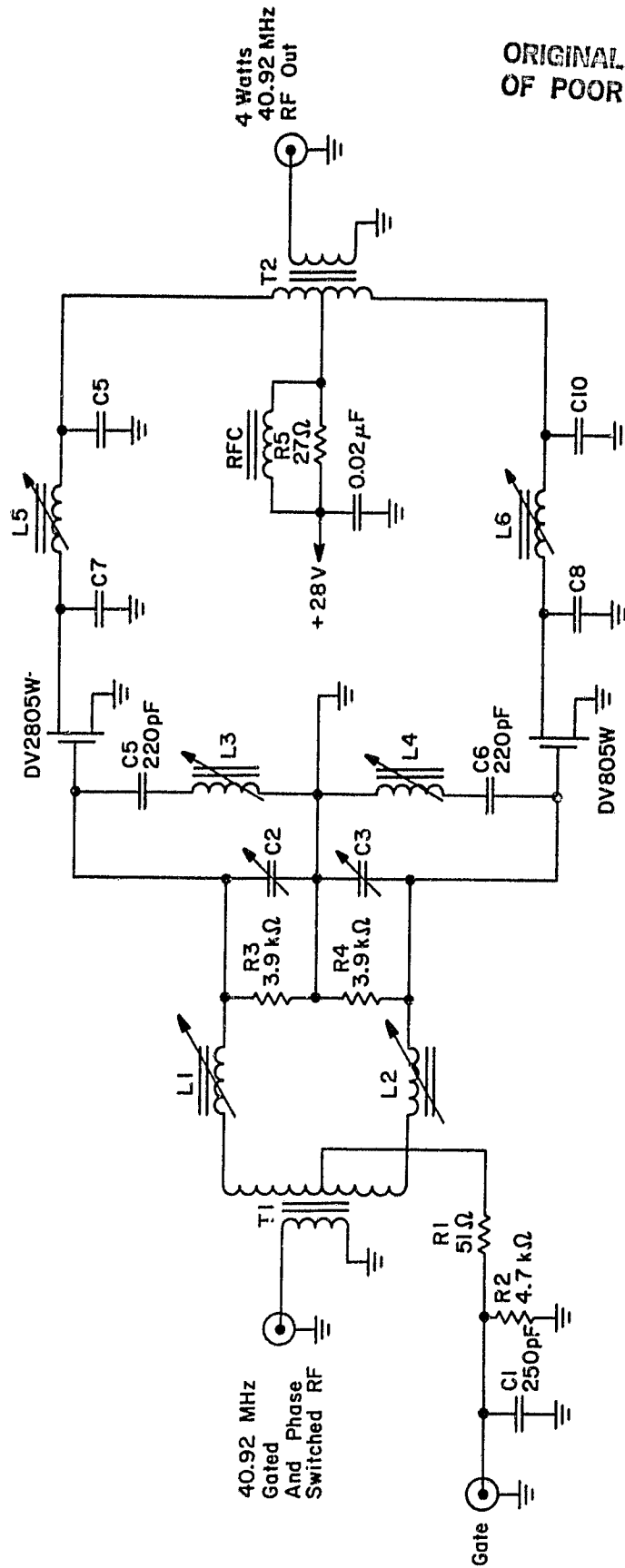
The gate pulse amplifier shown in Figure 3.6 turns the RF amplifier on and off via bias control. Q1 is a simple pulse amplifier, IC1 is in a Schmitt trigger circuit configuration, with the trigger point set by R6, with D1 and D2 selected for the desired on and off bias.

The RF output power detector shown in Figure 3.7 is basically a modified wideband 20 dB dual directional coupler based on the design by McDonald (1982). The modifications consist entirely of two 51 $\Omega$  detectors built into the transmitted and reflected power lines, and voltage dividers to assist in calibrating the meter.

Figure 3.8 is the circuit diagram of the peak power meter circuit devised to assist in monitoring the performance of the RF amplifier. Built onto the back of an existing Micromatch average power meter, this device provides an indication of transmitted power, reflected power, and S.W.R. It does, of course, require a gate signal which is taken from existing lines.

Pictures of these devices and circuits are shown in Figures 3.9 a, b, c, and d.

ORIGINAL PAGE IS  
OF POOR QUALITY



Note:

- All Caps Mica
- All Resistors 1/2 W

Figure 3.5 RF amplifier circuit diagram.

ORIGINAL PAGE IS  
OF POOR QUALITY

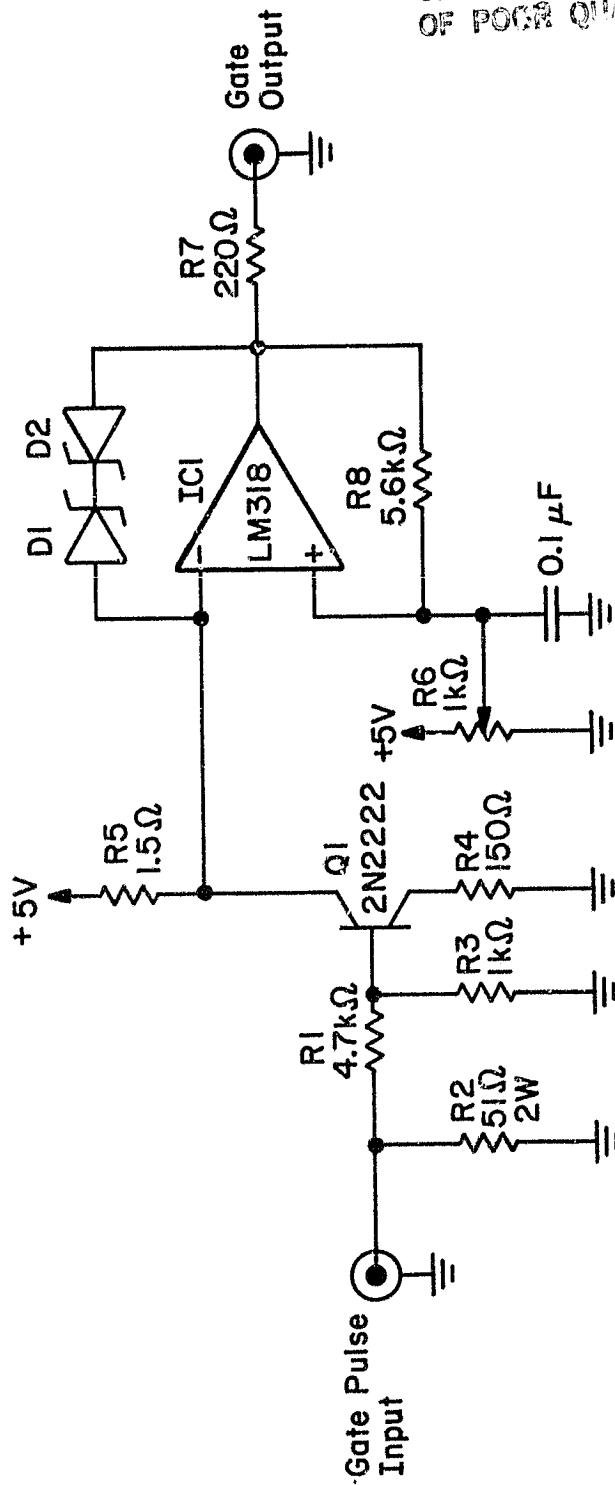


Figure 3.6 Gate amplifier circuit diagram.

ORIGINAL PAGE IS  
OF POOR QUALITY

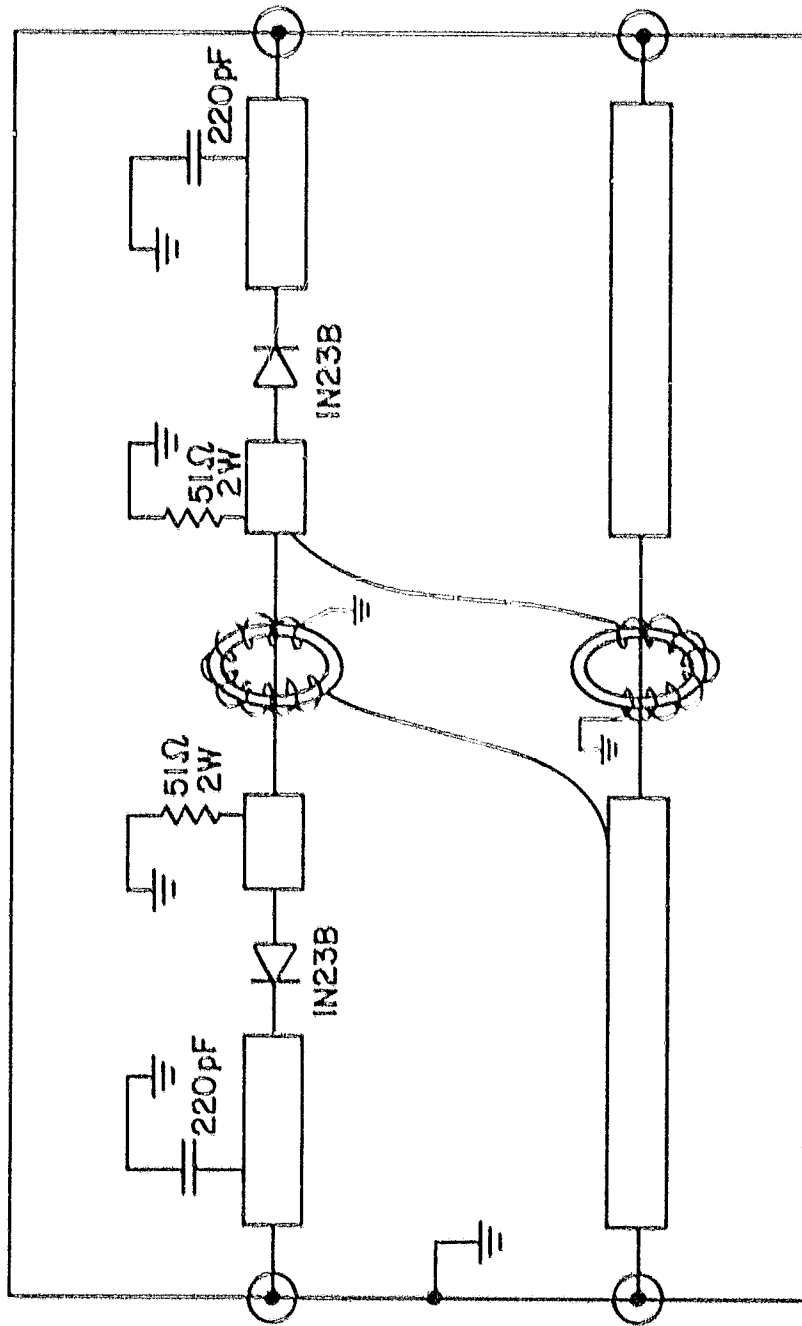


Figure 3.7 Output detector diagram.

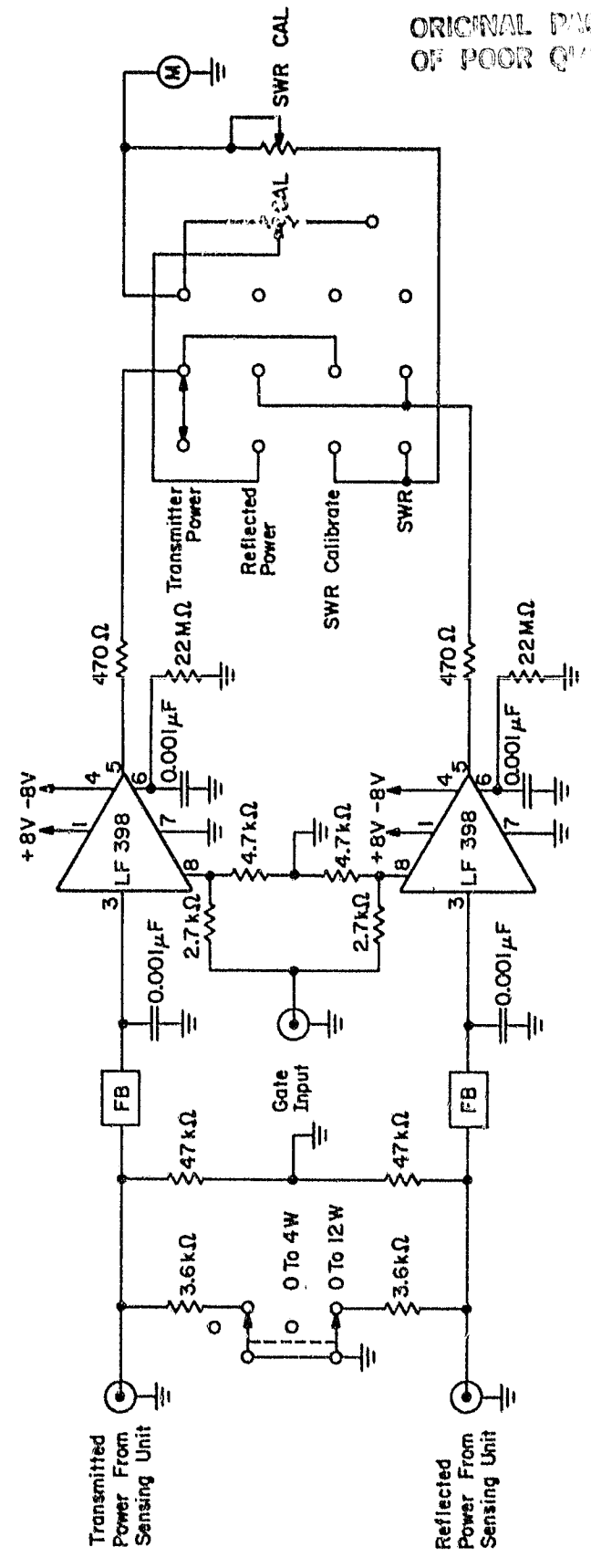
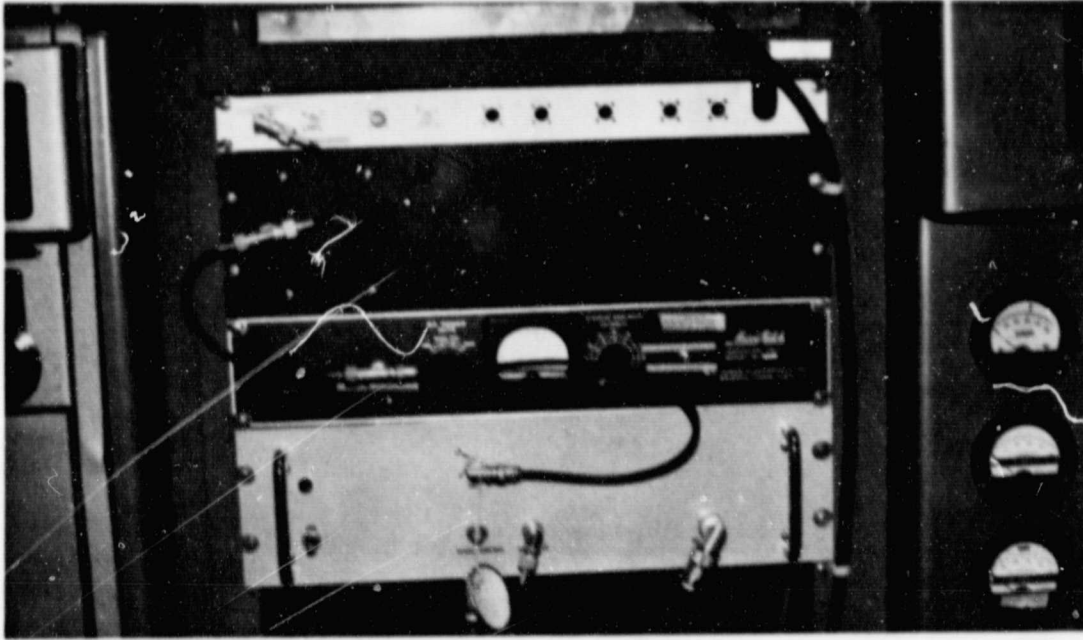


Figure 3.8 RF output power meter circuit diagram.

(a)



(b)

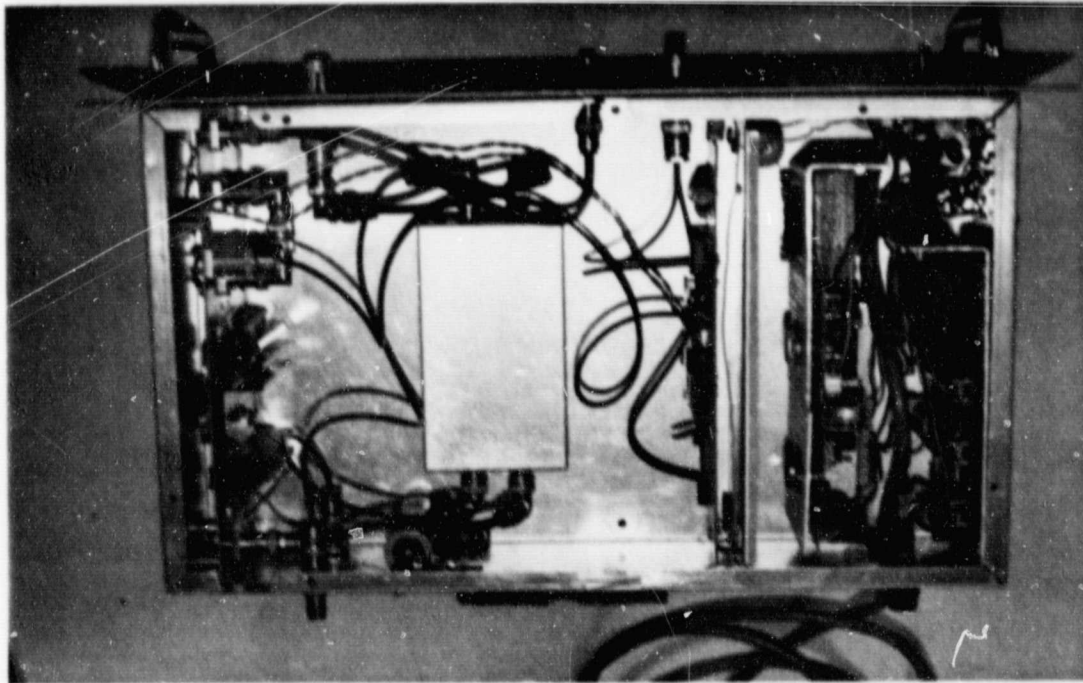
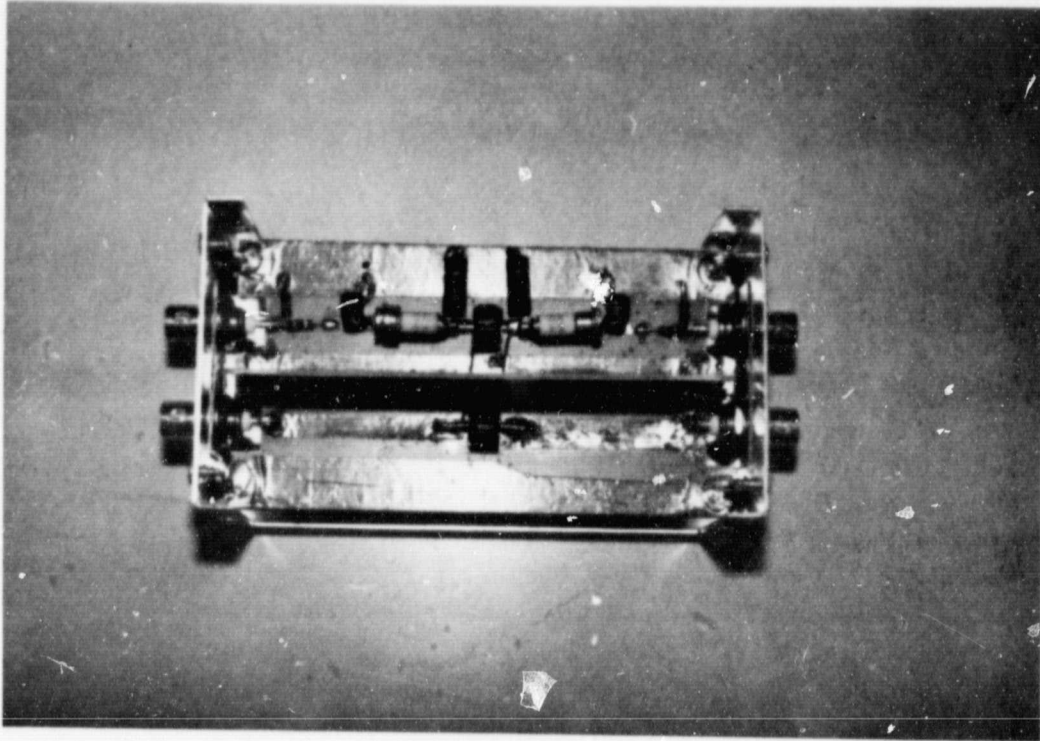


Figure 3.9 (a) RF amplifier shown mounted in equipment rack. The amplifier is the light gray unit on the bottom. The output power meter is shown mounted just above the amplifier. The next panel (black) is the mount for the 814B output power meter discussed in Section 2 of this chapter.  
(b) Chassis layout of the RF amplifier of unit 1.  
(c) Internal construction of the RF detector unit.  
(d) Component layout of the two circuit boards mounted in the unit 1 chassis.

(c)



(d)

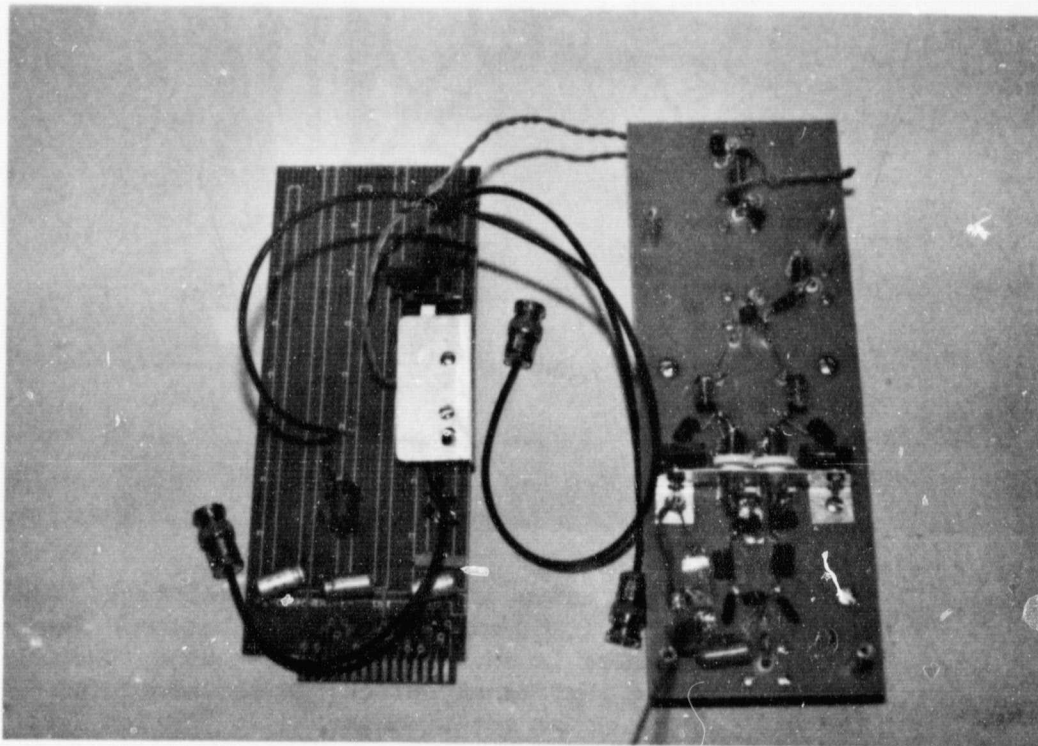


Figure 3.9 Continued.

### 3.3 The 814B Linear Amplifier

The 814B linear amplifier is a two tube class AB1 linear amplifier. Its basic specifications are summarized in Table 3.2.

Figure 3.10 shows the RF amplifier of the 814B. V101 and V102 are 4CX1000As operated in parallel. Greater stability is achieved by operating the screen at ground potential with the cathodes at -325V; the grids are biased 0 - 80V negative relative to the cathodes.

The dc power supply block diagram is given in Figure 3.11. The circuit diagram is shown in Figure 3.12.

The peak power meter and RF on detector circuit shown in Figure 3.13 performs two functions: it enables the output power meter of the 814B to measure peak power rather than average power, and it sends an "RF on" pulse to the logic and interlock module which enables the transmit pulse output for protection of the 4CX5000A stage. (Note: experience shows this amplifier is unstable if operated with a VSWR in excess of the rated maximum.)

### 3.4 The 4CX5000A Intermediate Power Amplifier

The schematic of the 4CX5000A intermediate power amplifier is shown in Figure 3.14. This device is operated class C. The input match network is a combination of a transmission line and conventional  $\pi$  network. The output match network is also a conventional  $\pi$  network. The tube and the output match network are located in a cylindrical pressurized container. Note that the plate voltage is derived from the modulator through a dropping resistor network and that if the RF input to the grid fails (hence no conduction) the entire modulator voltage will be impressed across the tube; arc damage is therefore possible, and special precautions are necessary to avoid this. The capacitor designated C213 is actually 8 each 1000-pF transmitter-type capacitors installed symmetrically around the socket; this is intended to improve the stability of the amplifier by providing superior screen by-

Table 3.2 Continental Electronics 814B specifications.

Peak power output	3 kW
RF input power	5-10 Watts Peak
Output impedance	51.5 $\Omega$
Output SWR	2:1
Input impedance	51.5 $\Omega$
Class operation	AB1
Plate voltage	+3 kV
Screen/cathode voltage	-325V
Plate current maximum	1.67 amps combined
Bandwidth	$\pm$ 573 kHz

ORIGINAL PART IS  
OF POOR QUALITY

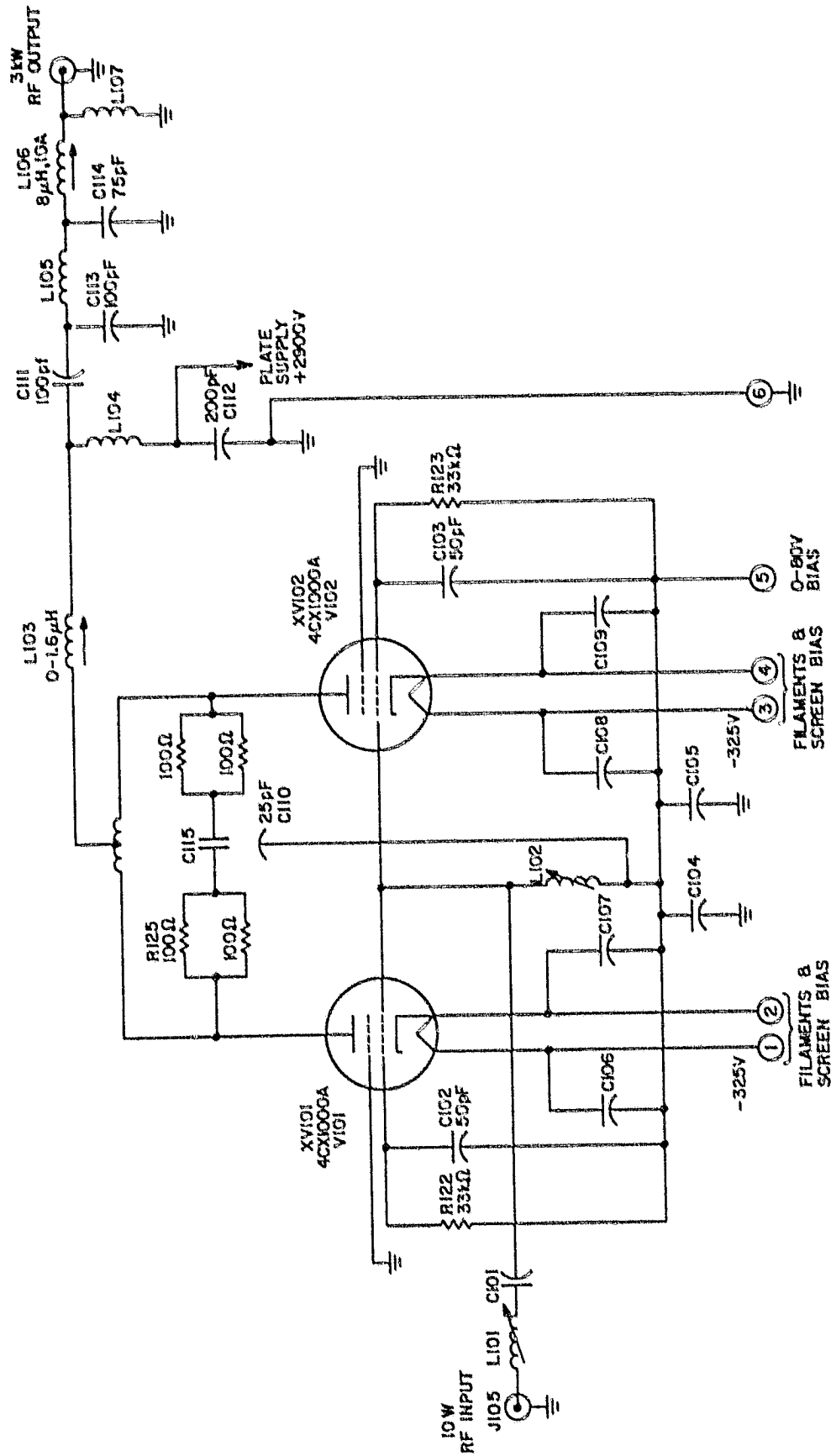


Figure 3.10 RF amplifier circuits of the Continental Electronics 814B VHF transmitter.

ORIGINAL PAGE IS  
OF POOR QUALITY

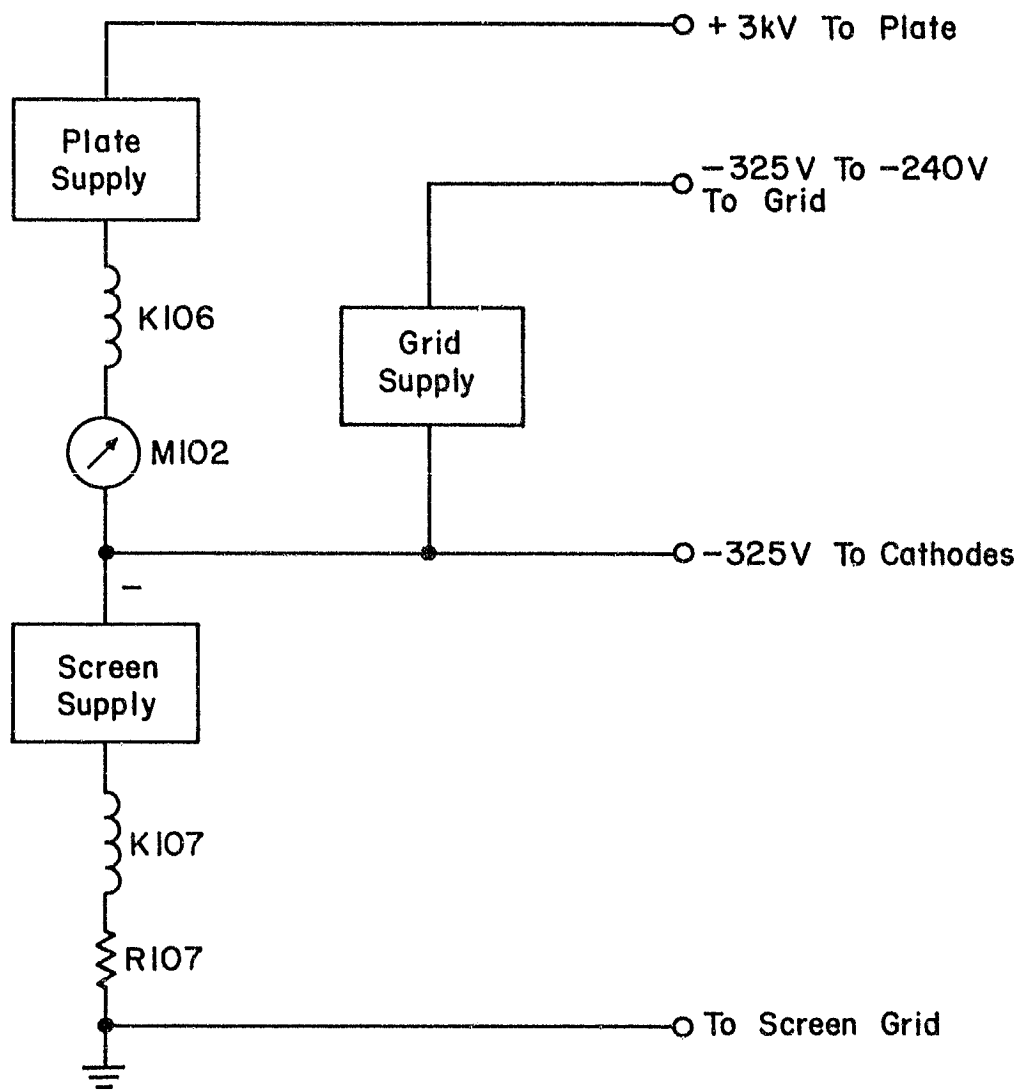


Figure 3.11 814B power supply block diagram.

ORIGINAL PAGE IS  
OF POOR QUALITY

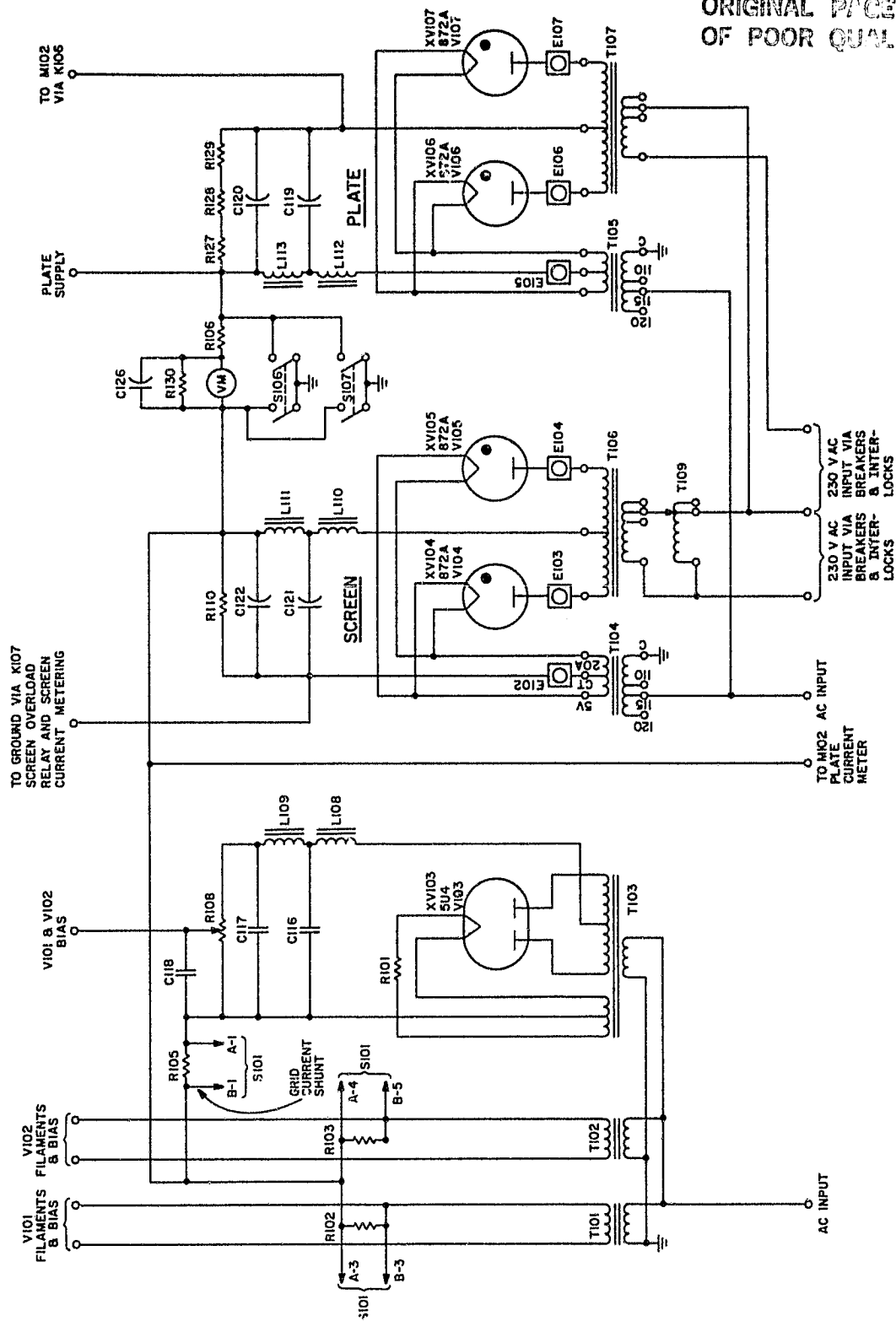


Figure 3.12 814B power supply circuit diagram.

ORIGINAL PAGE IS  
OF POOR QUALITY

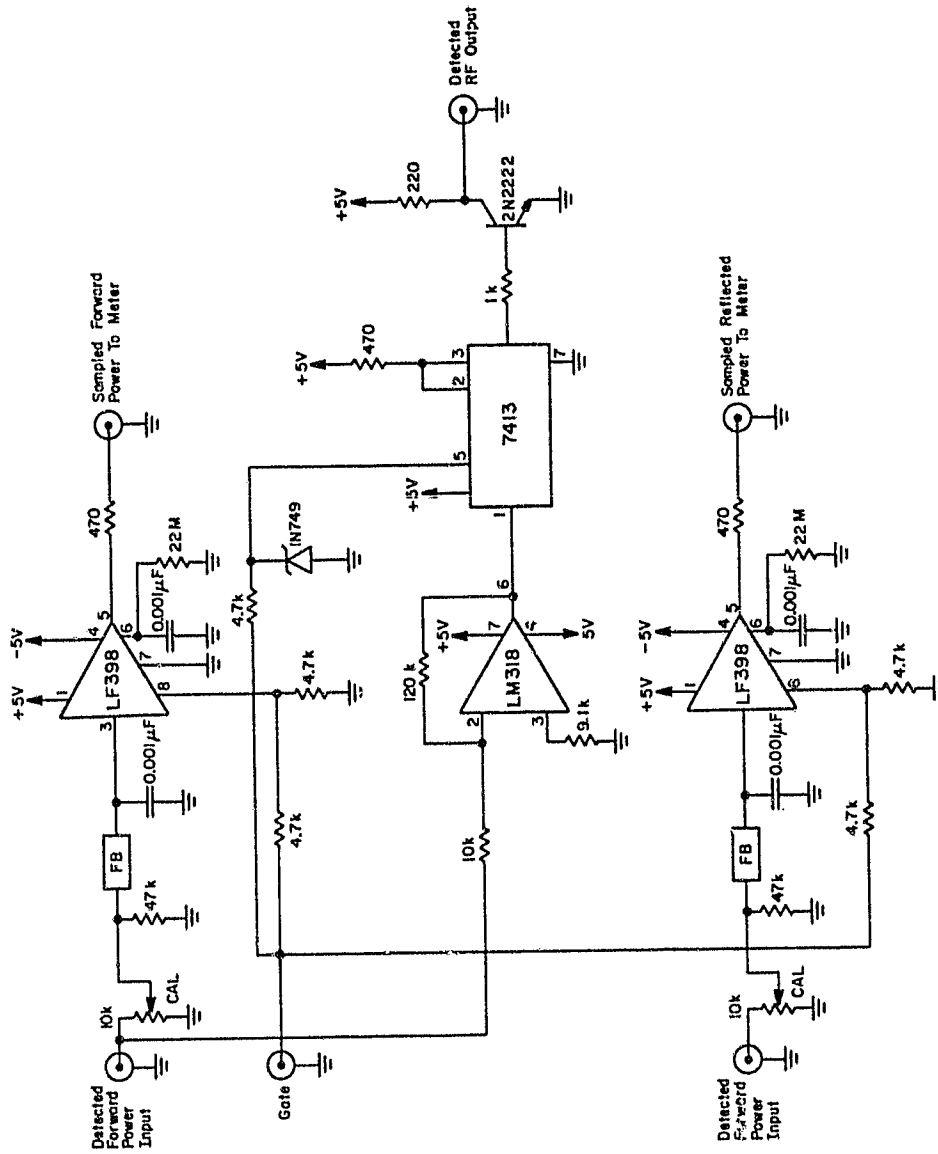


Figure 3.13 814B peak power meter and "RF on" detector circuit diagram.

ORIGINAL PAGE IS  
OF POOR QUALITY

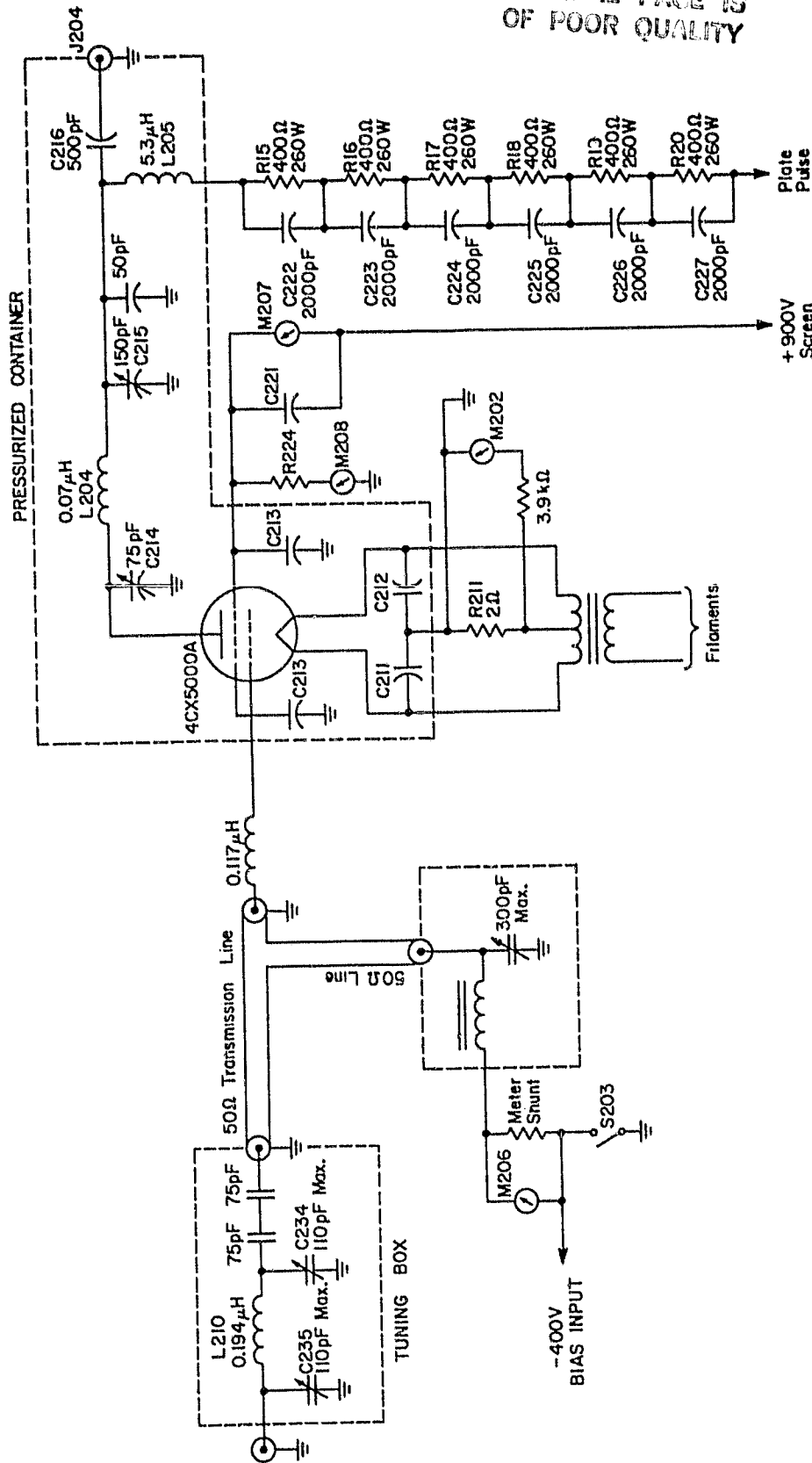


Figure 3.14 4CX5000A (unit 2) RF amplifier schematic.

pass. The socket reactance is by no means negligible; it is equivalent to about  $.17 \mu\text{H}$  in series and  $50 \text{ pF}$  in parallel with the tube input. Further, the output match has a fatal flaw when used in conjunction with the current match network at the drive input: it will match low resistance, high capacitance loads to high impedances as seen by the tube, thus tending to produce what looks like a match; (i.e., the plate current dips) but which limits the tube output power by presenting a high-impedance load to the plate.

Figure 3.15 is the schematic of the bias supply for the 4CX5000A. It is controlled through the use of a Variac in the ac supply.

Figure 3.16 shows the circuit of the screen supply; this is also variable using a Variac in the ac supply.

Figure 3.17 is a picture showing several major units of the transmitter. Closest to the camera and on the right in the picture is the unit 2 cabinet housing the 4CX5000A. Next is an equipment rack housing the gated RF amplifier (unit 1) in the top. The screen supply for unit 2 is shown installed in the bottom of the rack. Beyond the equipment rack is the Continental Electronics 814B transmitter used between units 1 and 2.

Figure 3.18 shows part of the transmission line match networks used in the input of unit 2.

### 3.5 Units 3 and 4: The Driver and PAs

Units 3 and 4 are the "work horses" of the radar. These two final stages boost the RF output to the 1 to 4 megawatt range. Since unit 3 is essentially identical to each of the four components of unit 4, only one model need be developed. Figure 3.19 is a simplified diagram of the physical structure of these devices. Note the single tube -- an ML-5682 -- mounted plate-down inside the unit.

Figure 3.20 is an enlarged version of the upper portion of the unit,

ORIGINAL PAGE IS  
OF POOR QUALITY

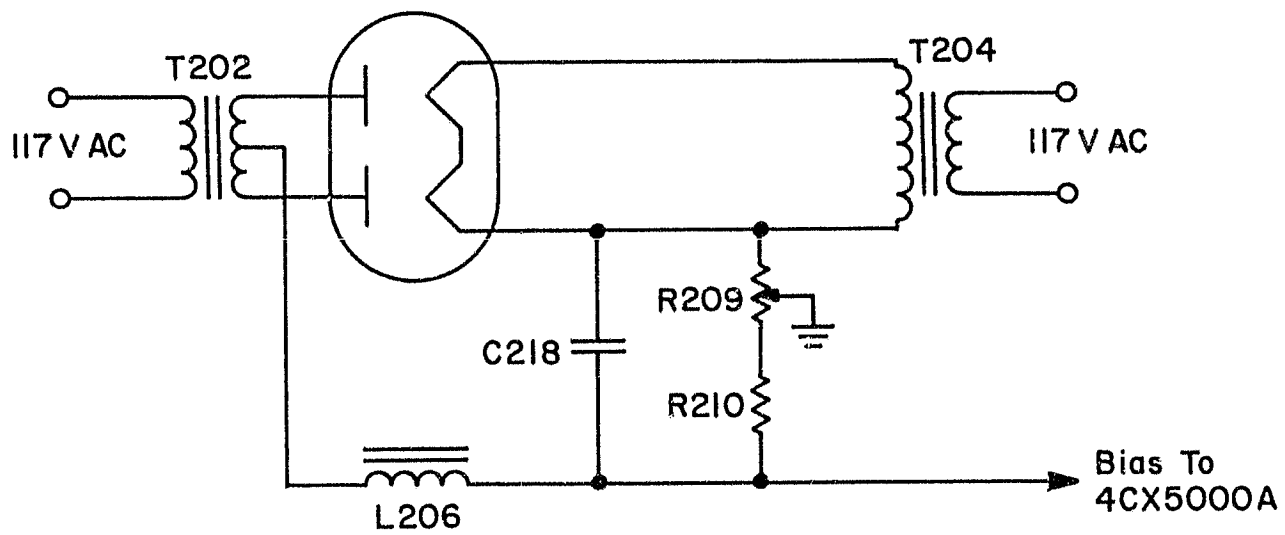


Figure 3.15 Unit 2 bias supply.

ORIGINAL PAGE IS  
OF POOR QUALITY

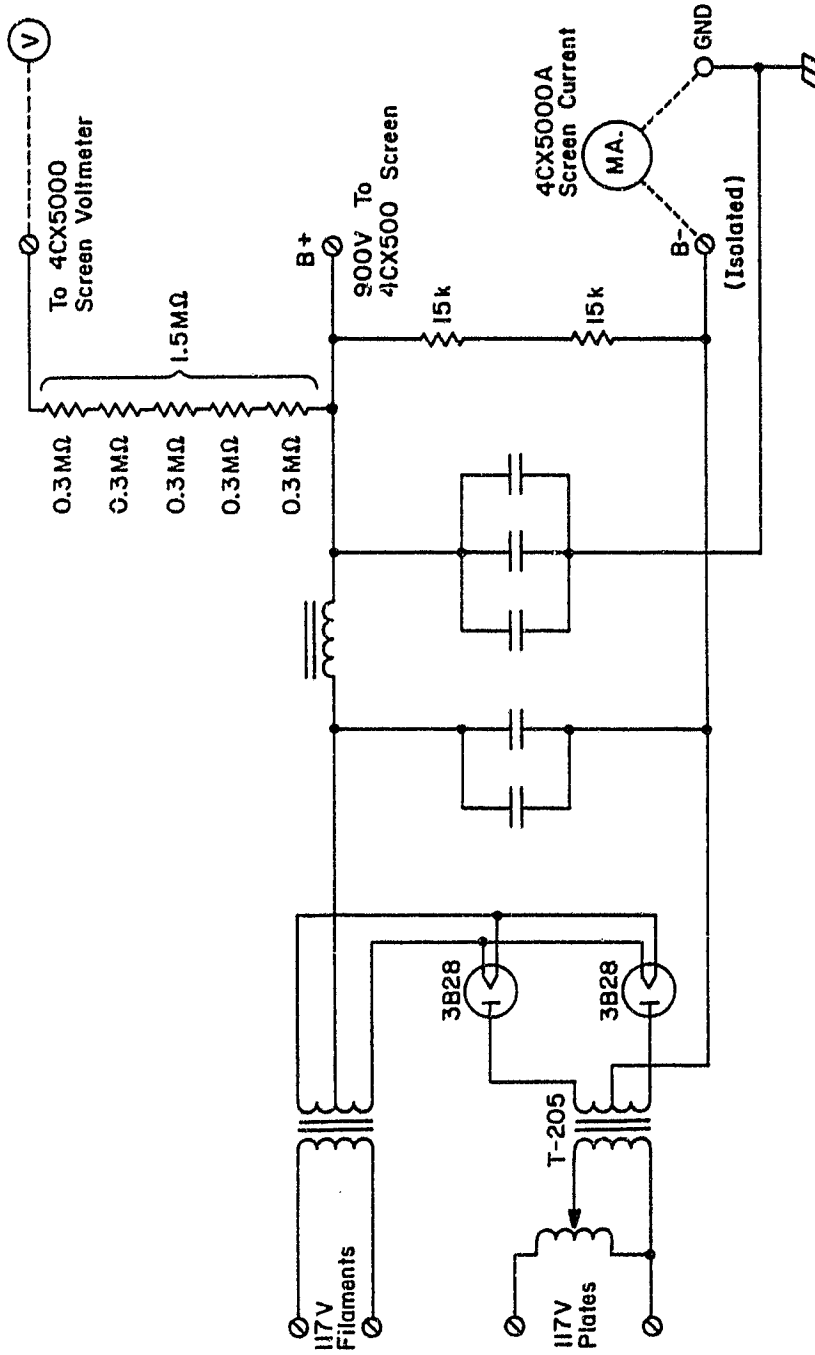


Figure 3.16 Unit 2 screen supply.

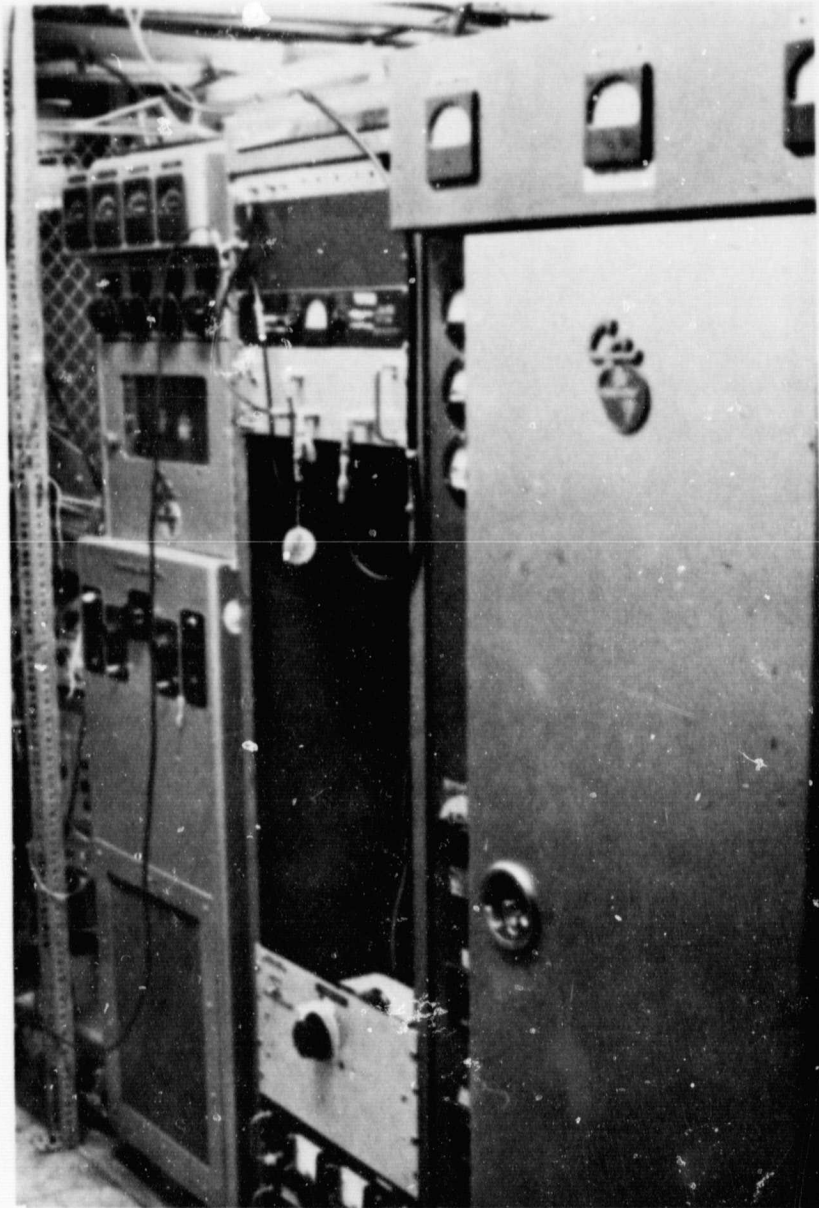


Figure 3.17 Picture of units 1, 2, and 3, showing unit 2 on the right, unit 1 in the center, and the 814B linear amplifier on the left.

ORIGINAL PAGE IS  
OF POOR QUALITY

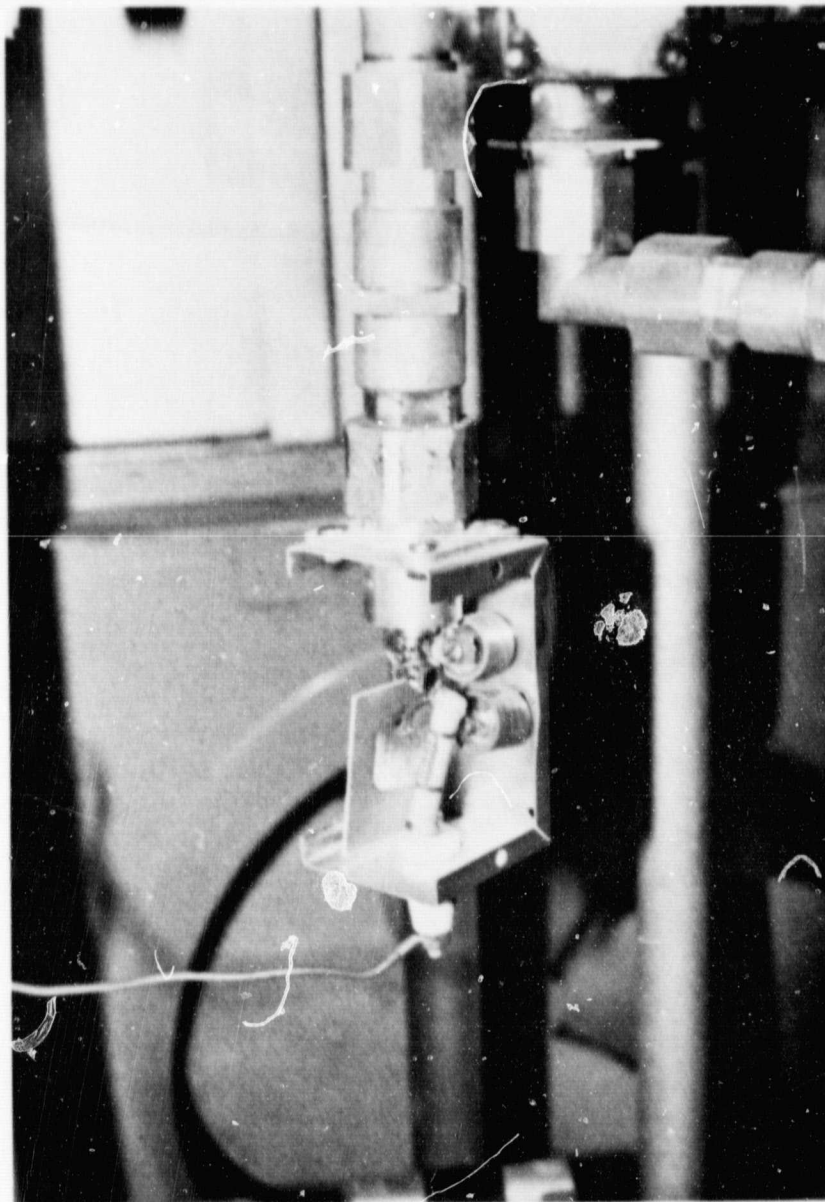


Figure 3.18 Detail of the bias input portion of the 4CX5000A input matching network.

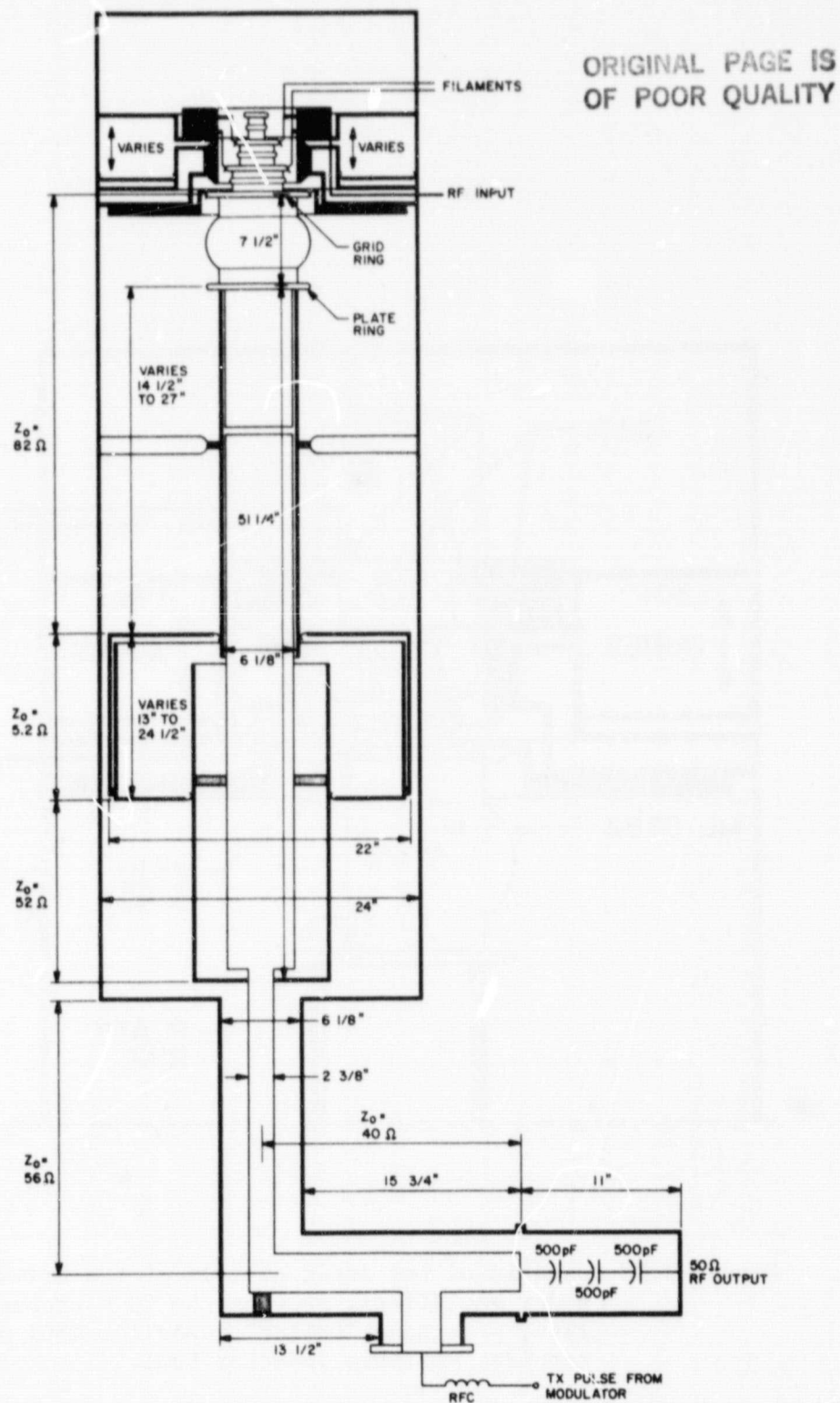


Figure 3.19 Simplified physical structure of the driver and power amplifiers.

ORIGINAL PAGE IS  
OF POOR QUALITY

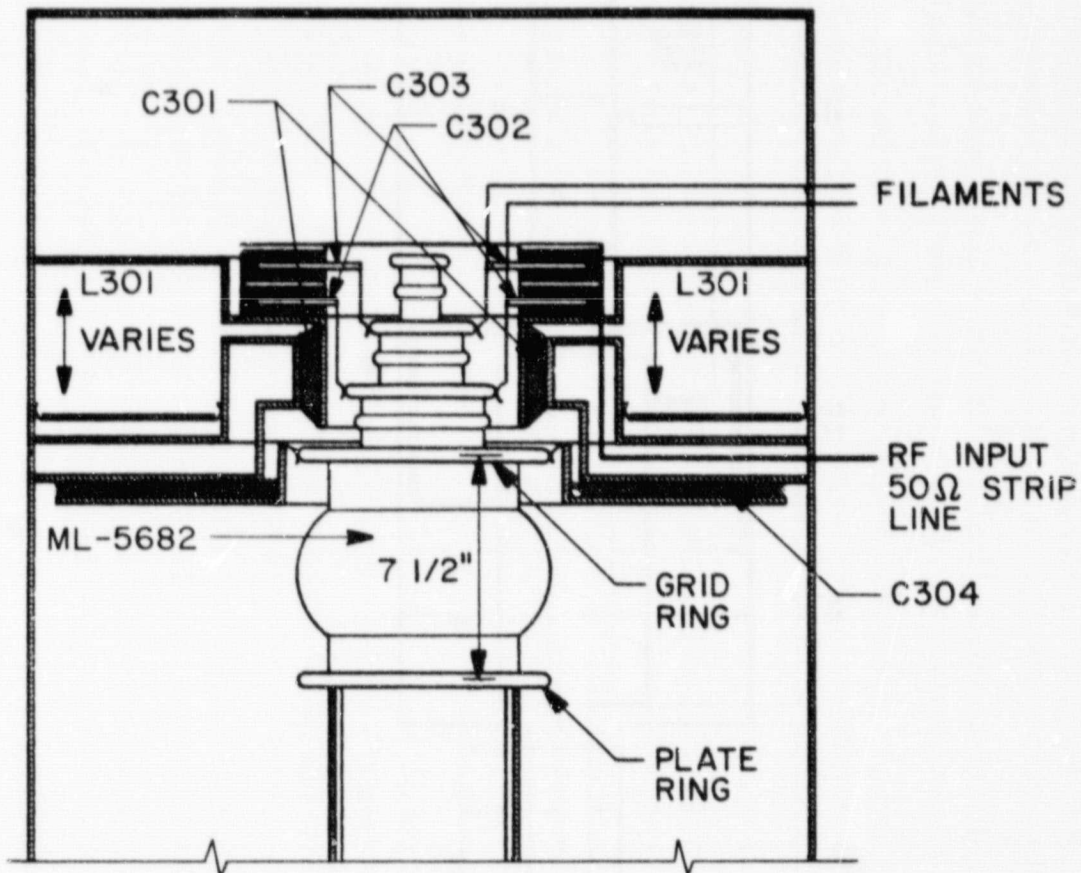


Figure 3.20 Details of the input circuit of the driver and power amplifiers, showing the 20  $\Omega$  transmission line, irathane "collar" capacitor C301 and the toroidal variable inductor L301.

which contains the input circuitry shown in Figure 3.21. This whole device is coaxial with the tube mounted on the axis. C301 is an 800 pF irradthane capacitor in the form of a collar which fits closely around the tube socket. C303 and C304 are mica rings mounted as part of the tube socket. L301 may be thought of as a high Q single turn toroidal inductor which may be varied with the input tuning controls. The tank circuit composed of L301 and C301 reduces distortion of the signal, which is conducted inward via a strip line of approximately  $20 \Omega$  characteristic impedance and 15" in length. C304 is another mica ring which keeps the grid at RF ground.

Again referring to Figure 3.19 we note that the output match network may be modeled as segments of transmission line of differing lengths and characteristic impedances, with junction capacitances at the ends of each segment. The model used to evaluate this network is shown in Figure 3.22, and is described as follows: the plate of the ML-5682 is fitted into the center conductor of an  $82 \Omega$  transmission line. This line then connects to a 5.2 line, and has a junction capacitance of 20 pF at the connection. The 5.2 line ends in a junction with a  $52 \Omega$  line, having junction capacitance of 17 pF. Thereafter follow lengths of  $56 \Omega$  line,  $40 \Omega$  line, and a blocking capacitor and transmission line structure having a characteristic impedance of about  $120 \Omega$ . The junction capacitances of the last 5 sections of line have been evaluated, then ignored as negligible. The two shown have been evaluated from the formulas provided by Somlo (1967) based on the work of Whinnery (1944). The 85 pF of the grid-plate interelectrode capacitance completes the matching network. Please note that the whole tube plate must be included as part of the  $82 \Omega$  line. The program called CAPAUG (Program 2, Appendix IV) computes the load impedance seen at the outputs of units 3 and 4. Its results are used by the program called PA MATCH (Program

ORIGINAL PAGE IS  
OF POOR QUALITY

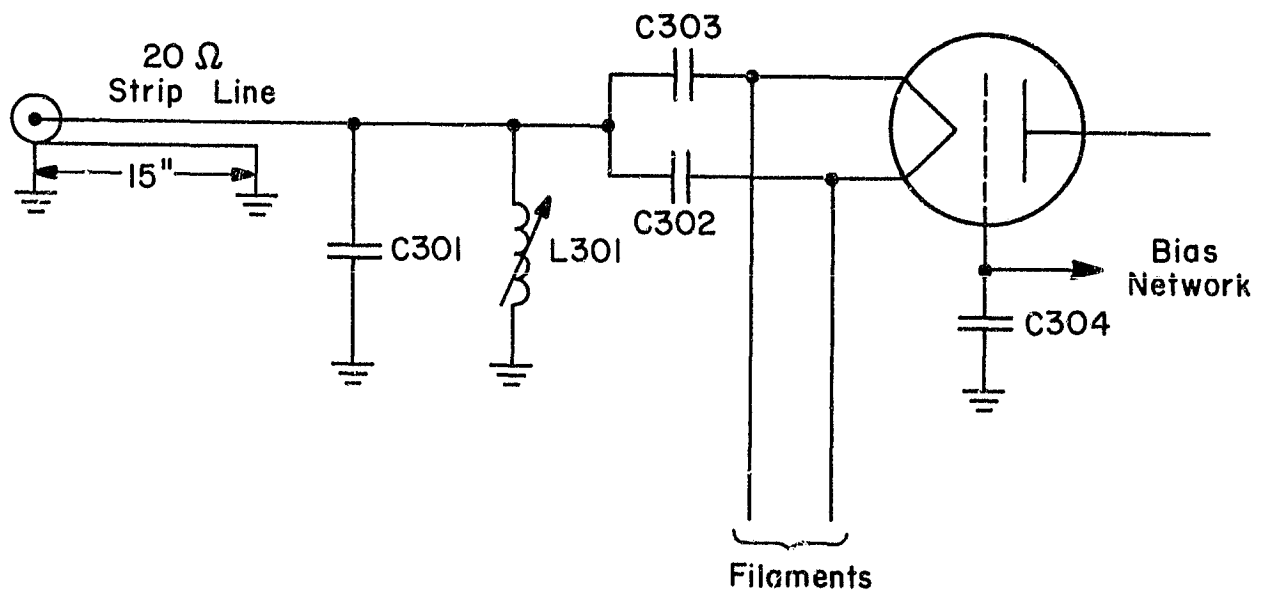


Figure 3.21 Simplified schematic of the input match network.

ORIGINAL PAGE IS  
OF POOR QUALITY

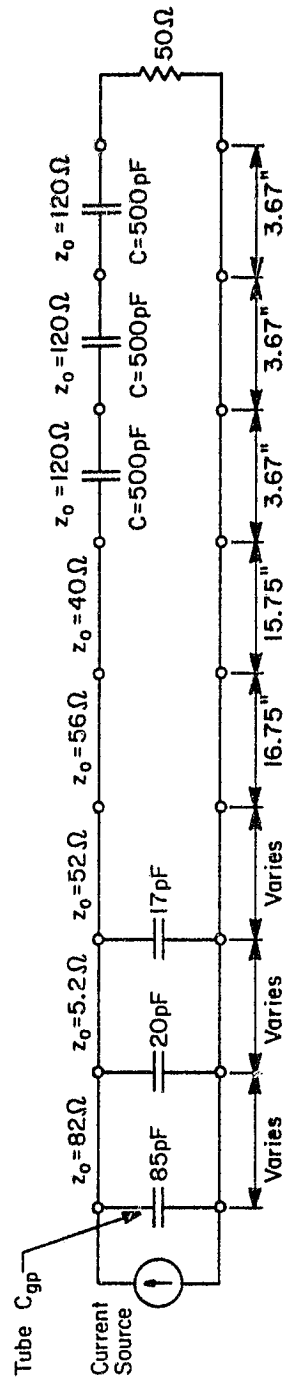


Figure 3.22 Model of the output match network.

1, Appendix IV), which was written to evaluate the possible range of loads seen by the tube. The program called PA BANDWIDTH (Program 3, Appendix IV) evaluates the bandpass of the match network for particular loads, using part of the data generated by PA MATCH for input and generating graphs of the transmission function, an example of which may be seen in Figure 3.23. Results from PA MATCH indicate that loads may be matched in the range from about  $300 \Omega$  to  $850 \Omega$  requiring that the ML-5682's load lines be kept in this range, which incidentally is also the range specified by the tube's manufacturer. Program descriptions and listings are included in Appendix IV. A simplified schematic of the bias circuit is shown in Figure 3.24. Note that the bias is part fixed and part grid-leak bias, and may be class AB, B, or C depending on the operating conditions. Most of the basic limitations of units 3 and 4 arise directly from the ML-5682 triode. Tubes are always rated conservatively, so one can usually expect to be able to exceed some of the limits some of the time. In point of fact the available peak plate voltage of the Urbana Radar greatly exceeds the manufacturer's specifications, but the point which has to arise is how much excess is tolerable? Killpatrick (1957) and Doolittle (1964) have demonstrated that these limits depend on the plate-grid spacing and the structure of the cathode. For the thorium-tungsten cathodes and 1.7 cm spacings of the ML-5682, the nomograph shown in Figure 3.25 taken from Doolittle (1964) suggests that a safe maximum for new ML-5682's is about 70 kV, twice the rated value. This ability to withstand high voltages is called high voltage stability; the Urbana Radar has no crowbar circuit in the modulator, having only some relay based (hence slow) protection circuits. Hence, once a flash arc occurs, it will continue until the power supply capacitors are discharged or until the tube is destroyed. Flash arc damage to a tube accumulates; i.e., a tube will always

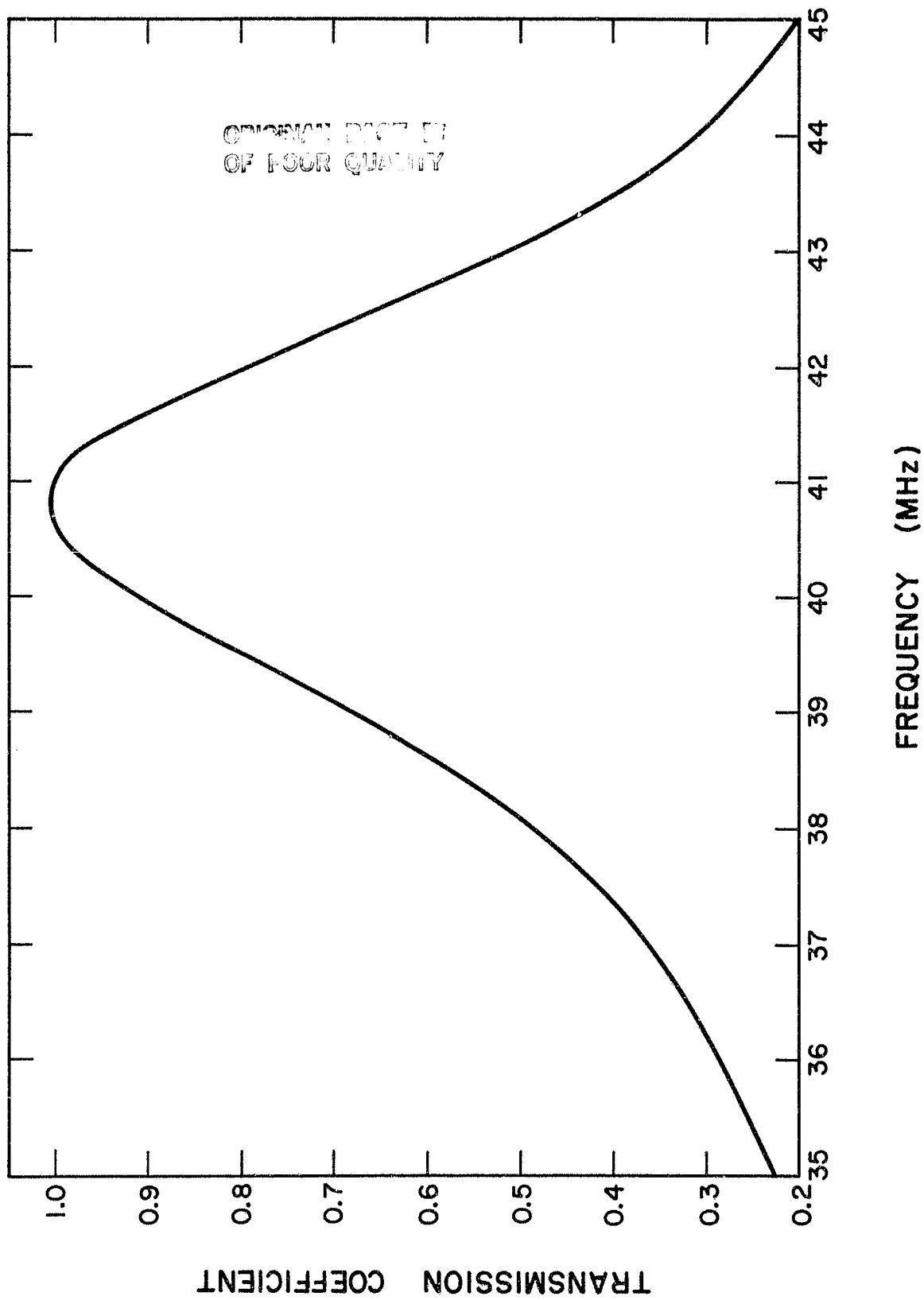
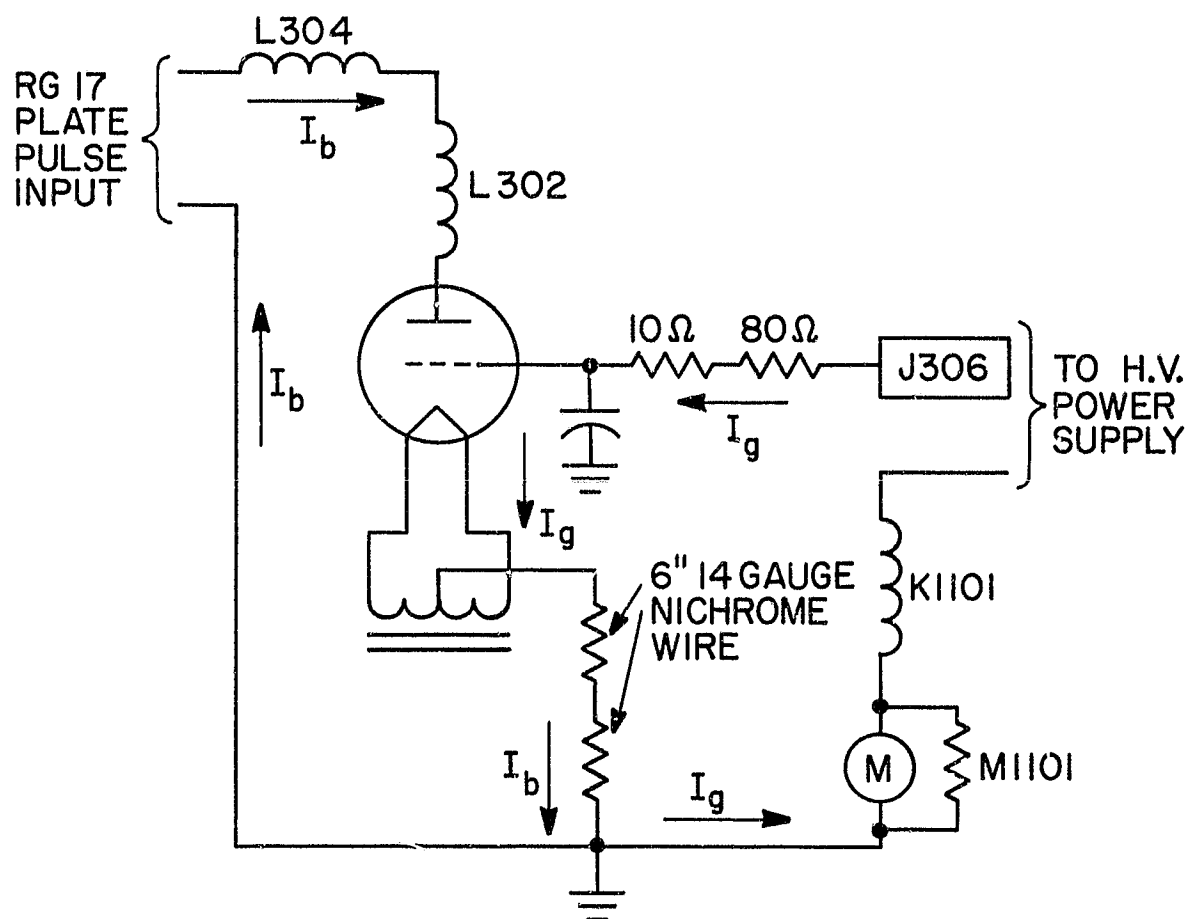


Figure 3.23 Typical passband of the output match network of units 3 or 4, as generated by the program named PA BANDWIDTH.

ORIGINAL PAGE IS  
OF POOR QUALITY



### BIAS CIRCUITS OF UNITS 3 & 4

Figure 3.24 Bias circuits of units 3 and 4.

ORIGINAL PAGE IS  
OF POOR QUALITY

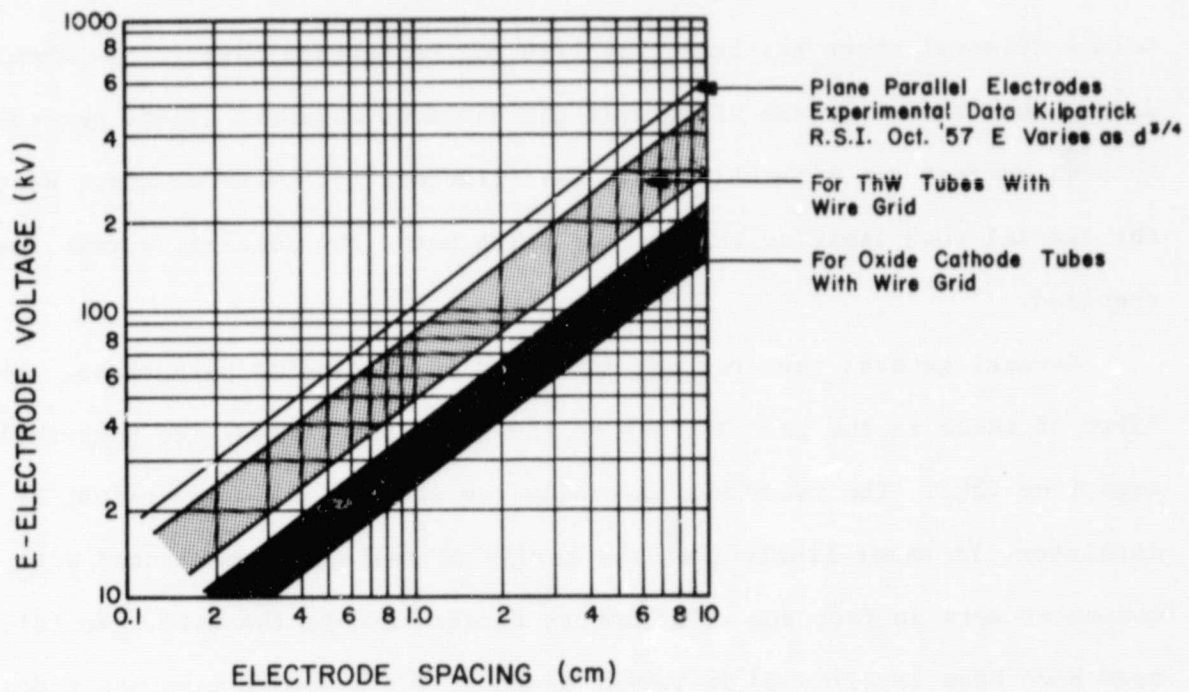


Figure 3.25 Anode voltage rating versus outer grid to anode spacing from Doolittle (1964).

tend to arc over more easily the second time. Arc damage causes pits and catwhiskers on the cathode wires, increasing the voltage gradient and probability of arc. Note that the modulator of the Urbana Radar is capable of 50 kV pulses; during operation the peak plate voltage of an RF amplifier would exceed 90 kV, well beyond the limits of the ML-5682. Care must be taken to keep the modulator output within the tube's limits. Like any tube of its kind, the ML-5682 requires a special filament transformer, and not only to provide the normal operating current of 325 amps @ 16.5 V. When cold a filament often has less than 1/10 the resistance than it has when hot; during the initial inrush of current the enormous magnetic fields generated by high current can literally twist the filaments off their mounts. Hence the special rush limiting transformer which keeps the initial current low is required.

Several general concerns are described in succeeding paragraphs. The first of these is the past history of the irrathene (irradiated polyethylene) capacitor C301. The radar was initially run at the full power output of the modulator. It seems likely that the series of failures experienced with this component were in fact due to flash-arc damage through the tube. No failures have been experienced in recent history, during which time the modulator output has been run at 16 kV dc input, with 15 kV pulses out.

Another area meriting discussion is the physical weakness of the blocking capacitor assembly. This consists of an 11-inch long segment of 6-inch diameter rigid copper coaxial line whose center conductor has been replaced by 3 each 500 pF 15 kV ceramic capacitors in series. Though they are not individually delicate, the stress encountered in assembly and disassembly has broken these devices in the past.

The ML-5682 is a water cooled tube. The cooling water is in actual

physical contact with the plate at all times, and hence demands a certain level of purity. Care should be taken to monitor this and change the cooling water when required. Note that no filtration or deionization system is in use, the water being changed about every 6 months.

The operating conditions of tetrodes and triodes may be analyzed using Fourier analysis of the various tube currents and voltages. One practical approach to this makes use of the Machlett Power Tube Calculator which consists of a cosine scale and a work sheet for tabulating and computing the results. The work sheet was automated using the Apple computer; the program is called Machlett Power Tube Calculator. The user draws the desired load line and uses the cosine scale to measure grid and plate currents at pre-selected points. These are tabulated by the program and various predicted operating conditions are computed and printed. Certain general statements can be made from analysis of the ML-5682: 1) The input impedance of this circuit is highly dependent on the bias voltage and on the size of the grid resistors. 2) Certain operating conditions are possible which will not permit matching in the circuits as they now exist. 3) Operating conditions also are possible in which the output is matched but which produce large mismatches at the input. Since the input match network is constructed for a  $20 \Omega$  input impedance careful design of the operating conditions is mandatory to ensure proper operation of these units.

One more point which should be discussed is the problems caused by the interaction between the input and output circuits of these units. Since these are common grid triode circuits the condition of the output match is reflected to the input; hence when tuning one must always adjust both, input and output, using a rocking procedure to achieve optimum match at both ends.

A picture of unit 3 is shown in Figure 3.26. It is virtually identical

ORIGINAL PAGE IS  
OF POOR QUALITY

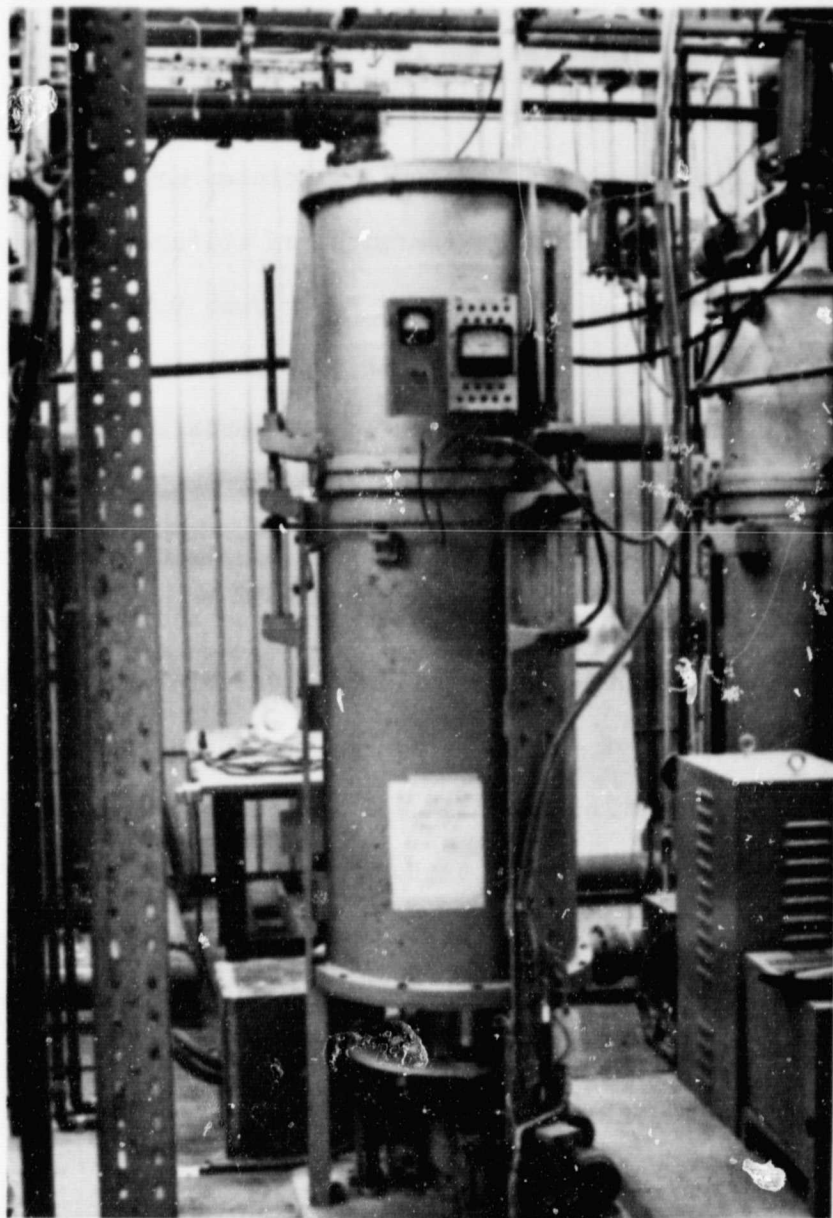


Figure 3.26 Picture of the driver (unit 3). Each of the four power amplifiers has an identical appearance.

in construction to all four parts of unit 4.

### 3.6 Driver Output Power Divider

The driver (unit 3) output must be equally divided 4 ways before it is applied to the PAs. Two of the inputs must also be phase shifted by  $180^\circ$ . The transmission line network which accomplishes this is shown in Figure 3.27. Parts of the system included on the diagram are the average power detector, the peak power detector, two hybrid dividers (standard "rat race" devices) and a coaxial t-splitter and match network. Power from the driver unit passes through the power detectors, through the 6" to 3" reducer, (in which both the inner and outer conductors taper identically, thus maintaining a constant  $50 \Omega$  characteristic impedance) to the 3" coaxial t, all arms of which are of  $50 \Omega$  characteristic impedance. Each of the two output arms then pass through a 62" length of  $72 \Omega$  impedance line to match to the  $50 \Omega$  line impedance following. One of these arms is routed to the hybrid divider serving units 4-1 and 4-2. The other is routed through an additional  $\lambda/2$  length of  $50 \Omega$  transmission line to provide the required  $180^\circ$  additional phase shift, then to the output divider serving units 4-3 and 4-4. The outputs of these dividers are matched to the  $20 \Omega$  PA inputs VIA a  $1/4\lambda$   $30 \Omega$  transmission line section.

Computer analysis of the coaxial t-splitter and match network reveals that when each output end is terminated in  $50 \Omega$ , the reflected power is less than 1% between the frequencies of 32 and 70 MHz; these results are shown graphically in Figure 3.28.

One addition should be made to this network to improve the tunability of the radar. Phase and amplitude comparators should be placed at the junction of each  $30 \Omega$   $1/4\lambda$  transform to permit tuning this device. This would enable the operator to cope more readily with the interactions between the



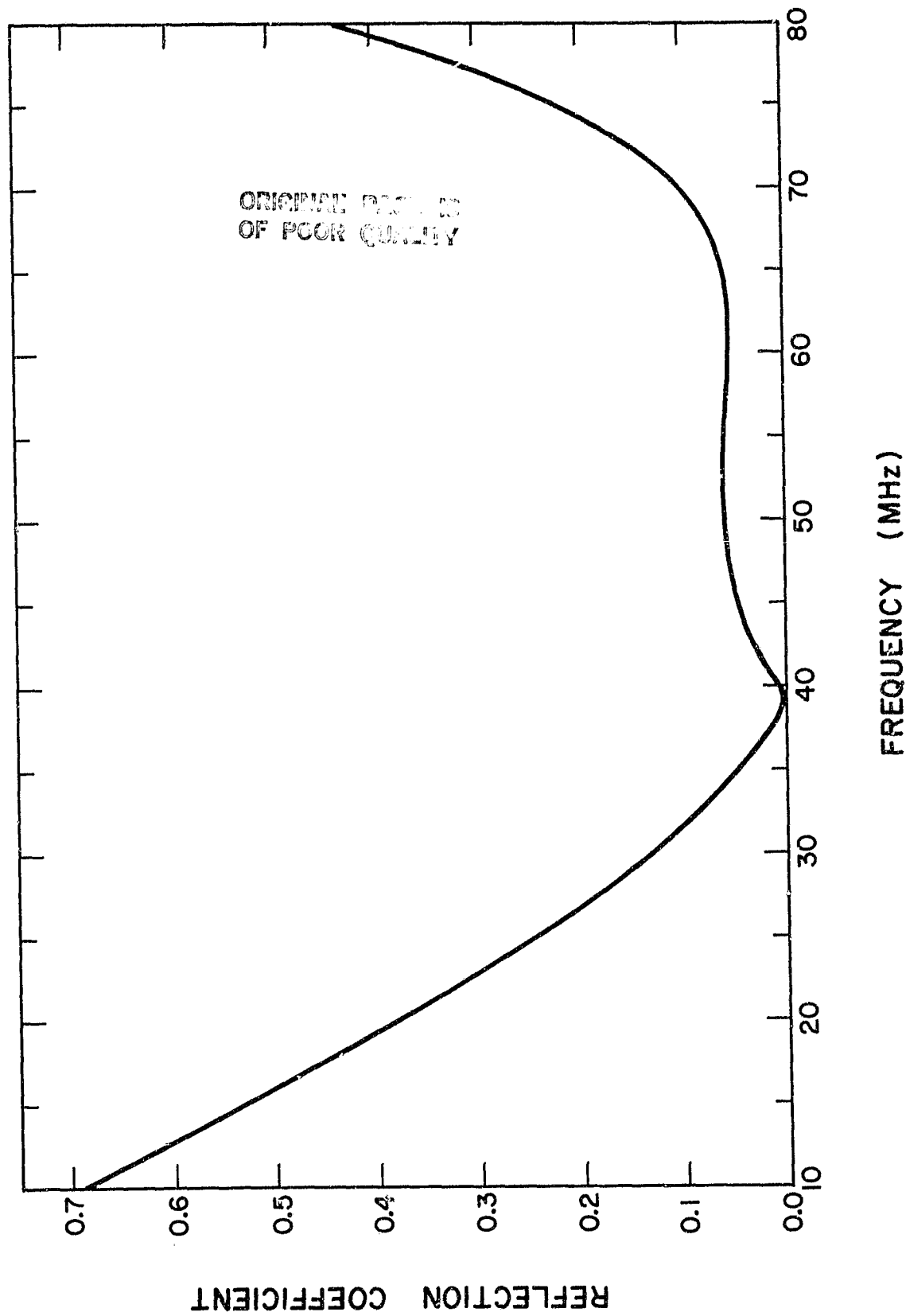


Figure 3.28 Bandpass of the asynchronous T-match network.

various outputs. Note that the outputs are not isolated from each other here. Isolation only may occur if both output lines are terminated in  $50 \Omega$ . In addition, the T-match network should be refabricated using 3" line to avoid arcs caused by high moisture, high power, and the high VSWR encountered during tuning; arc damage has been observed in this area. Drains should be installed at the low points of the hybrid splitters to permit an easy test for standing water in the lines.

### 3.7 Final Output Combiner Networks

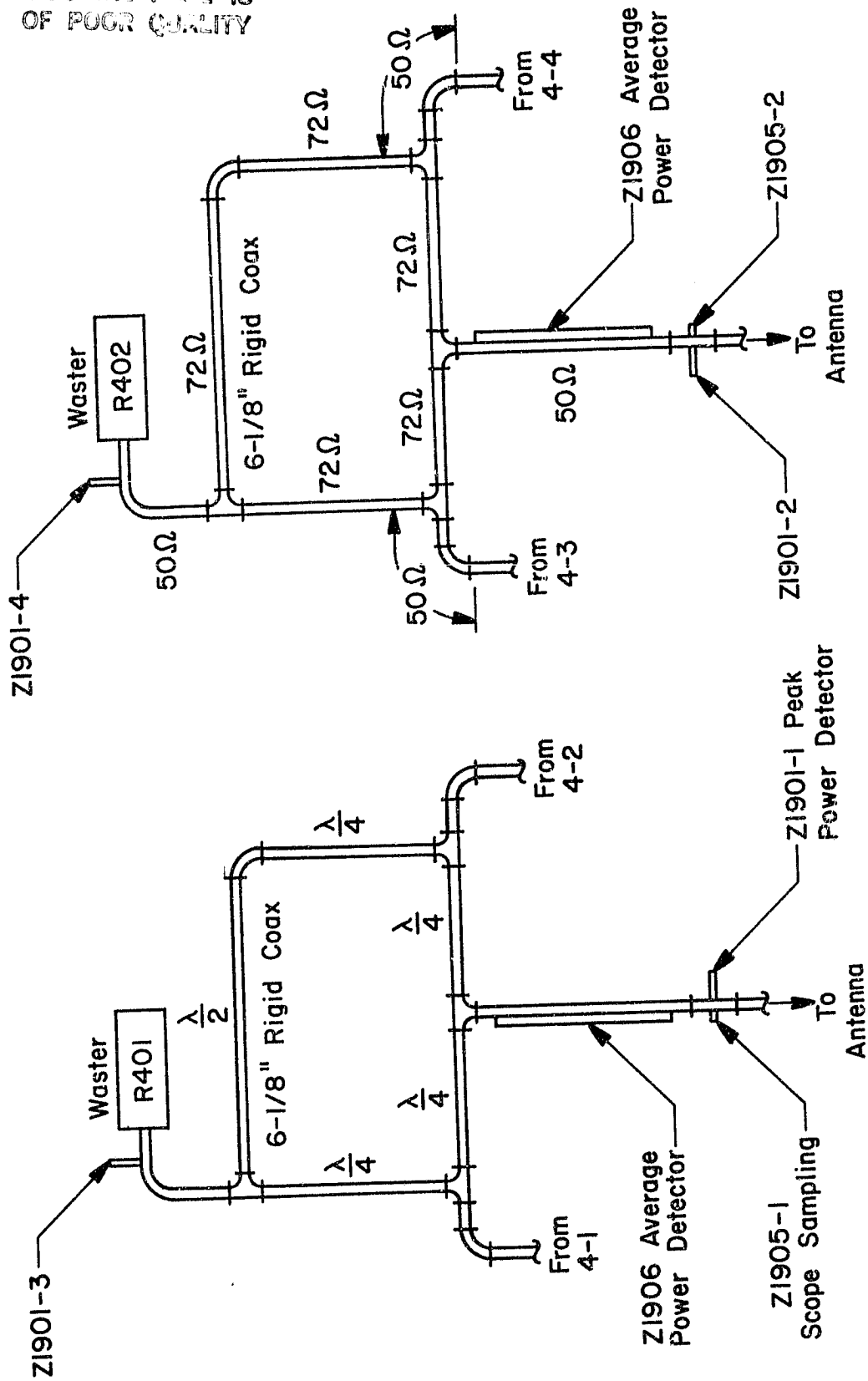
The final output combiner networks each combine the outputs from two power amplifiers. In addition they provide isolation between amplifiers. In normal operation the PA outputs are in phase and of the same magnitude, in which case no power is lost in the waster. When an imbalance in phase or magnitude occurs, however, that imbalance is "burned up" in the waster. From the research of Brown and Morrison (1949), we see that this device is typically better than 90% efficient with relative phases of less than  $30^\circ$ , if the magnitudes are equal. On the other hand, if one of the amplifiers fails completely, only 50% of the output of the remaining amplifier will reach the load. Both combiners are constructed of 6 1/8" rigid copper coaxial lines. The lengths and characteristic impedances of the lines are shown in Figure 3.29. The nominal bandwidth of these devices is about 7% for proper isolation.

### 3.8 TR-ATR Switch

The TR-ATR switch permits use of the same antenna and feed lines on both transmit and receive. It performs two functions: it keeps the high power transmit pulse off the receiver input during transmit and provides a  $Q = 100$  tank circuit on the receive portion of the duty cycle.

Since the feeder line is of the balanced type, one T/R switch is

ORIGINAL PAGE IS  
OF POOR QUALITY



## FINAL OUTPUT COMBINER NETWORKS

Figure 3.29 Final output combiner networks.

required for each line; since they are identical, only one is shown in Figure 3.30. Operation is as follows:

The TR tubes short the receive cavities during the transmit portion of the cycle. When shorted, each of the arms presents an effective open circuit to the transmitter; essentially all of the power, therefore, is conveyed to the antenna. When the TR tubes open (on receive) the arm closest to the antenna presents a tank-circuit-like appearance to the antenna; hence it is in effect a high Q filter. The other arm reflects a short to the junction where it connects to the feed line. This in turn reflects an open at the junction of the first arm, effectively isolating the transmitter from the antenna on receive, ensuring that all received signal is routed to the receiver. The TR-ATR switch assembly imposes two limits on the transmitter-receiver system: (1) The bandwidth of 400 kHz imposed on the received signal limits the minimum pulse length to about 6  $\mu$ sec, (2) The TR tube recovery time of about 400-600  $\mu$ sec minimum limits the minimum range to about 40 miles (65 km). This could be shortened further by adding water vapor to the tube fill, but this will decrease TR tube life. For details of the design, construction and maintenance of the TR switch see Allman and Bowhill (1976).

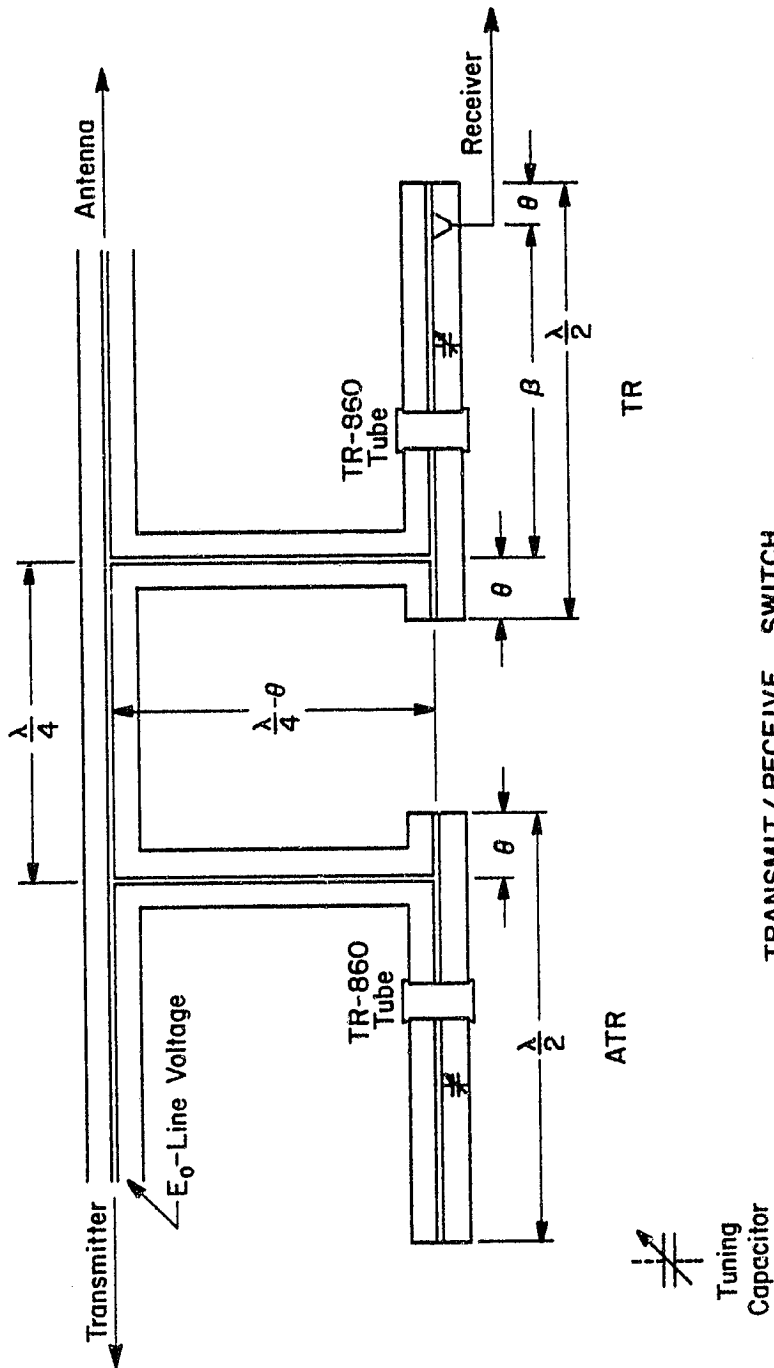
### 3.9 High Voltage and Bias Supplies

The high voltage supply consists of the 4 major units shown in Figure 3.31: an 87 KVA primary supply transformer followed in turn by the high voltage rectifiers, a 10 Henry choke, and a capacitor bank.

The 87 KVA primary supply transformer has variable output voltages, changed by selecting a switch position and either a Y or Delta connection. The possible combinations of switch position, connection, and output voltage are tabulated in Table 3.3.

ORIGINAL PAGE IS  
OF POOR QUALITY

(One of Two)



TRANSMIT/RECEIVE SWITCH

Figure 3.30 T/R switch diagram.

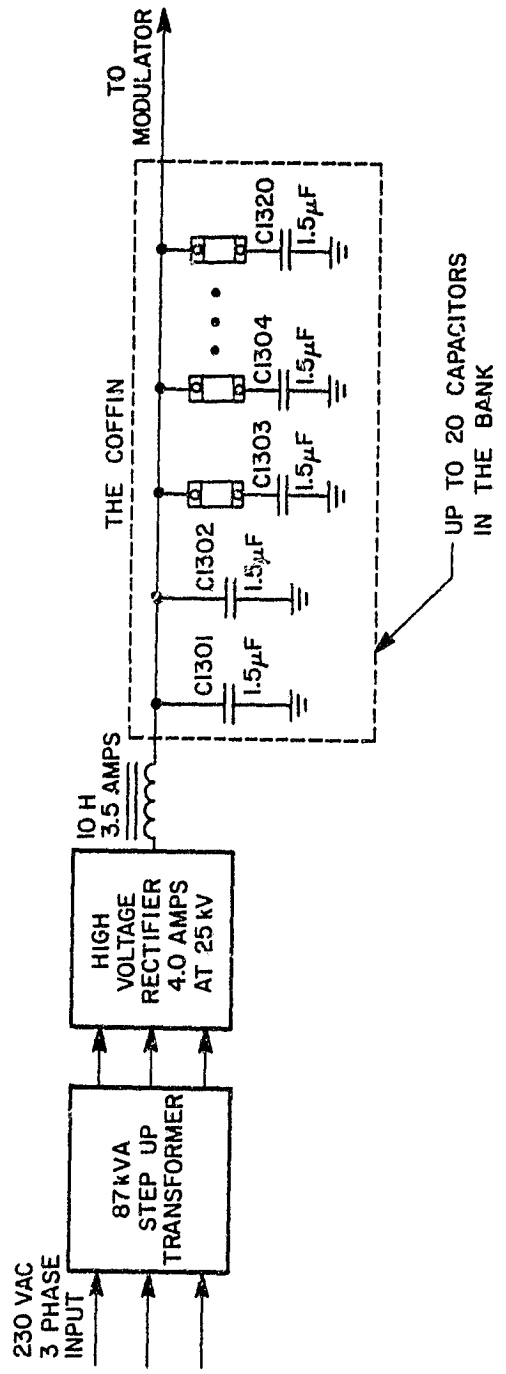


Figure 3.31 25-kV power supply block diagram.

Table 3.3 87 KVA plate supply taps.

Primary Tap Position	Secondary Delta Connection Output	Secondary Y Connection Output
1	7,200 V	12,456 V
2	8,300 V	14,359 V
3	9,170 V	15,864 V
4	10,000 V	17,320 V
5	10,900 V	18,850 V

The high voltage rectifier is rated at 4.0 amps. The circuit now in use is shown in Figure 3.32. The original rectifier tubes have been replaced by Westinghouse diode stacks, but the original ballast resistors are still in place.

The 3.5 amp rating of the 10 Henry choke is one of the primary factors limiting extension of the duty cycle.

The capacitor bank contains 20 large 1.5  $\mu$ F capacitors in a large horizontally mounted box. For normal use only two are connected, but for long pulses more must be added. The switches involved in adding capacitors are spring loaded and function as fuses; if one capacitor shorts, overall operation should not be affected.

The high voltage supply delivers 16 - 25 KVDC at 3.5 amp to the modulator.

The bias supply for units 3 and 4 is located in the same cabinet with the high voltage rectifier, and is also shown in Figure 3.32. It provides rectified and filtered bias voltage to the grids of the ML-5682s. Unfortunately there is presently no way to bias unit 3 and unit 4 differently.

### 3.10 The Modulator

The modulator currently used in the Urbana Radar was originally designed (see Martin-Vegue, 1961) to deliver 16 MW pulses at a duty factor of .004, with output voltages selectable from 30-50 kV (specifications are given in Table 3.4). This is, one might suspect, a bit much for a radar transmitter rated at 4-6 MW peak power output. No significant changes have been made to the initial design of this unit.

A simplified schematic of the modulator is shown in Figure 3.33. V601 is a simple pulse amplifier circuit built around an 807 tetrode. This stage has its own plate and bias supply shown in Figure 3.34(a). V602 is also a

ORIGINAL PAGE IS  
OF POOR QUALITY

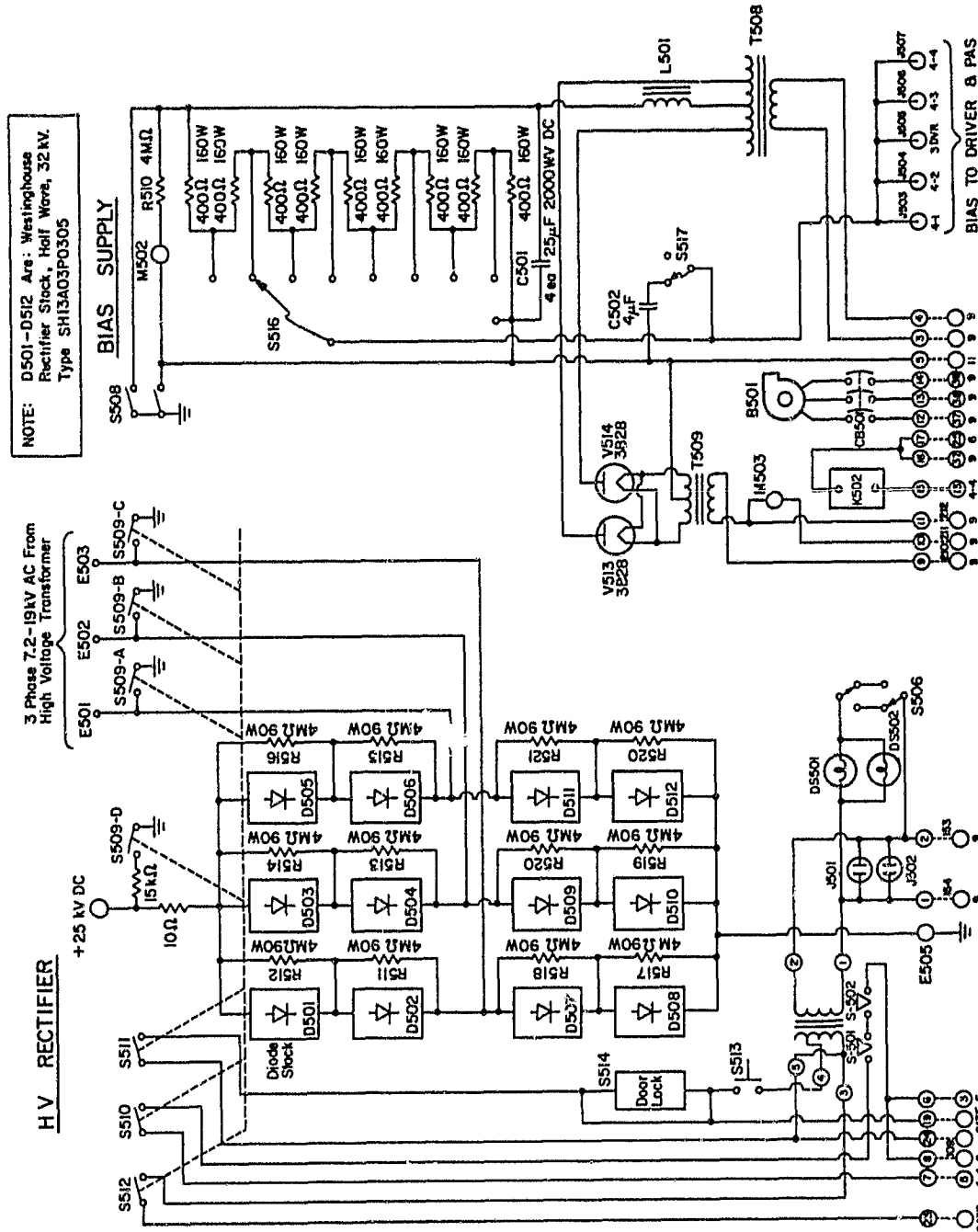


Figure 3.32 25-kV power supply and bias supply for units 3 and 4 circuit diagrams.

Table 3.4 Modulator specifications.

Peak output power	16 MW
Pulse length	3 - 100 $\mu$ sec
Duty cycle	.004 nominal
Droop	10% maximum
Input pulse	shaped +15V pulse provided by V1101
Output voltage	15 - 48 kV pulses
DC supply	16-24 kV
AC supply	220 VAC
Rise time	3 $\mu$ sec with T617B & T618B 8 $\mu$ sec with T617A & T618A

ORIGINAL PAGE IS  
OF POOR QUALITY

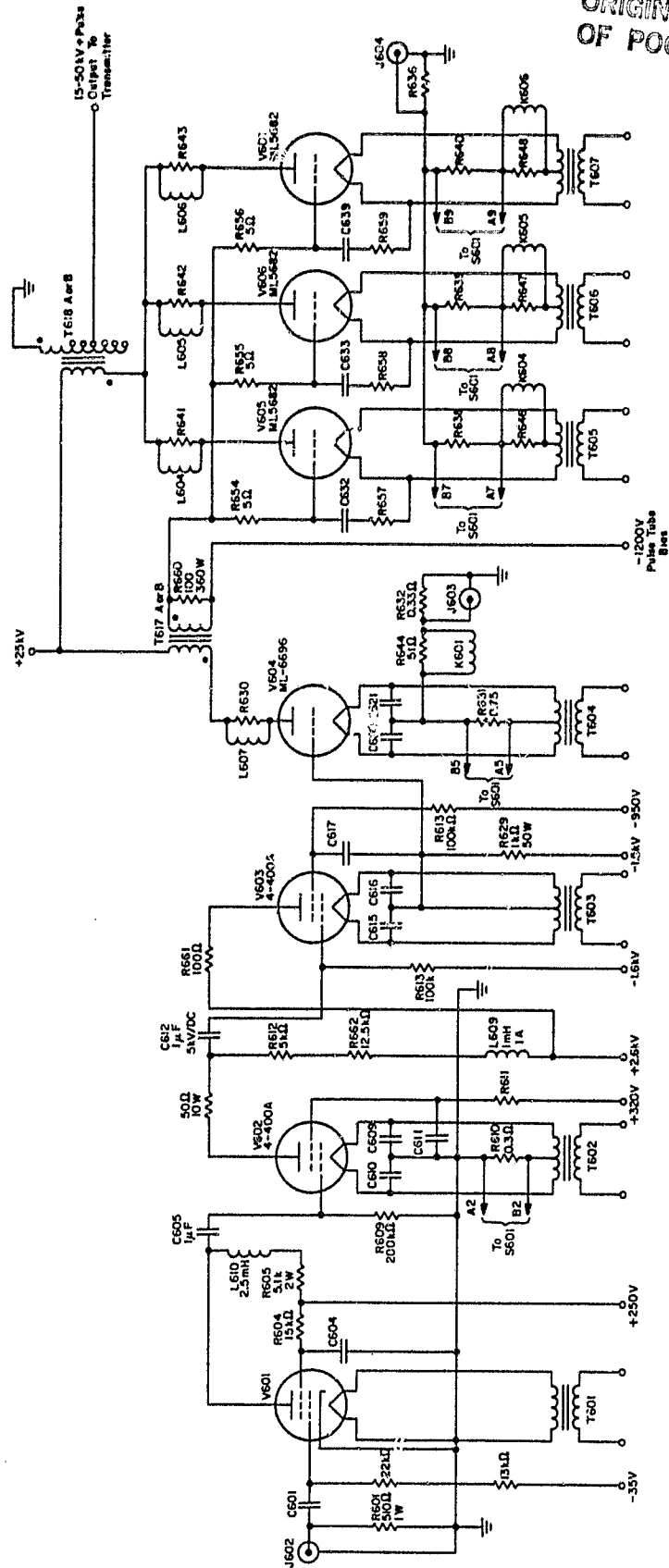
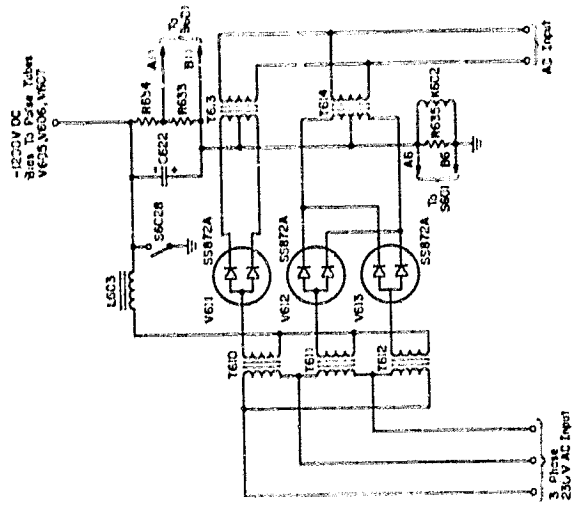
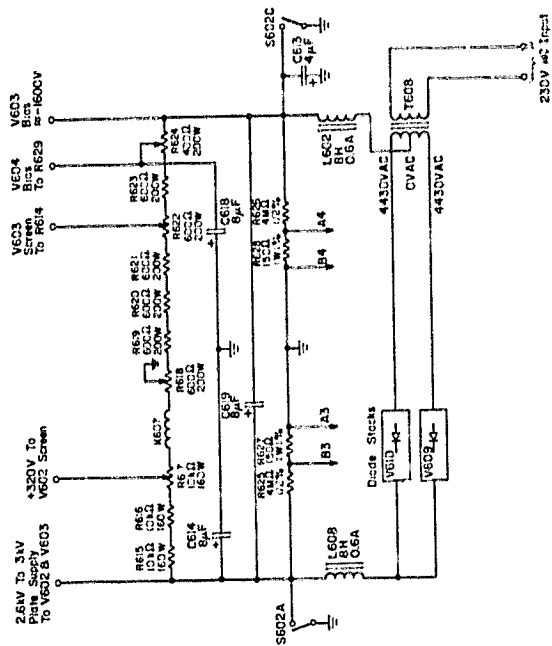


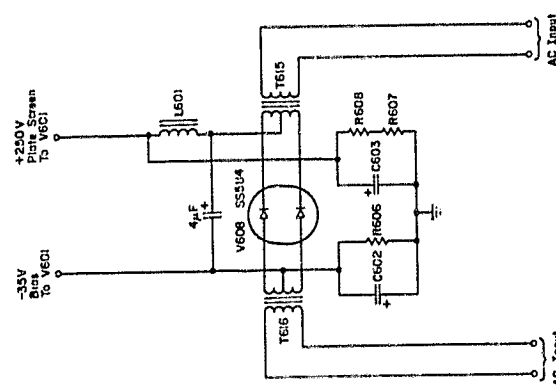
Figure 3.33 Modulation simplified schematic.



(a)



(b)



(c)

Figure 3.34 Modulator power supplies (a) supply for V601; (b) supply for V602, V603, and bias for V604; (c) bias supply for V605, V606, and V607.

pulse amplifier, designed around an Eimac 4-400A tetrode. This is the only stage which is normally conducting in the modulator. In addition one should point out that the rise time of the modulator is somewhat limited by the time constant of the plate circuit.

The third stage consists of a 4-400A in cathode-follower configuration. This choice was dictated by the input capacitance of the following stage. Note the direct connection between the cathode of V603 and the grid of V604. This is made possible by the power supply shown in Figure 3.34(b).

V604 is an ML-6696 Machlett pulse triode in a typical pulse amplifier circuit. The output of stage four is transformed by T617 and applied to the paralleled inputs of V605, V606, and V607, all ML-5682 8 MW pulse triodes. These inputs are bootstrapped to increase the input impedance and improve rise time. R546, R565, and R566 are parasitic suppressors in the grid circuits. More suppressors in the form of parallel R-L networks are present in each plate load. -1200V bias is supplied through T617 from the supply in Figure 3.34(c).

The output of the final stage is taken from the output pulse transformer T618, which has a tapped secondary for various output pulse voltages. T617 and T618 are actually each present in two versions; T617a and T618A are for long pulses -- 10  $\mu$ sec to 100  $\mu$ sec or longer. T617B and T618B are for short pulses -- 3 to 10  $\mu$ sec. The output connections for various desired voltages are shown in Tables 3.5 and 3.6.

One difficulty which has arisen in the operation of T618 is the very large backlash present in the modulator. This has been alleviated somewhat through the use of a shaped pulse -- with short rise time and long fall time characteristics as the input to stage 1. The pulse shaper circuit is shown

Table 3.5 T618 output connections.

Assume Primary Pulse = 21 kV

Secondary Voltage Desired	Required Terminal Connection
50 kV	3 to 10
45 kV	4 to 10
40 kV	5 to 10
35 kV	6 to 10
30 kV	7 to 10
20 kV	output to 9 only

Table 3.6 T617 internal connections.

Primary Input Pulse Voltage	Internal Connection	Output Voltage
16 kV	3 to 7	3 kV
18 kV	4 to 7	3 kV
20 kV	5 to 7	3 kV

in Figure 3.35.

Figure 3.36 shows the three ML-5682 switch tubes used in the modulator output and the ML-6696 driver stage (the smaller tube in the back). Clearly shown are the parasitic suppressors and the large straps required for current distribution.

Figure 3.37 depicts the cabinet containing the first four modulator stages and their respective power supplies.

The ML-6696 and all the ML-5682 triodes are water cooled devices which receive their cooling water from a heat exchanger at 18 gal/min @ 40 psi. Interestingly enough, none of these devices are operated anywhere near their dissipation limits; a larger duty cycle could be achieved through use of a 25 kV power supply with more current output.

### 3.11 Timing and Control

The basic timing diagram of the Urbana Radar is shown in Figure 3.38. This describes the various functions which are controlled by the radar director. Currently, the radar director is either a FORTH program resident in an Apple II plus computer, or a hardware device documented in Hess and Geller (1976). However, the hardware device does not possess phase control capabilities. Since the thrust of this project involves phase coding the hardware director is not discussed here.

Figure 3.39 shows how the various commands generated by the FORTH program are transmitted. The commands generated in the Apple II plus computer are sent to the John Bell interface card, which is actually located in slot 7 of the Apple. It is shown as a separate unit here for emphasis and convenience. Port 2 of the John Bell card is connected through a 16 Pin Dip Header plus and ribbon cable to the interlock and high current adaptor.

The interlock and high current adaptor provides three functions:

ORIGINAL PAGE IS  
OF POOR QUALITY

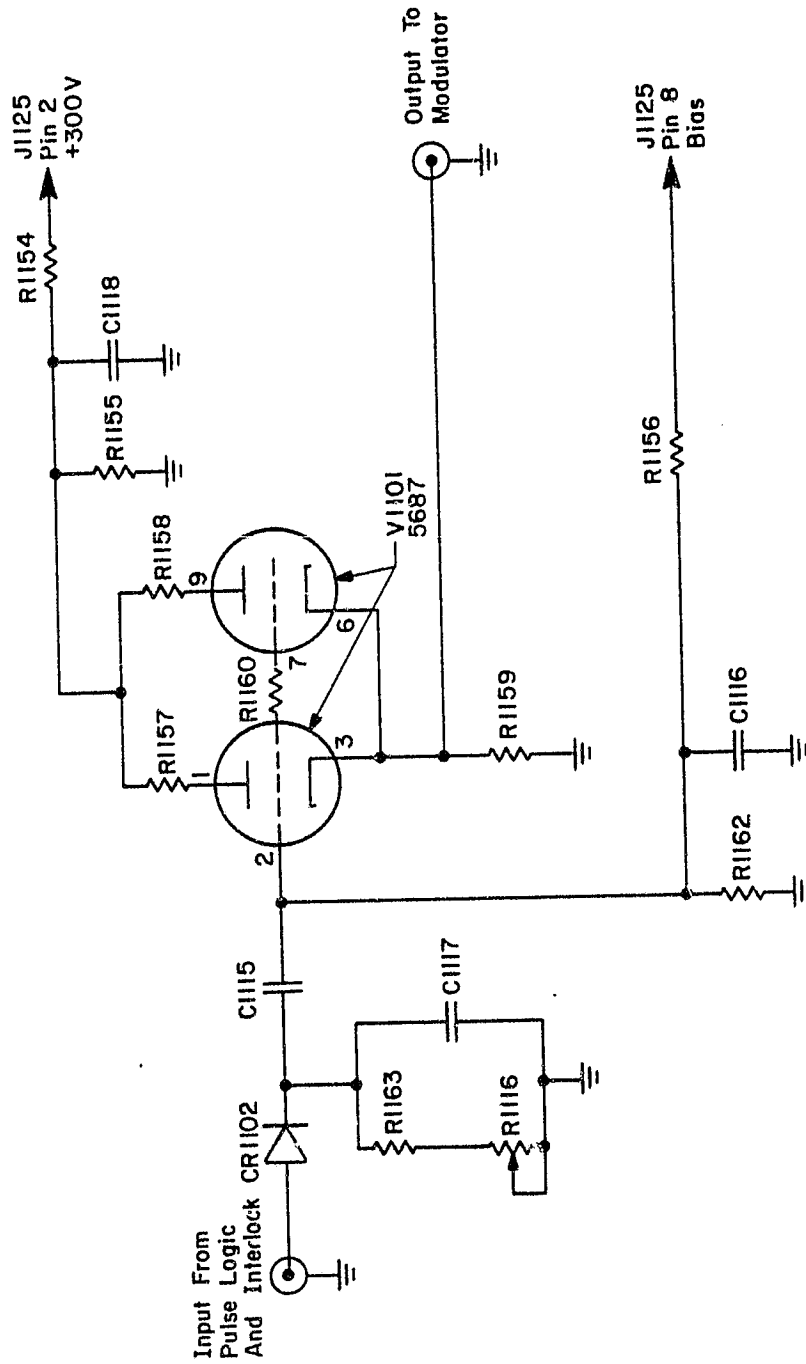


Figure 3.35 Pulse shaper circuit diagram.

ORIGINAL PAGE IS  
OF POOR QUALITY

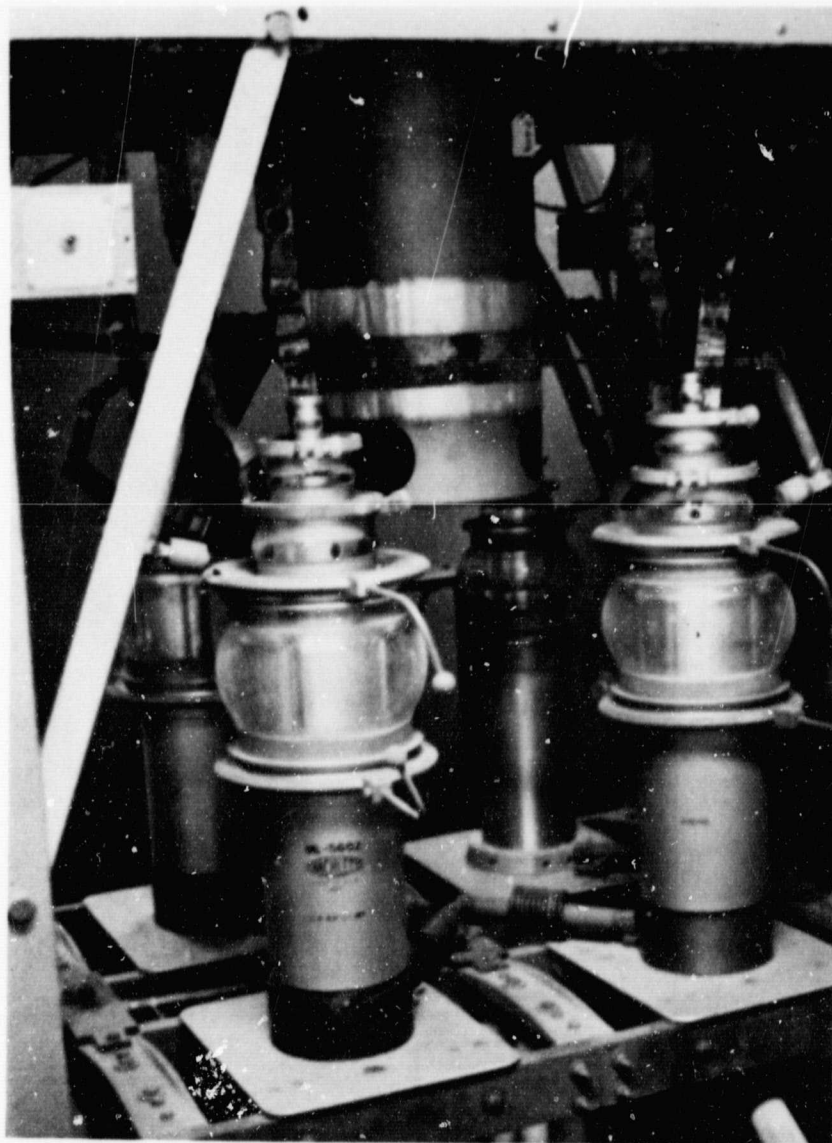


Figure 3.36 Picture of V604, V605, V606, and V607.

ORIGINAL PAGE IS  
OF POOR QUALITY

77

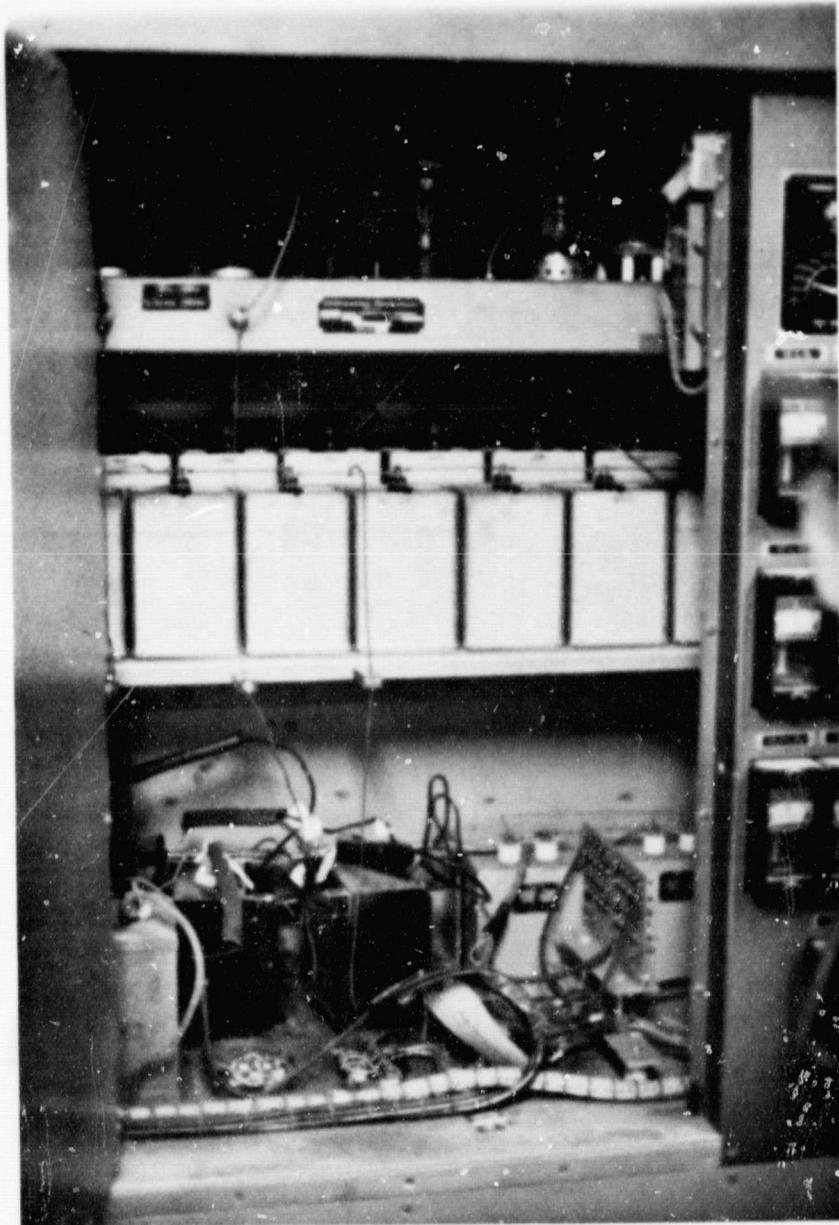


Figure 3.37 Modulator chassis layout.

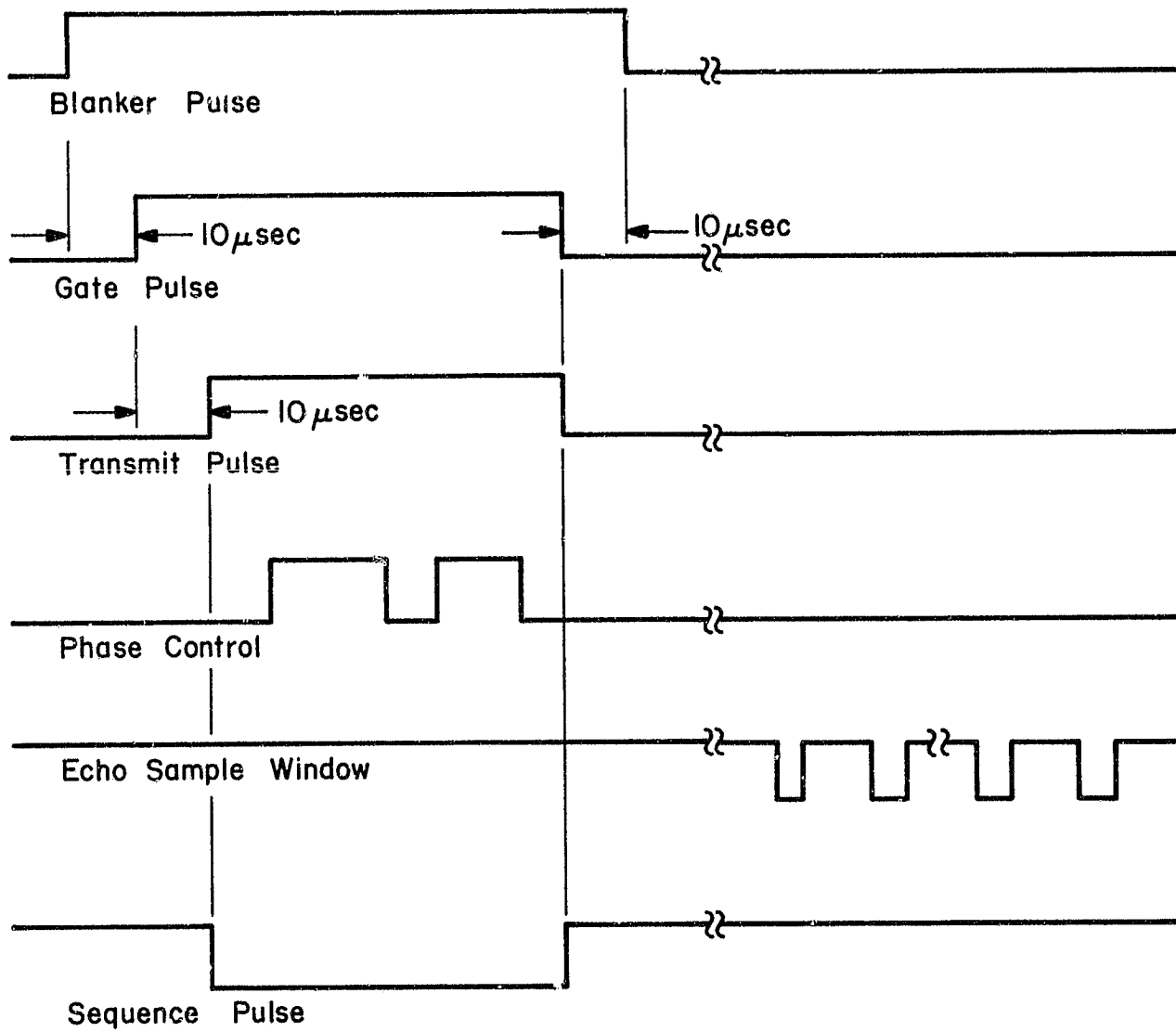
ORIGINAL PAGE IS  
OF POOR QUALITY

Figure 3.38 Radar timing diagram.

ORIGINAL DOCUMENT  
OF JOHN BELL

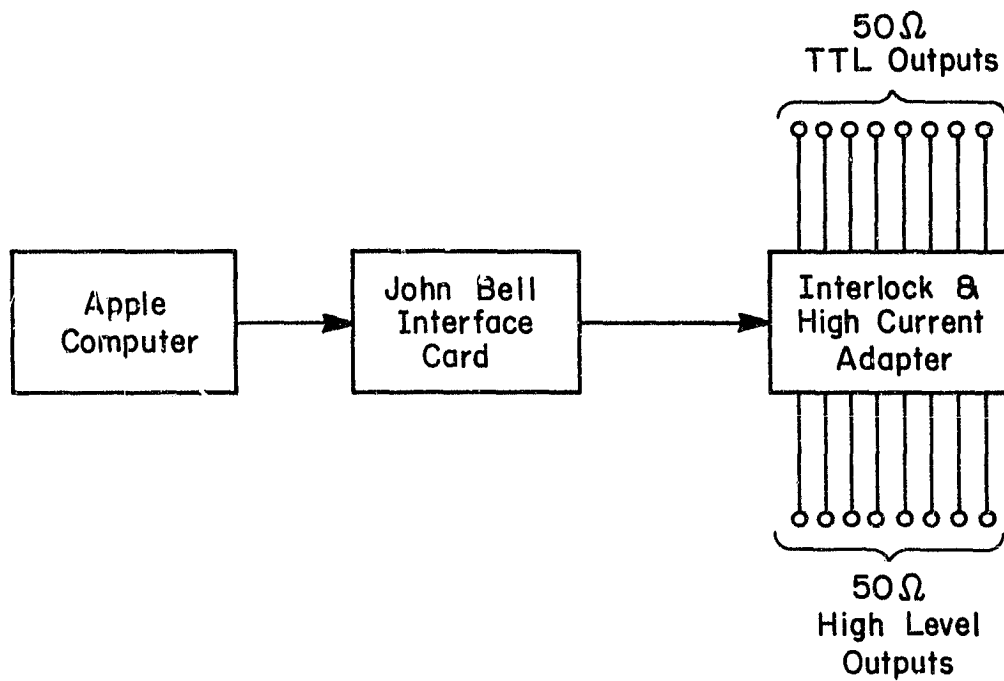


Figure 3.39 Apple radar director block diagram.

(1) it interlocks the blanker, gate and transmit control lines to protect the transmitter and receiver systems; (2) it provides a  $50\ \Omega$  TTL compatible output for each control line capable of driving a large number of loads; and (3) it provides a +12V  $50\ \Omega$  for each control line for driving high level lines into the high interference environment of the transmitter room. The schematic of this device is shown in Figure 3.40.

Referring again to Figure 3.38, we wish to describe the sequence of normal operations of the transmitter: First, the blanker is to protect the sensitive receiver system preamp during the transmit cycle.

Next, the gate pulse causes the RF signal to be generated, amplified, and applied to the grid of the 4CX5000A (unit 2). Please note that the 40.92 MHz signal is generated in a binary fashion such that it only exists during the gate pulse; this prevents the oscillator from interfering with the sensitive receiver system during the receive portion of the cycle.

Next the transmit pulse is generated and applied to the logic and interlock module. If transmitter conditions permit, the signal is then routed to the pulse shaper, and from there to the modulator where it energizes the three final stages of the transmitter and puts the RF pulse on the air. Note that the delay between the start of the gate pulse and the start of the transmit pulse protects the 4CX5000A stage from flash arc damage.

The phase control pulse will change the phase of the transmitter by  $180^\circ$  each time it changes state. Please note that the pattern of these changes and the overall length of the blanker, gate, transmit, and phase control pulses are functions of the program and are hence easily modified for different experiments.

The echo sample window and the sequence pulse control the analog to

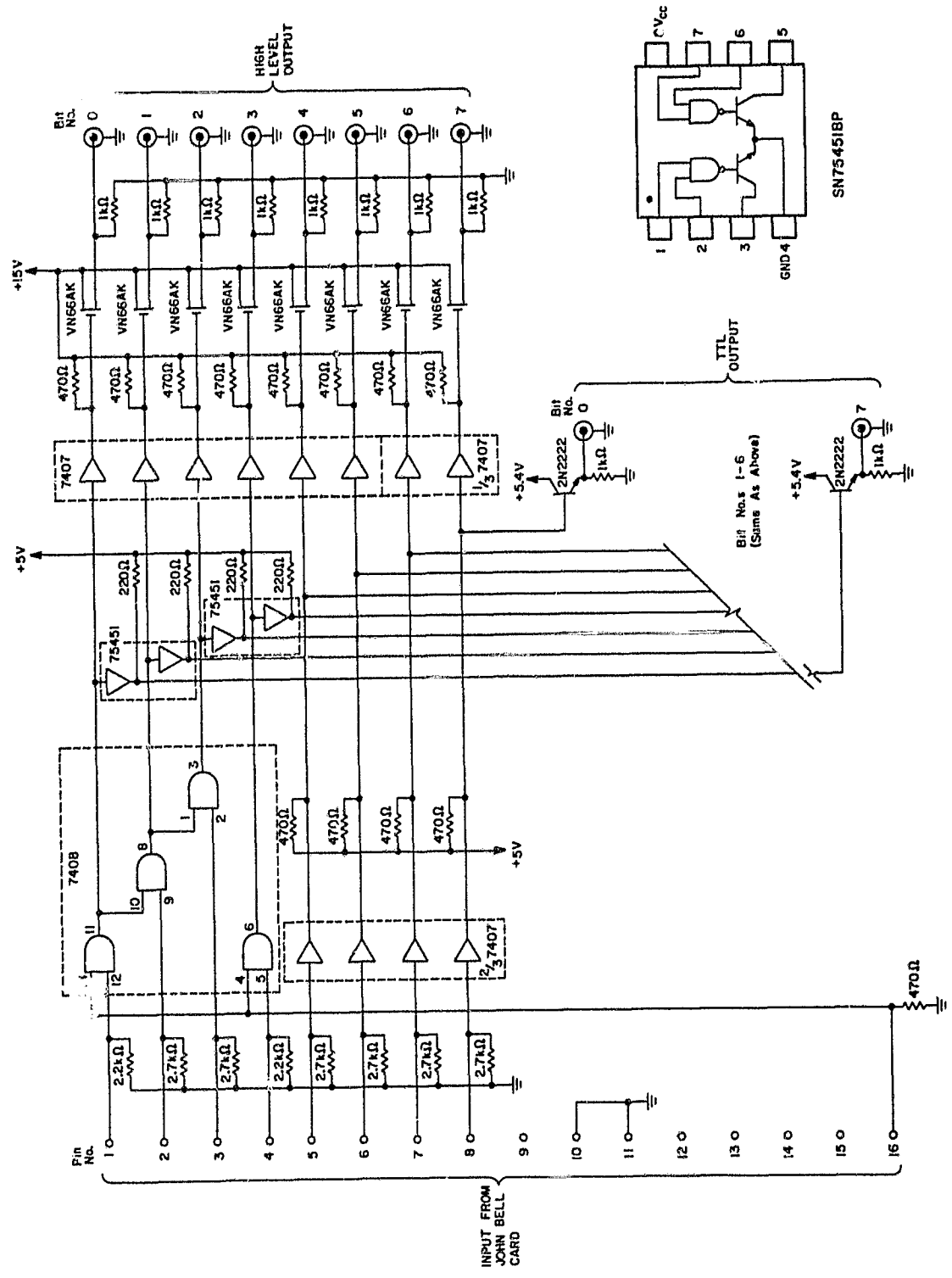


Figure 3.40 Interlock and high current adaptor circuit diagram.

digital converter used to sample the data. The sequence pulse is used to select the channel and the echo sample window selects the various ranges sampled during the receive cycle.

Figure 3.41 is the circuit diagram of the logic and interlock module shown in block form in Figure 3.1. The rectified output of the transmitter is amplified by the circuit in (a), then applied to the pulse integrator in (c). The rectified output of the 814 amplifier is amplified by the circuit in (b) then added in (c) to permit an output. The logical functions of parts (a), (b), (c) and (d) are illustrated in the block diagram of Figure 3.42.

Figure 3.43 details the construction of the interlock and high current adaptor diagrammed in Figure 3.40. Part (a) shows the logic control board. Part (b) shows the mounting of the line driver transistors and the rest of the major units. Part (c) shows the front panel of the completed device.

### 3.12 The Receiving System

The receiving system is summarized in this section and key elements are described.

The block diagram of the receiving system is shown in Figure 3.44. A coaxial T-combiner network combines signals from both halves of the antenna and applies them to the blanker. The blanker has the function of removing the transmit pulse RF and associated transients not removed by the T/R switch; it is constructed with PIN diodes shown in Figure 3.45, and its drive circuitry is shown in Figure 3.46. The output of the blanker is applied to the preamplifier, the specifications of which are given in Table 3.7. Essentially this is a wideband low noise device. The blanker and preamplifier are located in the same chassis and physically mounted in the T/R switch shed.

The important characteristics of the receiver are its IF bandwidth,

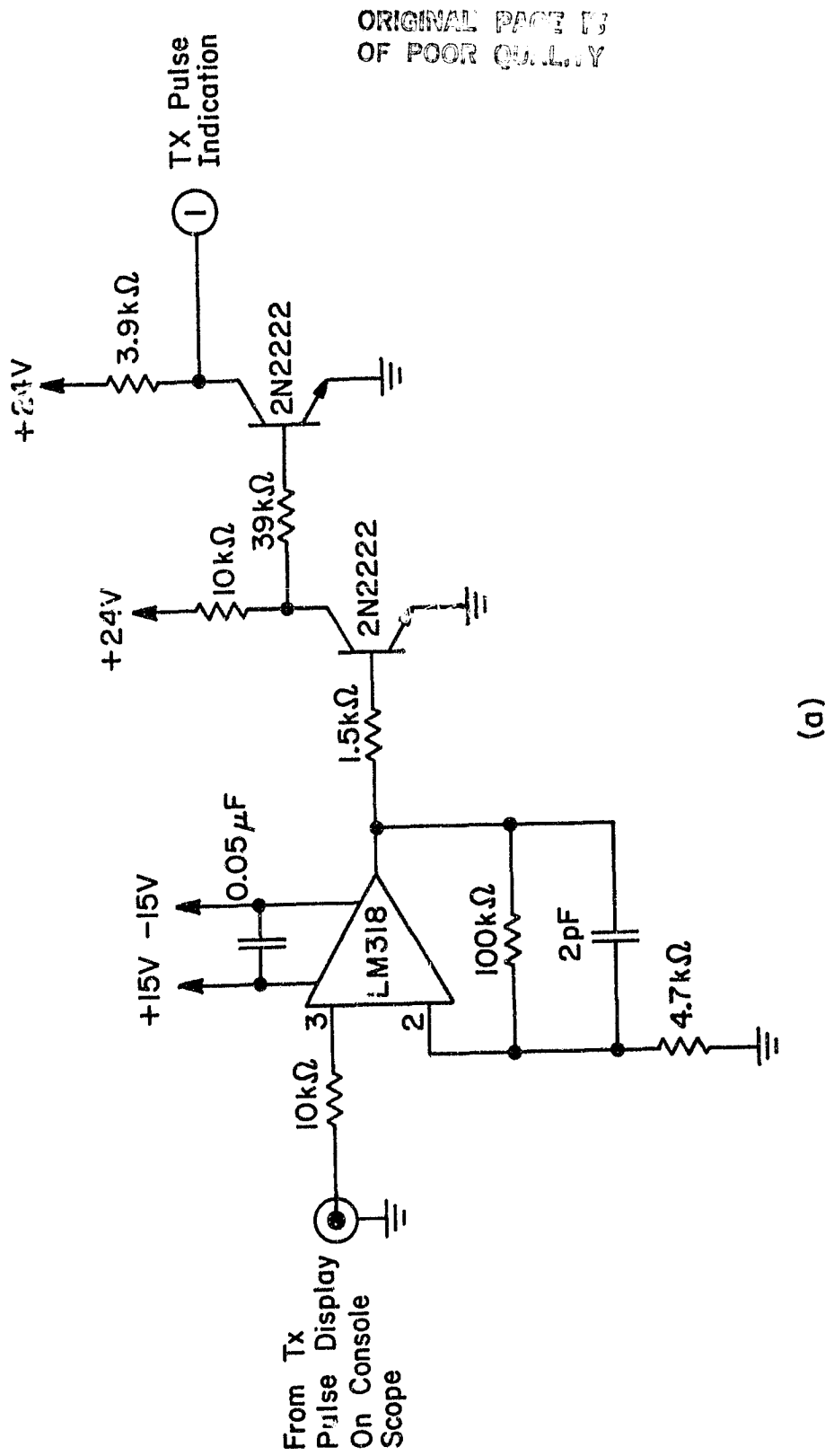
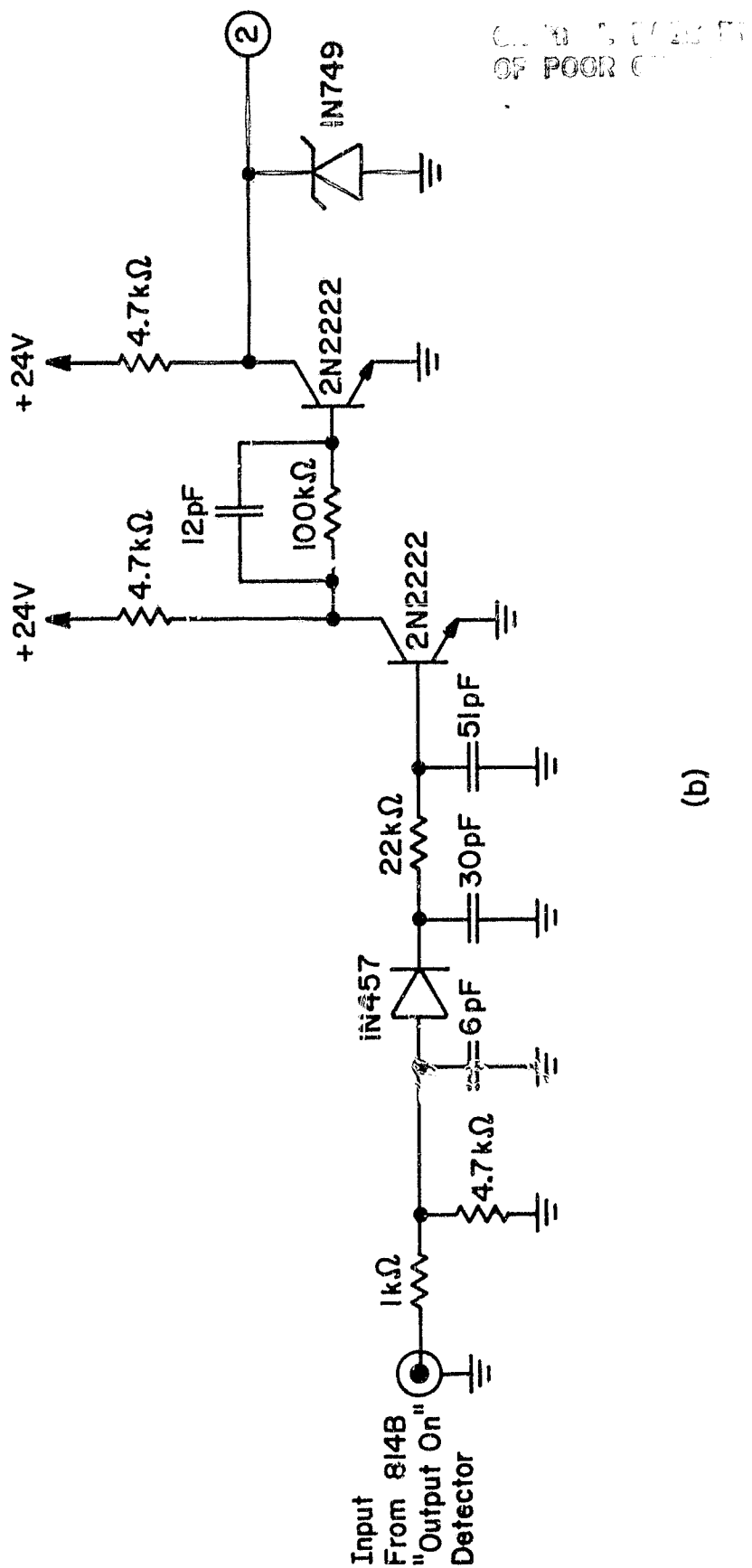


Figure 3.41 Logic and interlock module (a) transmitter output detector (b) "814 OUTPUT ON" amplifier (c) pulse length control, duty cycle exceeded tester, and TX output present tester circuits and (d) RF gate pulse control.

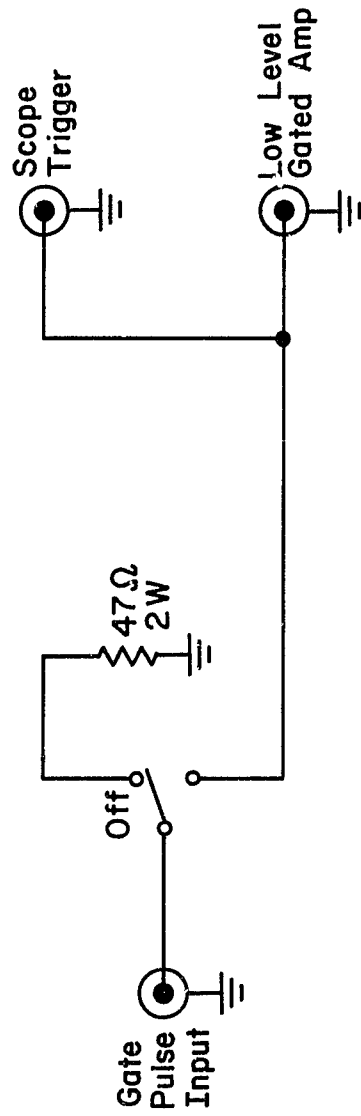


(b)

Figure 3.41 Continued.



ORIGINAL PART IS  
OF POOR QUALITY



(d)

Figure 3.41 Continued.

ORIGINAL PAGE IS  
OF POOR QUALITY

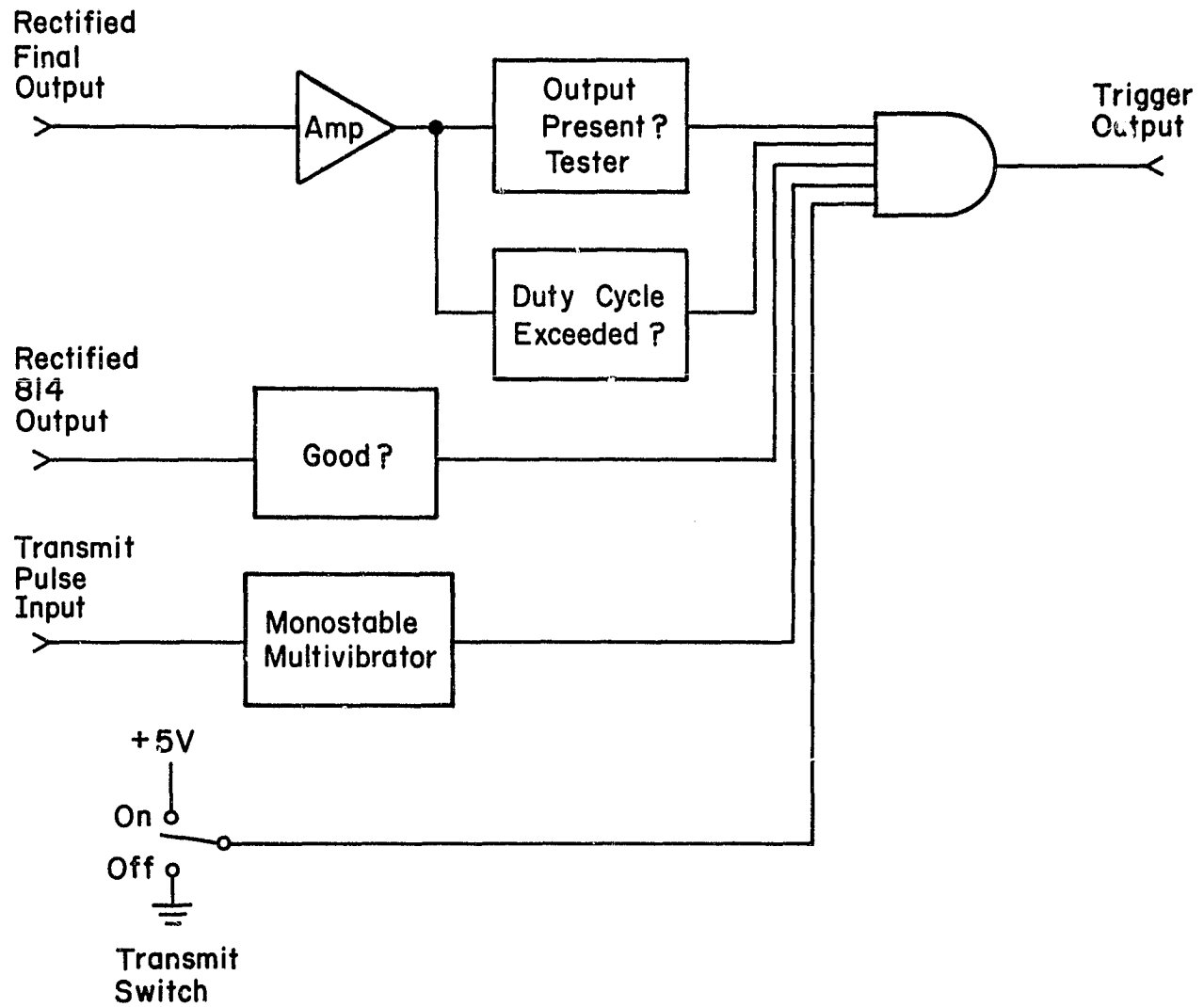
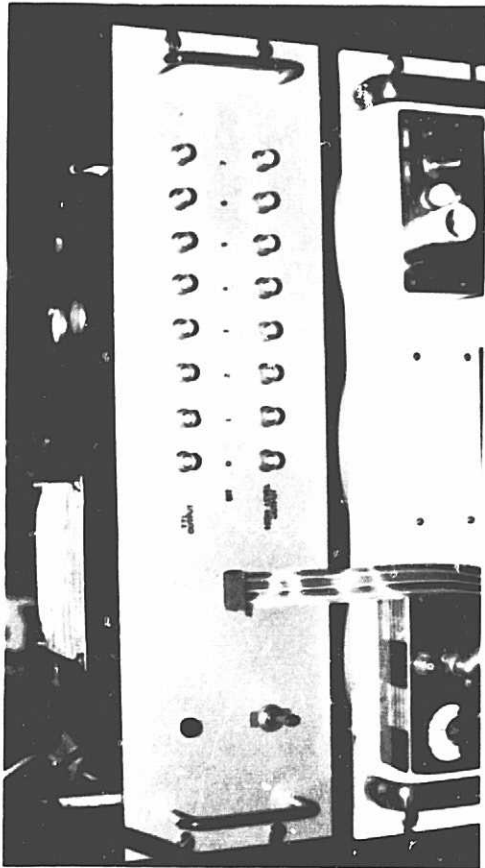
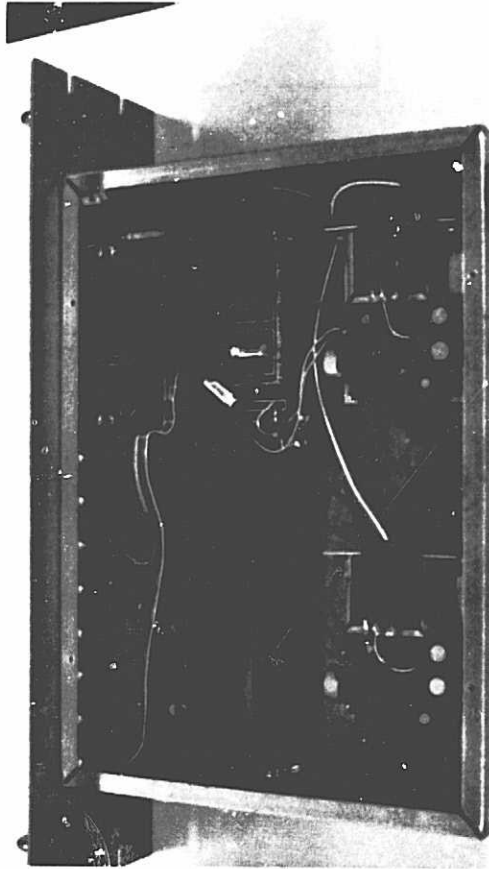


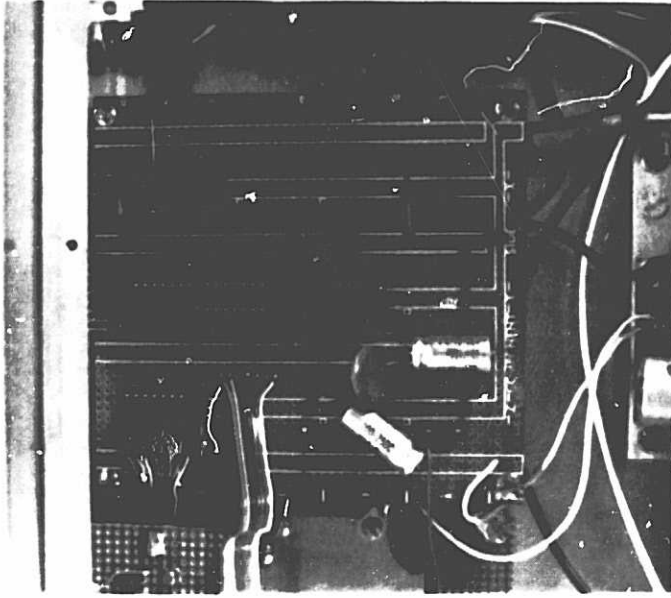
Figure 3.42 Equivalent logic of Figure 3.41 (c).



(a)



(b)



(c)

ORIGINAL PAGE IS  
OF POOR QUALITY

Figure 3.43 Pictures of the interlock and high current adaptor.  
(a) front panel (b) chassis layout (c) logic board layout.

2

1

ORIGINAL PAGE IS  
OF POOR QUALITY

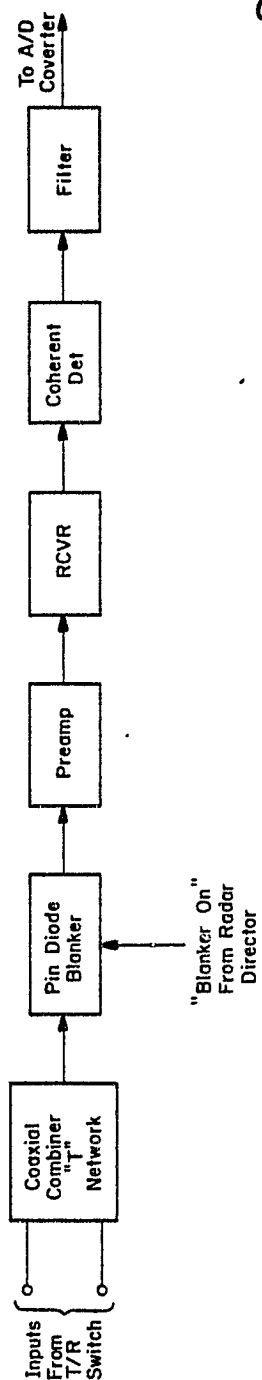
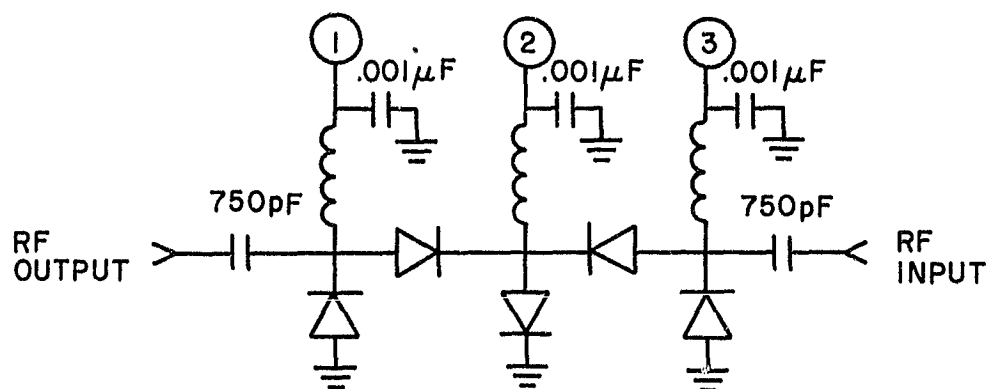


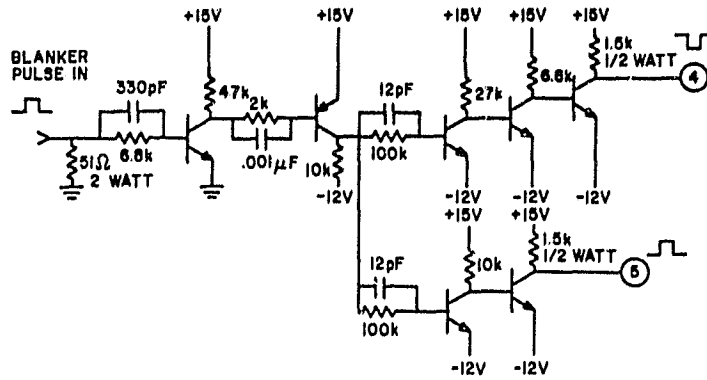
Figure 3.44 Receive system block diagram.

ORIGINAL PAGE IS  
OF POOR QUALITY



PIN DIODES ARE UNITRODE UM 9401  
COILS ARE T30-6 CORES WITH  $\sim$  40 TURNS # 34 WIRE  
(RESONANT AT 41 MHz)

Figure 3.45 PIN diode blanker.



ALL NPN TRANSISTORS ARE 2N2222  
ALL PNP TRANSISTORS ARE 2N1131

ORIGINAL PAGE IS  
OF POOR QUALITY

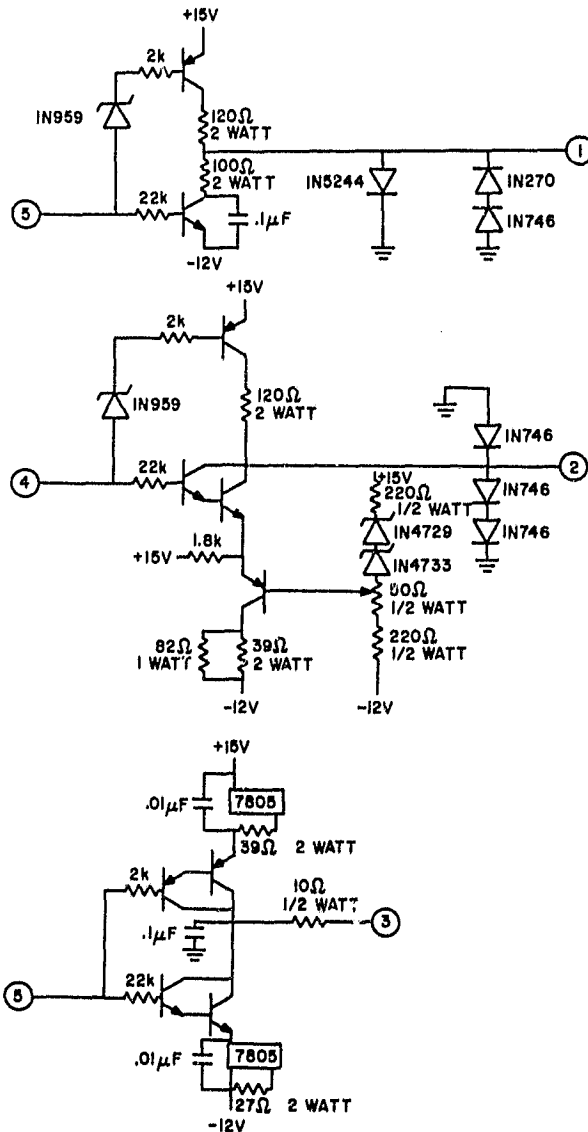


Figure 3.46 Drive and control circuitry for the PIN diode blanker.

Table 3.7 Characteristics of the preamplifier in the Urbana Radar receiving system.

Frequency range (MHz)	5-110
Noise figure max (dB)	1.7
Gain min (dB)	22
P min @ 1 dB comp (dBm)	+9
Gain flatness ( $\pm$ dB)	0.5
Intercept point (dBm)	+22
VSWR max in unitless	2.0
VSWR max out unitless	2.0

which is about 250 kHz, its passband shape, which is approximately Gaussian, and its IF output of 5.5 MHz. This IF output is coherently detected by the device shown in Figure 3.47, the outputs of which are filtered (if required) and channeled to the analog-to-digital converter.

### 3.13 Suggestions for Improvements

The Urbana Radar Transmitter was never fully developed to its fullest capacity. This leaves many areas where refinement would be of great interest. Only a few of these are listed below.

1. Due to advancements in solid-state switch technology, the first three stages of the modulator could now be replaced with a single stage or perhaps two stages of power MOSFET devices. Two alternate versions are shown in Figure 3.48(a) and (b). This would permit two improvements: greater electrical efficiency and improved rise time.

2. Currently the modulator output is distributed to units 2, 3, and 4 via RG-17 coaxial lines. The resonance of these lines and the secondary of the modulator output transformer cause envelope distortion of the transmitted RF pulse. This could be reduced by going to a high impedance twin lead distribution system.

3. The 814 linear amplifier is now replaceable with a solid-state device having superior characteristics, specifically wider bandwidth. This would enhance reliability and resolution of the transmitter. At the time of writing, the 814 linear amplifier shows need of either a major overhaul or outright replacement of the tuning sections, both input and output. Difficulties have been encountered during tuning which result from intermittent operation of these circuits.

4. The control and monitoring console needs to have each monitoring function tested and overhauled or re-designed. The simple vacuum-tube

ORIGINAL PAGE IS  
OF POOR QUALITY

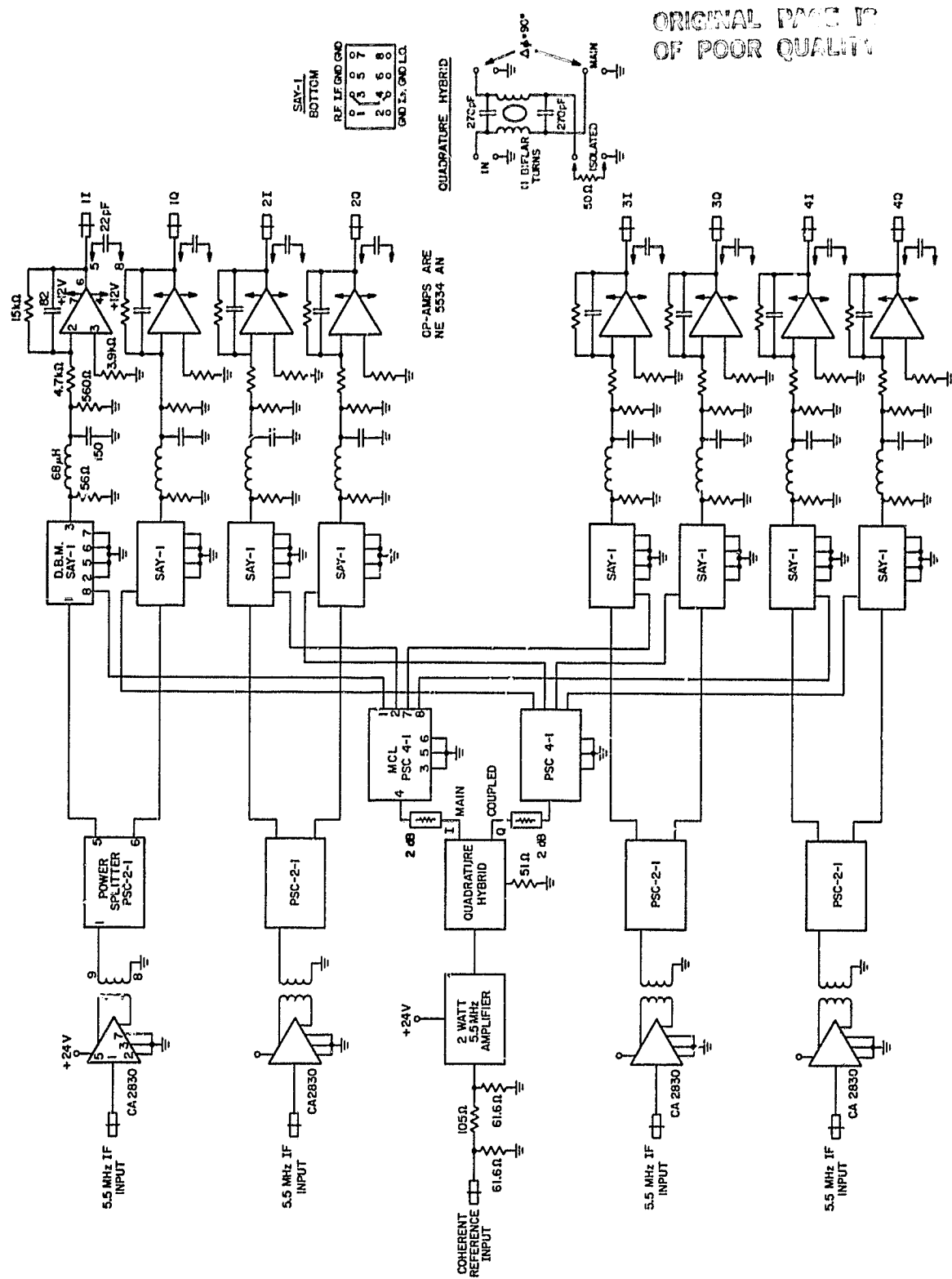


Figure 3.47 Phase detectors used by the coherent-scatter radar and meteor radar.

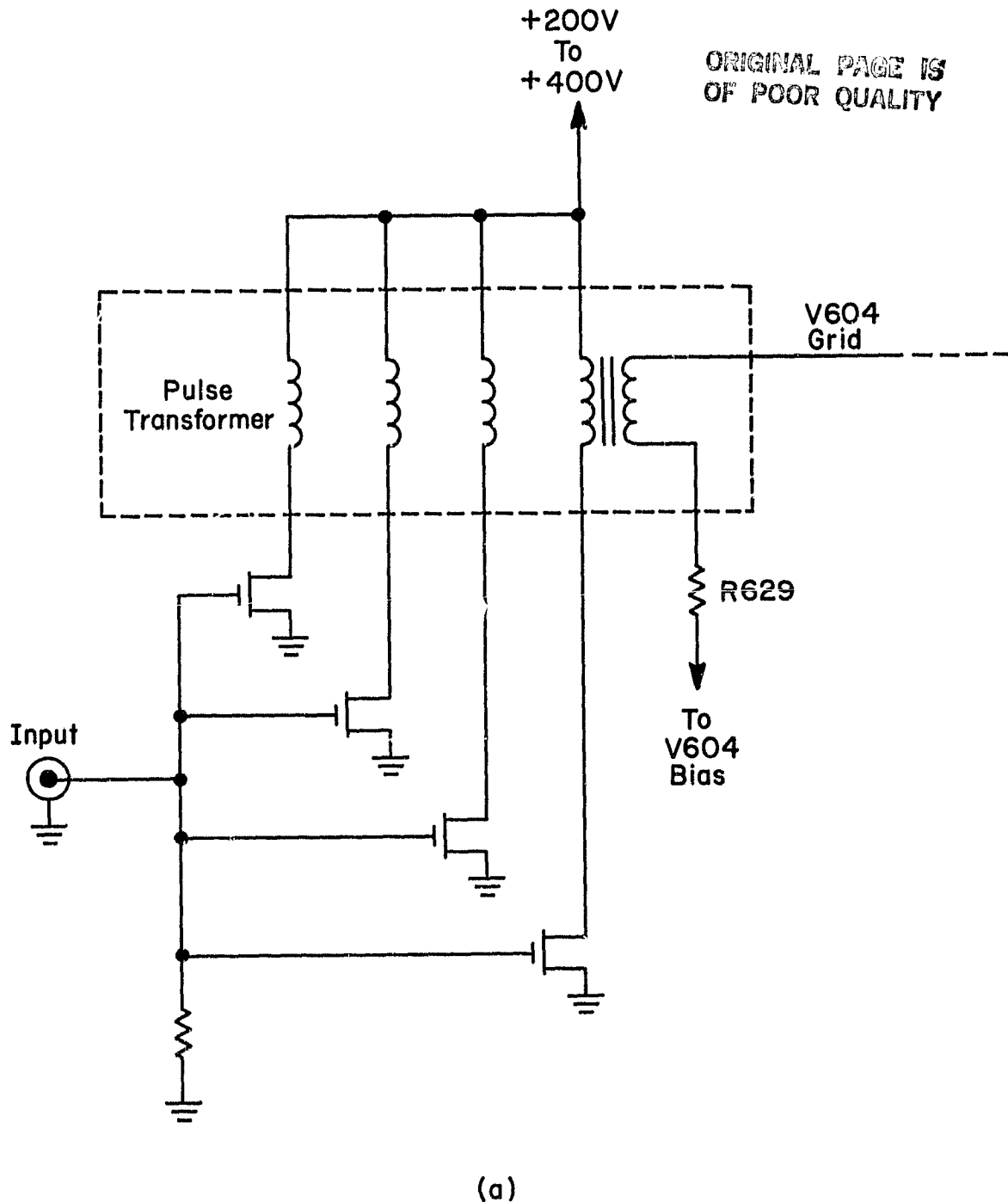


Figure 3.48 (a) and (b) Two methods to improve modulator efficiency and rise time.

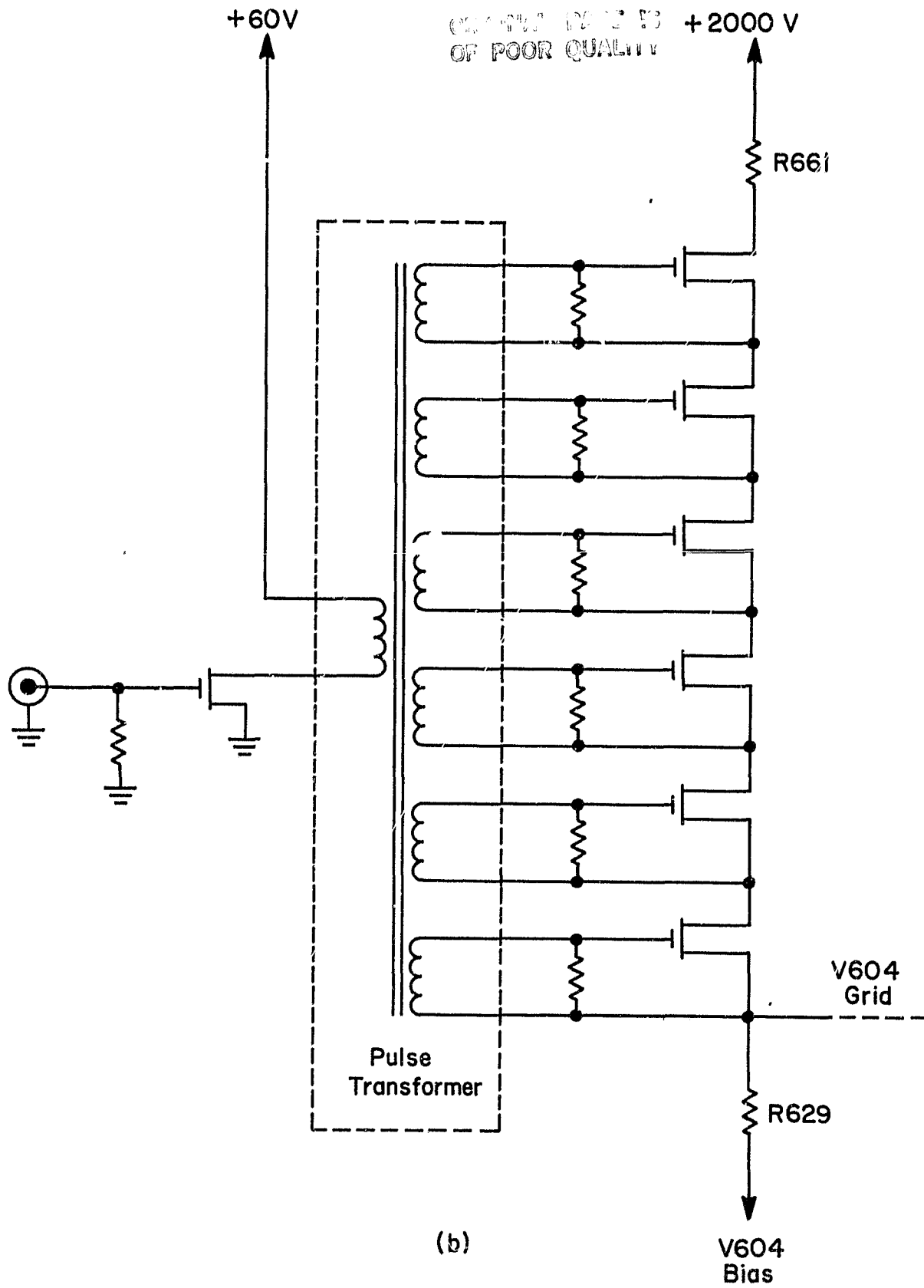


Figure 3.48 Continued.

differential amplifiers and vacuum-diode sensing units should be replaced with more reliable and economical solid-state devices; a phase monitoring system should be added to facilitate tuning.

5. Arrangements should be made to permit operation of the 4CX5000A and driver into  $50\Omega$  loads to facilitate proper tuning. Currently there exists too much interaction between stages to permit the operator to ascertain proper tuning from the monitor console. Addition of this capability should control this problem.

### 3.14 Summary

This chapter has been an analysis of the Urbana Radar. The approach has been a stage-by-stage intended to provide enough understanding to facilitate its use by future engineers and scientists.

## 4. DESIGN CONSIDERATIONS FOR THE URBANA RADAR

### 4.1 Introduction

Of primary importance in the design of any instrument is the phenomena which it is intended to measure. In the case of a radar transmitter, the transmitted waveform is designed to optimize the expected return. Its period, frequency, waveshape, and modulation characteristics comprise a statement concerning the present state of knowledge of the target. The final choice of a waveform suggests how closely we can devise circuits and make wise compromises in the approach to an ideal in our search for increasing accuracy in measurement. In the first sections of this chapter, we deal with the general requirements for transmitting phase coded signals and in the latter discuss the limitations and compromises involved in actually transmitting them.

### 4.2 Frequency Selection

The earth's atmosphere has long been known to be comprised of several layers. Among these the E and F regions are frequently highly ionized and hence can reflect a large fraction of the energy below the plasma frequency. For HF communications it has long been a practice in propagation studies to measure or compute a MUF or maximum usable frequency based on the need for point-to-point communications. Below the MUF radio waves may be reflected back to earth very little attenuated. For study of the mesosphere, which is only lightly charged if at all, and to be able to sense the small changes in  $\epsilon$  caused by turbulence one must therefore select a transmitter frequency conveniently above the MUF such that the E and F regions are transparent, and any energy not reflected from the mesosphere is conveniently "lost"; unable to return and confuse measurements. The 40.92 MHz transmitter

frequency assigned to the Urbana transmitter is above the MUF in the main lobe of the antenna; however, this is not always the case for hypothetical sidelobes, and observations substantiate this.

#### 4.3 Bandwidth Criteria

A phase modulator similar to the one in the Urbana Radar may be modeled as shown in Figure 4.1, as a multiplier circuit. Since the phase modulator simply changes the phase of the carrier by  $\pm \pi$ , it is mathematically equivalent to the process of multiplication by  $\pm 1$ . Letting the modulating waveform be represented by  $m(t)$  and the carrier by  $c(t)$  we can then describe the output of the modulator by

$$s(t) = m(t) c(t) \quad (4.1)$$

and from the theory of modulation one would expect the spectrum of  $s(t)$  to be

$$S(w) = M(w) * C(w)$$

where  $S(w)$  = the spectrum of  $s(t)$

$M(w)$  = the spectrum of  $m(t)$

$C(w)$  = the spectrum of  $c(t)$

where  $S(w)$  would exhibit two sidebands but no carrier.

Since  $m(t)$ , the modulating waveform, will be one of a number of Barker codes or complementary codes, it is not practical to compute the spectrum for each possible  $m(t)$ . However, it is possible to compute an upper bound of sorts by assuming  $m(t)$  to be a square wave with a period of 12  $\mu$ sec, 6  $\mu$ sec being the minimum bit length available in the present configuration of the radar. We, therefore, can use Fourier analysis to write

$$m(t) = \frac{4}{\pi} \sum_{n=1}^{\infty} \frac{1}{2n-1} \sin\left[\frac{2\pi(2n-1)}{T} t\right] \quad (4.2)$$

where  $T$  = the period of the square wave.

ORIGINAL PAGE IS  
OF POOR QUALITY

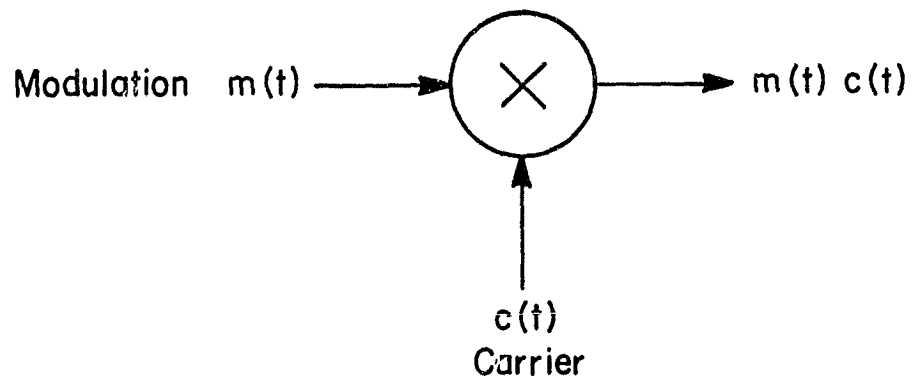


Figure 4.1 Mathematical model of the modulator in the Urbana Radar.

Now, assuming  $c(t)$  to be sinusoidal and of magnitude 1 we have

$$c(t) = \sin(\omega_0 t)$$

where  $\omega_0$  = the angular frequency of the carrier

then

$$s(t) = m(t) c(t) = \frac{4}{\pi} \sum_{n=1}^{\infty} \sin\left[\frac{2\pi(2n-1)}{T} t\right] \sin(\omega_0 t) \quad (4.3)$$

$$= \frac{4}{\pi} \sum_{n=1}^{\infty} \frac{1}{2n-1} \cdot \left\{ \frac{1}{2} \cos\left[\left(\omega_0 - \frac{2\pi(2n-1)}{T}\right)t\right] - \frac{1}{2} \cos\left[\left(\omega_0 + \frac{2\pi(2n-1)}{T}\right)t\right] \right\} \quad (4.4)$$

Now 4.4 is in a recognizable form. Each element in the spectrum of  $s(t)$  is represented by a magnitude term

R. |

$$M(n) = \frac{2}{\pi} \cdot \frac{1}{2n-1}$$

and two frequency terms

$$W(n) = \omega_0 + \frac{2\pi(2n-1)}{T} \quad \text{and} \quad \omega_0 - \frac{2\pi(2n-1)}{T}$$

Evaluating the magnitude terms we have

$$M(1) = \frac{2}{\pi} \cdot \frac{1}{1} = \frac{2}{\pi} = .637$$

$$M(2) = .212$$

$$M(3) = .127$$

$$M(4) = .091$$

Hence the fundamental plus the first 3 harmonics of  $m(t)$  contain 95% of the available transmitted power in the signal. For  $T = 12 \mu\text{sec}$  we then can state that if the transmitter bandwidth is 333 KHz or more it will transmit at least 95% of the power available from the modulator.

#### 4.4 Pulse Length Considerations

In a phase coded system the range resolution is determined by the bit

or baud length and equals  $c\tau/2$  where  $c$  = the speed of light and  $\tau$  = the baud length. For the case where  $\tau = 6 \mu\text{sec}$ , the minimum set by the equipment, the resolution corresponds to 900 meters.

Overall pulse length must be selected as a compromise involving the average transmitter power and the PRF, plus the desired compression ratio and the type of code being used. The maximum length is set by the equipment, though, and falls between 100 and 140  $\mu\text{sec}$ .

#### 4.5 Code Selection

Code selection must be governed by several variables. Among these are (1) the desired compression ratio, (2) the maximum available duty cycle, (3) the processing capabilities present, (4) the correlation time of the mesosphere, (5) the amount of integration to be used, and (6) aliasing. Longer codes will require longer pulses, forcing lower PRFs to keep within average power limits. Also, for the more complex codes the cycle time, (that is, the period from the beginning of the sequence of codes until it begins again) can approach or exceed the correlation time of the mesosphere. One good compromise might be transmission of a pair of complementary 16-bit codes, or perhaps a set of 8, 8-bit codes. For the former, the cycle time is about .02 seconds and about .04 seconds for the latter. However, increased complexity is involved in processing the longer codes; this in itself can become prohibitive.

Shorter codes, with shorter cycle times, are more prone to aliasing problems than the longer codes. In fact, one of the prime characteristics of the complementary codes is that the cross-correlation between the individual sequences of the pairs or sets is small; hence by their nature they tend to reduce aliasing problems.

Phase coding and integration are complementary techniques; however, in

practical use the designer is faced with a choice of how much pulse compression and how much integration to use during processing. Use of pulse compression techniques tends to reduce the amount of integration for which an improvement in signal-to-noise ratio may be had.

#### 4.6 Summary of Design

In equipment like the Urbana Radar, in which the required output is so high, the normal method of procedure is to amplify a signal through a series of amplifier stages, up to the desired power level. Here the Urbana Radar is no exception. In the interests of efficiency, therefore, the designer should carefully construct the matching networks between stages in such a manner that they provide good transfer of energy across the desired bandwidth. One point which is often not sufficiently stressed is the necessity for keeping the paths of circulating currents as short as possible. Perna (1979), in a set of articles published, demonstrated that points of low impedance and high current deserve special attention. Circuit losses in these conditions can approach (or exceed) 50%. High VSWR on transmission lines can exhibit an exactly similar pattern of unexplained losses.

Efficiency is the prime measurement of the effectiveness for a high-power amplifier. An amplifier which is properly designed, driven, and tuned exhibits a class-C conversion efficiency of 60-85%. Until these figures are reached, no class-C amplifier can be thought properly matched.

Bias is another consideration worthy of discussion here. In general, (and certainly true for the Urbana Radar), is the fact that given more forward bias, a given amplifier produces more gain. No amplifier should be designed without careful attention to the effects of bias on the matching networks, gain, and efficiency of the device.

The power supply is an important element of an amplifier, and one serious impediment to improved operation of the Urbana Radar is the inadequacy of the present power supply, which limits both the duty cycle and the average power transmitted.

The modulator is the last basic equipment to be discussed here. The Urbana Radar modulator is of the hard-tube type, and is responsible for the wide selection of available pulse widths, output power, duty cycle, etc. Central to the modulator is the pulse transformer, T618, and the capacitor bank or coffin. The pulse transformer has wide bandwidth and a wide selection of output taps to choose from. The capacitor bank may be switched in as necessary to prevent excessive droop during long pulse operation.

## 5. RESULTS AND CONCLUSIONS

### 5.1 Results

Verification of the proper operation of the phase modulation system proved simple. The Apple radar director was used, including a FORTH program written by Dr. Sidney Bowhill which included the necessary controls for transmission of a 7-bit Barker code. Verification consisted of simply demodulating the transmitted signal and displaying the results on an oscilloscope as shown in Figure 5.1. Figure 5.2(a) displays the RF signal taken directly from a monopole antenna. Note that switch intervals occur in proper locations, as this pulse is phase coded. Figure 5.2(b) displays the receiver output with phase modulation turned off. This is the expected output for this situation. Figure 5.2(c) displays the receiver output with phase modulation turned on. The phase reversals plainly indicate the transmission of the 7-bit Barker code.

### 5.2 Conclusions

The Urbana Radar transmitter now has the capability for phase modulation. The work represented here has resulted in analysis of and documentation for the transmitter.

ORIGINAL PAGE IS  
OF POOR QUALITY

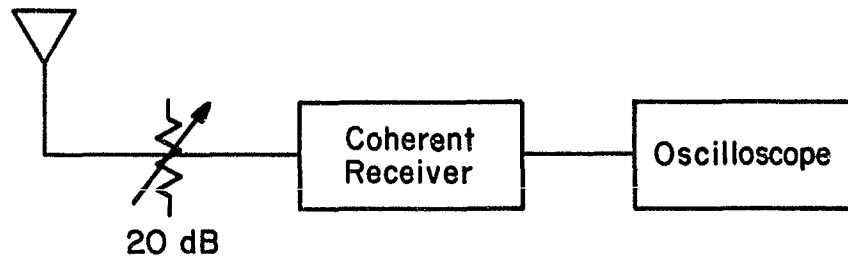
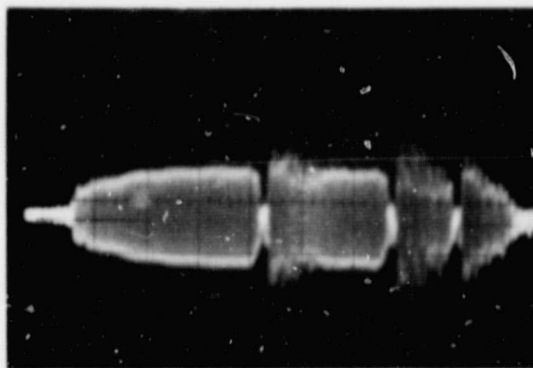


Figure 5.1 Block diagram of the verification system.



ORIGINAL PAGE IS  
OF POOR QUALITY

Figure 5.2(a) Picture of the coded RF pulse taken on a 100 MHz oscilloscope connected to a dipole antenna. The effects of phase coding are clearly visible on the envelope. Taken at 5  $\mu\text{sec}/\text{cm}$ .

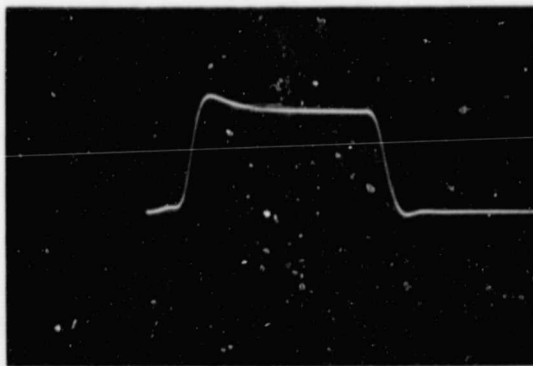


Figure 5.2(b) Coherently detected RF pulse with no phase coding applied. Taken at 10  $\mu\text{sec}/\text{cm}$ .

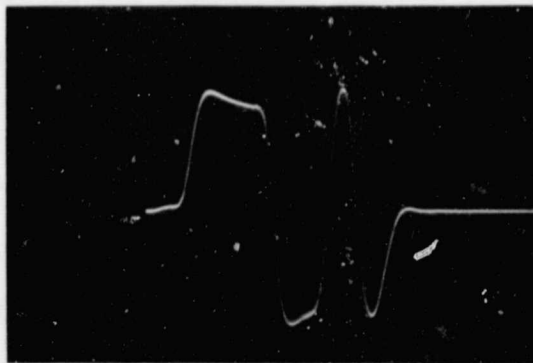


Figure 5.2(c) Coherently detected RF pulse phase modulated with a 7-bit Barker code. Taken at 10  $\mu\text{sec}/\text{cm}$ . The effects of limited system bandwidth are plainly visible.

## APPENDIX I. WIDEBAND FERRITE TRANSFORMERS AND DEVICES

## I.1 Introduction

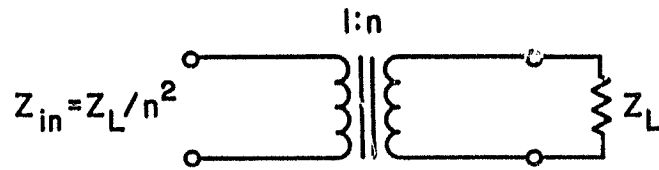
Wideband transformers are ferrite-and-wire devices of three distinct types: (1) the conventional transformer with its primary-and-secondary structure which provides impedance transformation and D.C. isolation between input and output; (2) the autotransformer which provides impedance matching but no D.C. isolation; and (3) the transmission line transformer which provides impedance matching and an exceptionally wide bandpass characteristic. Each type is illustrated in Figure I.1.

These devices and the more complex structures one may make from them comprise a simple, economical means of coupling, matching, combining, and dividing in wideband (.1 - 1000 MHz) radio frequency circuits.

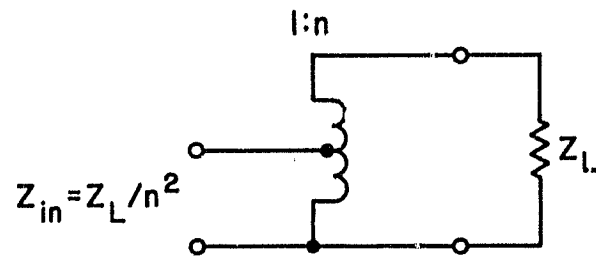
## I.2 Conventional Wideband Transformers

A commonly used model for a conventional wideband transformer is shown in Figure I.2.  $R_p$  and  $L_p$  represent the primary loss and primary inductance respectively. Both decrease with frequency and are hence the primary factors determining the low frequency cutoff, shown as  $f_1$  in Figure I.3.  $L_\ell$  and  $C_d$  represent the leakage inductance and winding capacitance of the finished transformer. Between them they determine the high frequency cutoff shown as  $f_2$  in Figure I.3.

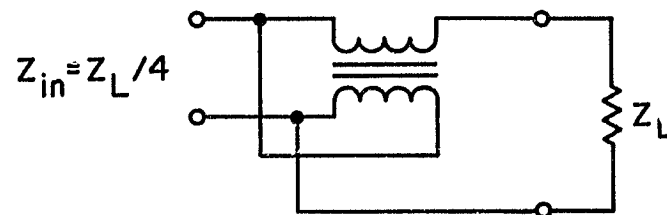
Figure I.4 shows flux lines in a typical ferrite core, passing inside and around the winding which excites them. Magnetic circuit theory assures us that the core's reluctance will decrease as the effective area available to pass flux (called  $A_e$ ) increases, and will increase as the effective magnetic path length (called  $\ell_e$ ) increases. Applying this to the transformer in Figure I.2, if  $A_e$  increases, so will  $R_p$  and  $L_p$ ; if  $\ell_e$  increases,



(a) Conventional Transformer



(b) Autotransformer



(c) Transmission Line Transformer

Figure I.1 Schematic representations of the three types of wideband ferrite transformers.

ORIGINAL PAGE IS  
OF POOR QUALITY

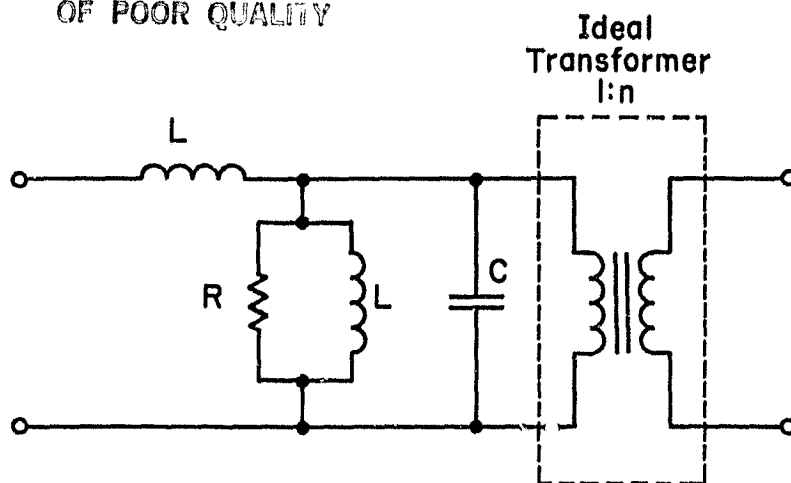


Figure I.2 Diagram of a commonly used model of a conventional wideband transformer.

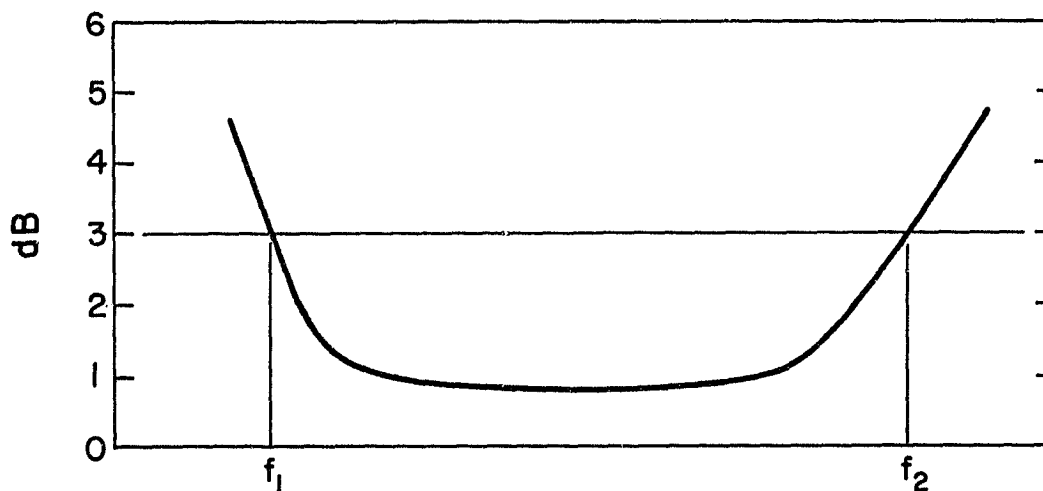


Figure I.3 Typical transmission loss versus frequency chart of a wideband transformer.

ORIGINAL PAGE IS  
OF POOR QUALITY

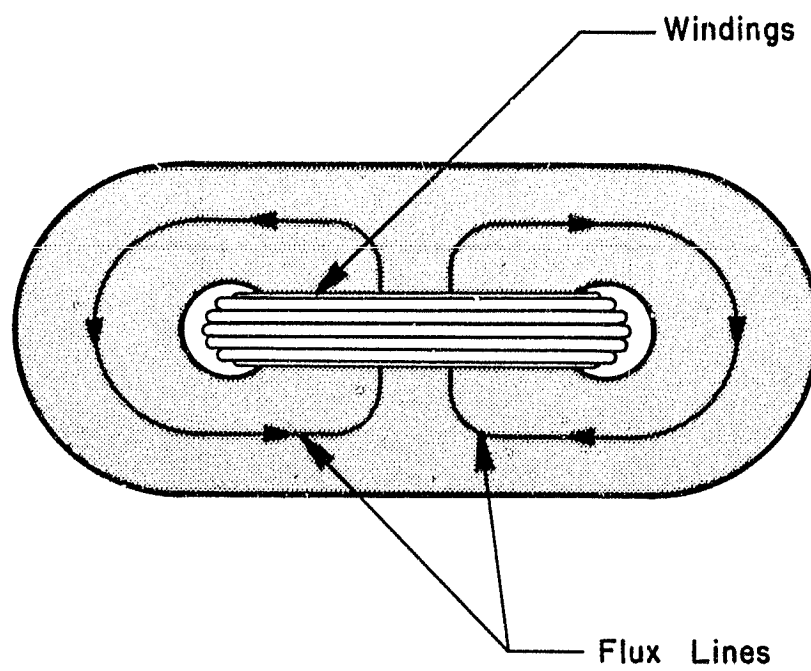


Figure I.4 Typical magnetic flux path in a BALUN type ferrite core.

$R_p$  and  $L_p$  will decrease.  $A_e$  and  $\ell_e$  are sometimes (Snelling, 1969) combined in one constant called the "core factor",  $Cl$ , where

$$Cl = \ell_e / A_e$$

Knowledge of the core's  $Cl$ , its size, and the magnetic characteristics of the core material give one a basis for estimating the low frequency response of the core.

For a particular core, one would expect the leakage inductance,  $L_\ell$ , and the winding capacitance,  $C_d$ , to increase with the number of turns one uses. In other words,  $L_\ell$  and  $C_d$  increase with the length of the winding, and for a particular core, the longer the winding required to provide the necessary low frequency response, the lower the high frequency cutoff will be. If  $\ell_w$  is defined as the length of wire required for one turn on the core, one would then expect  $f_2$  to depend on  $\ell_w$ .

For a wideband response we therefore desire a core with a small  $Cl$  and a short  $\ell_w$ . FAIR-RITE Products Corp. (1977) has combined these two concepts in a single geometry-dependent expression called the Form Factor:

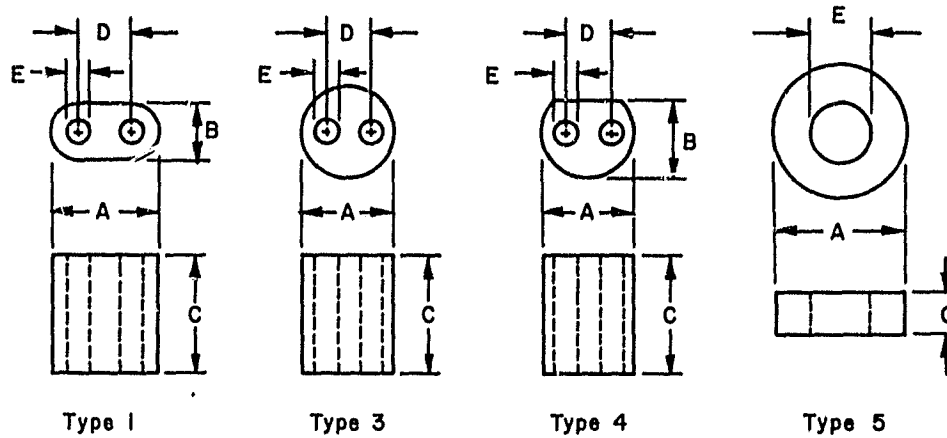
$$F.F. = \ell_w Cl$$

The Form Factor is used to express the wideband capabilities of cores (the smaller the Form Factor the wider the bandwidth). A table of various core shapes and the Form Factors thereof are provided in Figure I.5. The cores are all part of the "Joule Box" the company provides at a nominal cost.

Other manufacturers provide similar data on their products, but usually in a different form. They often provide the user with  $A_e$ ,  $\ell_e$  and the physical dimensions - hence one can easily compute the Form Factor for comparison between sources.

Note that in Figure I.2 we do not include a term describing the series resistance of the windings. The observed fact is that for transformers of

ORIGINAL FIGURE  
OF POOR QUALITY



List of Ferrite Core Shapes in Wide Band Transformer Sample Kit

Item	Part Number	Core Shape	Nominal Dimensions					Form Factor
			A	B	C	D	E	
1	28__000302	Type 1	.525	.295	.407	.225	.150	13.0
2	28__002402	Type 1	.277	.160	.244	.114	.071	14.3
3	28__002302	Type 1	.136	.079	.093	.057	.034	14.0
4	28__001802	Type 3	.250	—	.242	.100	.050	9.5
5	28__001702	Type 3	.250	—	.471	.100	.050	8.8
6	28__000902	Type 4	.284	—	.218	.104	.052	8.8
7	28--002802	Type 3	.220	—	.250	.090	.035	7.8
8	26--002402	Type 5	.380	—	.190	—	.197	29.0

Figure I.5 Core shapes, sizes, and form factors for Fair-Rite Products Corp. cores.

the type discussed here, using a good core and below a few hundred megahertz both the skin effect and D.C. resistance are negligible when compared to the core losses.

The loss target,  $\tan(\delta/\mu)$ , is another method of representing the core losses (previously call  $R_p$ ). This method (Ferronics 77) expresses the core losses in the form  $\tan(\delta/\mu) = \frac{1}{\mu Q} = R/\mu 2\pi fL$  where R and L are in series, not in parallel as in  $R_p$  and  $L_p$  of Figure I.2. Another method simply plots the Q as a function of frequency. Both methods may be easily converted to the more useful parallel form of Figure I.2.

Ferrite is a heat sensitive material. It may crack or be destroyed by excessive power dissipation. The limits suggested in Ferronics (77) are that  $100\text{-}600 \text{ mW/cm}^3$  will produce a  $40^\circ\text{C}$  rise in core temperature. Since most cores are small, one would expect to use them in relatively low power applications.

The following is a list of general construction tips for conventional wideband transformers:

1. Use a low Form Factor core. (Toroids are definitely not the lowest Form Factor cores, but can be used, of course).
2. Choose the smallest low F.F. core acceptable from low frequency response, saturation, and dissipation considerations.
3. Twist the primary and secondary windings together for tighter coupling and reduced self-winding capacitance, using multifilar windings to extend the transformation ratios where necessary.
4. Keep the windings as short as possible and still meet the required low frequency response. Granberg (1975) suggests the minimum primary inductance is:  $L = 4R/2\pi f$   
where L = primary inductance in  $\mu\text{H}$

$R$  = load impedance in ohms to the input

$f$  = lowest frequency in megahertz.

5. Use the largest wire which can be comfortably and tightly wound on the core.

Snelling (1969) Chapter 7 offers an extensive discussion of wideband transformers.

### I.3 Wideband Autotransformers

Wideband autotransformers permit a good range of impedance match ratios and an extended frequency response. Nagle (1976) discusses their advantages and details simple construction methods. His work is extended by Burwasser (1981) in a 2 part article. Burwasser demonstrated the construction of monofilar autotransformers having transformation ratios of 1:15, 1:2, 1:3, 1:4, 1:5, 1:6.25, 1:7.5, 1:9, and 1:16. With the single exception of the 1:16 device, the 1 dB points of all these transformers are below 1 MHz and above 200 MHz. The results demonstrate that for frequencies between 1 and 100 MHz or more, the monofilar autotransformer has lower transmission loss than comparable types of either conventional or transmission line devices.

The rules for the construction of monofilar autotransformers are the same as those for conventional devices except that monofilar wire is used and "pig tailed" at desired tap points.

### I.4 Transmission Line Transformers

Transmission line devices operate differently than conventional transformers, using the ferrite not to increase the coupling between turns, but instead to increase the line-to-line coupling of a 2-conductor transmission line wound in close proximity to it. This usage results in a device which does not have the fundamental upper frequency limit of the conventional

transformer. Ruthroff (1959) in a classic article reports devices with bandwidth ratios as high as 20,000 to 1. There are problems, though, arising from the new mode of operation; as one might expect, these arise out of the problems inherent in the construction of transmission lines suitable to the purpose. Several different types of transmission lines can be used; the most common one, however, the twisted pair (bifilar) line is well covered in the literature. Lefferson (1971) applies transmission line principles to simplify the construction of the twisted pair magnet wire transmission lines used in the manufacturing of many transmission line devices. The effects of variations of line lengths and of variations of characteristic impedance are discussed by Pitzalis and Couse (1968).

Successful devices have also been constructed using coaxial lines and, for low impedance lines, pairs of flat conductors separated by a dielectric.

Although transmission line devices have the widest frequency response of the devices discussed here, they have some drawbacks which limit their use: (1) They are limited to the "squares" ratios of impedance transformation: 1:1, 1:4, 1:9 ..., and often require more than one core to realize these; (2) They often have higher losses than comparable conventional transformers or autotransformers. They do have the advantage that they can be made physically larger and hence handle more power. Granberg (1975) reports devices capable of handling in excess of 400 w.

The following is a list of construction tips for transmission line devices:

1. Choose a core material having low losses over the whole frequency range of interest.
2. The low frequency response may be calculated exactly as in conventional devices. The core must be such that the total line length is less than one tenth of the wavelength of the highest frequency

of interest. If not, a new core material or geometry may be appropriate.

3. Keep the windings as short as possible. The longer the windings are, the more problems arise out of winding irregularities etc.
4. Twist bifilar windings by machine when possible. Hand twisted windings are not as uniform.

#### I.5 RF Combiners and Dividers

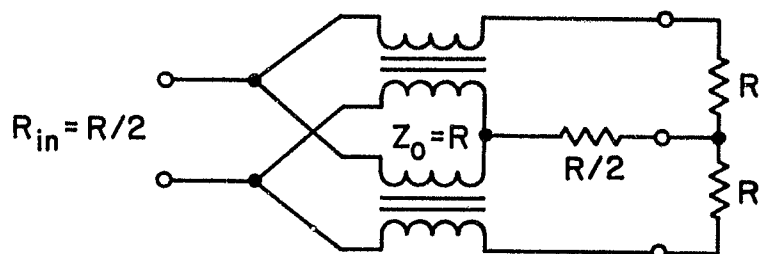
Each circuit by its nature is different from the next. The combiners and dividers presented here are by no means a complete selection. Any designer dealing with this frequency range must select devices to fit the requirements of his circuit. Some of the considerations involved in designing are: (1) bandwidth; (2) power level; (3) dc isolation requirements; (4) matching requirements; (5) size requirements, etc.

Figure I.6 demonstrates two versions of a hybrid combiner/splitter constructed of transmission line transformers. The version (a) can be wound on a single core. It has a balanced input and output and no dc isolation. Note that the transmission lines have characteristic impedances of  $R$  in both windings. The device in (b) has similar properties except that the addition of an unbalanced port places the whole device at dc ground potential, and requires an extra core with a different characteristic impedance winding.

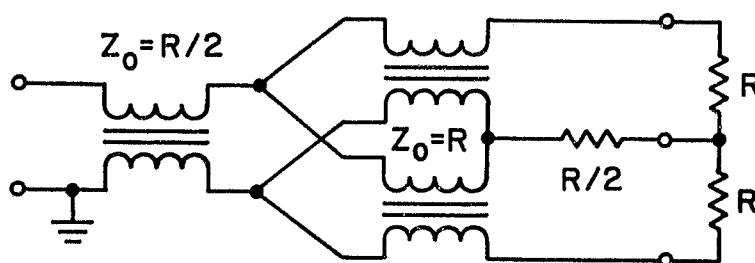
Figure I.7 shows the conventional equivalent of Figure I.6(a). Grounding one side of the input makes it unbalanced, equivalent to I.6(b). This device does have dc isolation but can have the narrower bandpass associated with a conventional device. For a more complete discussion see Sartori (1968).

Figure I.8 demonstrates a practical hybrid constructed from different device types. T1 is a transmission line device which supplies collector current to the two transistors; it is wound as shown in (b), enabling it to

ORIGINAL PAGE IS  
OF POOR QUALITY



(a) Symmetrical Hybrid



(b) Unbalanced Symmetrical Hybrid

Figure I.6 Two approaches to wideband hybrid combiners/splitters.

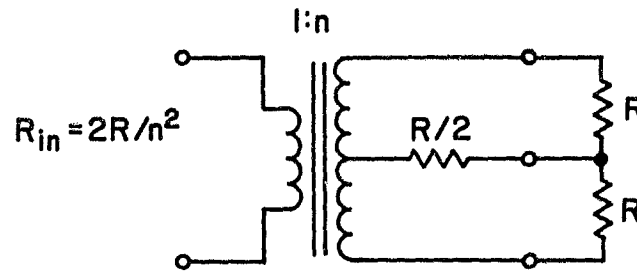


Figure I.7 A conventional wideband hybrid combiner/splitter.

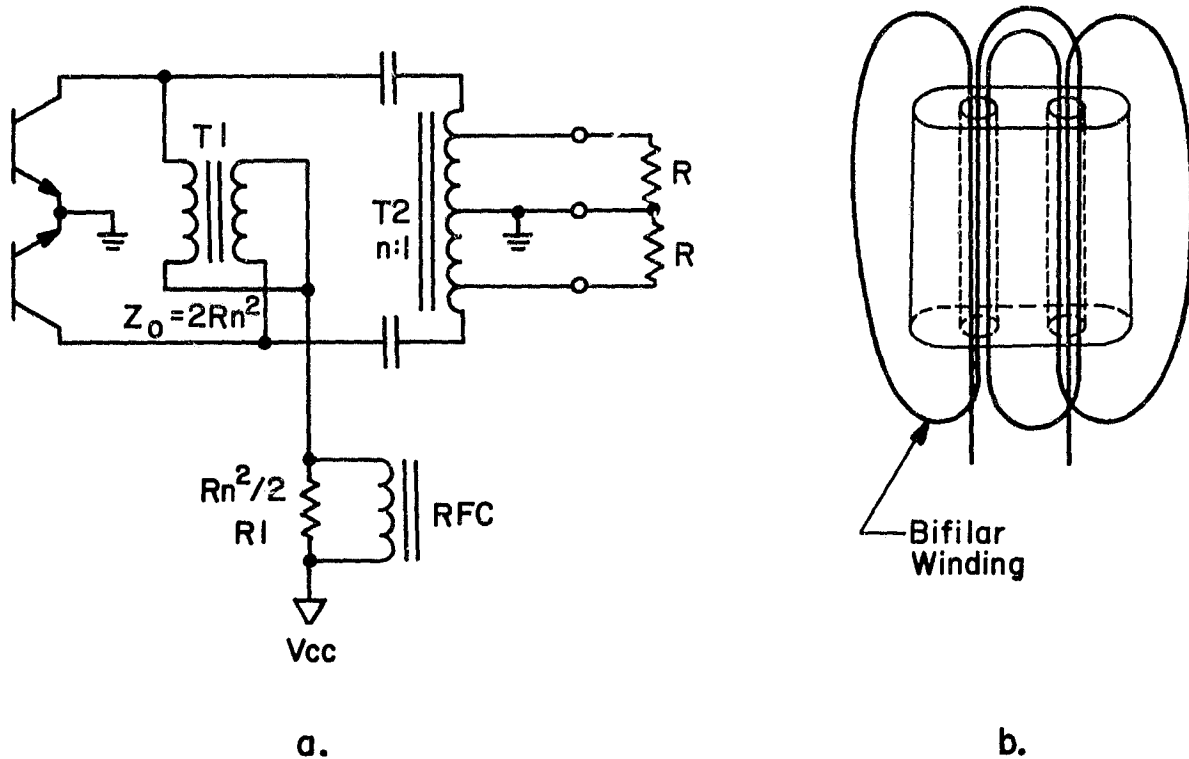


Figure I.8 (a) Method whereby two 180° transistor outputs may be combined  
(b) Method for winding a transmission line transformer which permits upright mounting.

be mounted upright on a printed circuit board. Note that the collector currents pass through T1 in opposite directions in effect cancelling and avoiding saturation effects. The radio frequency choke provides a low impedance path for dc but a very high impedance to R.F.; thus any imbalance in the RF outputs of the two transistors tends to be dissipated in R1. The autotransformer T2 provides an impedance match. It might as easily have been a conventional transformer or a transmission line device; the choice depends on circuit requirements.

#### I.6 Summary

Careful design of wideband RF transformers using Ferrite cores provides simple, economical methods for matching, isolation, and the construction of hybrid combiners and dividers. Small cores yield high frequency devices. Larger cores produce higher power devices.

APPENDIX II. IMPEDANCE MATCHING OF NONLINEAR LOADS

A nonlinear load is any load in which the magnitude of the current waveform is not directly proportional to the voltage waveform. Common examples of concern are transistor and vacuum tube inputs. For nonlinear loads, the matching network design depends on the power to be applied. If this power is to vary in the course of the normal operation of the device, the engineer is faced with the necessity of constructing a network capable of being adjusted to match an entire range of impedances. If we assume that the applied current waveform is a periodic waveform, with a fundamental angular frequency  $\omega_0$  then we can write

$$i(t) = I_0 + \sum_{n=-\infty}^{\infty} i_n e^{-jn\omega_0 t}$$

Since the problem of matching a nonlinear load at an infinite number of frequencies becomes rather large we make a simplifying assumption: we assume that the nonlinear element is bypassed with an LC circuit with a large enough  $Q$  such that  $v(t)$  in Figure II.2 is approximately sinusoidal. When this is applied to a nonlinear load with a voltage-current characteristic such as the one shown in Figure II.1 we can write an expression for the current through the load as:

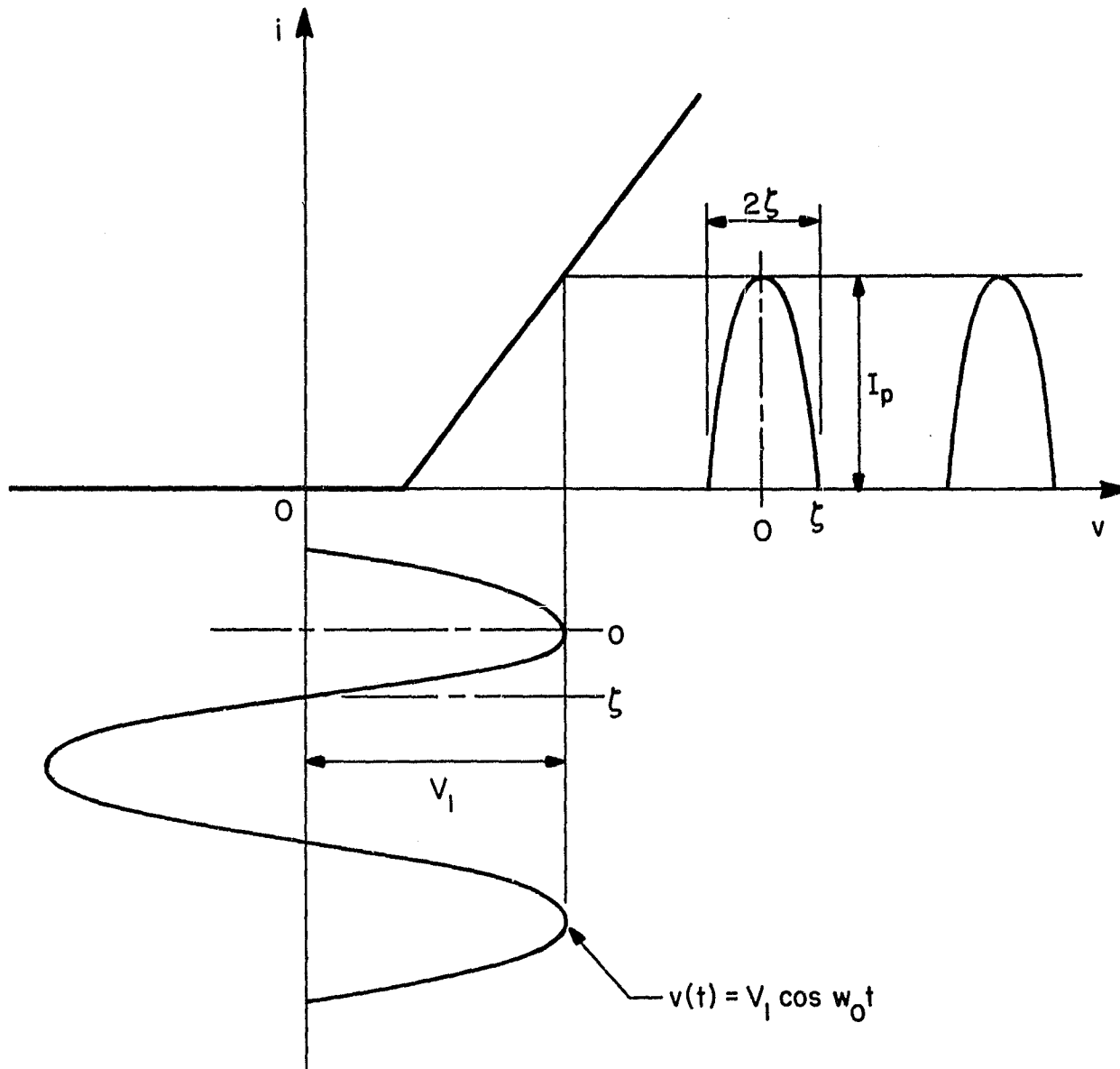
$$i(t) = I'_0 + \sum_{n=-\infty}^{\infty} i'_n e^{jn\omega_0 t}$$

Note that our assumption of a high  $Q$  "tank" circuit having very low impedance except at  $\omega_0$  causes the dc component and any harmonics of the input waveform to be "shorted" to ground; hence, only the fundamental frequency of the input current has much effect. To a good approximation, then, we can write

$$\frac{v_1 e^{j\omega_0 t}}{i_1 e^{j\omega_0 t}} = \frac{v_1}{i_1} = Z[v(t)]$$

Hence: 1) if we know the current/voltage characteristics of the nonlinear load; 2) if we assume an applied sinusoidal voltage we can solve for  $Z[v(t)]$

ORIGINAL PAGE IS  
OF POOR QUALITY



OGR. 1

Figure II.1 Applied voltage versus current waveforms for a nonlinear load of the piecewise continuous type.

ORIGINAL PAGE IS  
OF POOR QUALITY

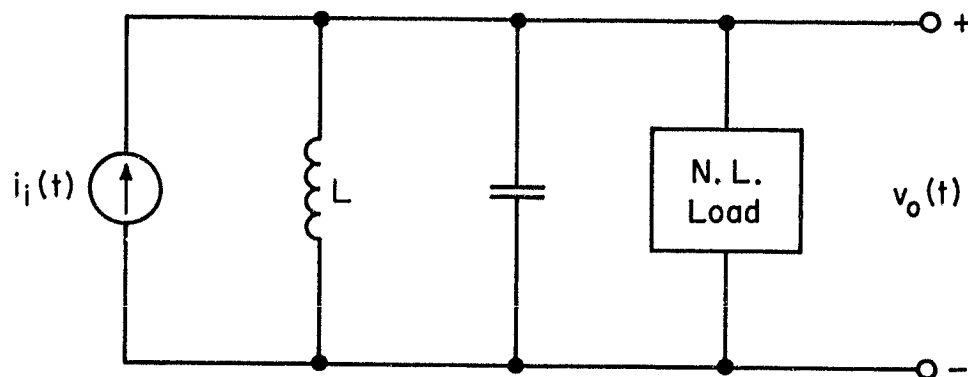


Figure II.2 Nonlinear load bypassed with a high Q tank circuit.

R. ↑

either analytically or graphically. We can then design our matching network for this impedance. If we insure that the  $Q$  of the match network is high enough to meet our initial assumption, then we have sufficient justification for this technique. In many cases a network  $Q$  of 10 to 20 is quite sufficient. If the input waveform is sinusoidal in the first place it eases this requirement somewhat.

Several techniques are available for the above analysis. The Machlett Power Tube Calculator is a graphical technique based on Fourier analysis of the current waveforms of the power tube in question. It permits the user to evaluate within 10% the operating conditions of a power tube using a particular load line. An excellent source for a mathematical approach to several types of nonlinearities is Clarke and Hess (1971). Finally, a more direct approach is the physical measurement of the S-parameters of a device using a method similar to the one shown in Figure II.3.

The direct measurement technique is applicable even when the device power level is higher than would ordinarily be permitted by most test equipment. 1) The system is set up as shown. 2) The input is adjusted for zero reflected power at a predetermined input power level. 3) The output is then adjusted for maximum power output. 4) Steps 2 and 3 are repeated until no further improvement occurs. 5) The device under test is then removed from the test setup. 6) The vector impedance of the input match network looking back toward the generator is measured using a vector impedance meter or network analyzer. 7) The vector impedance of the output match network is similarly measured. Note that steps 6 and 7 can be accomplished with low power equipment, since at this point no high-power levels are present. 8) The desired input and output impedances are simply the complex conjugates of the values measured in steps 6 and 7.

ORIGINAL PAGE IS  
OF POOR QUALITY

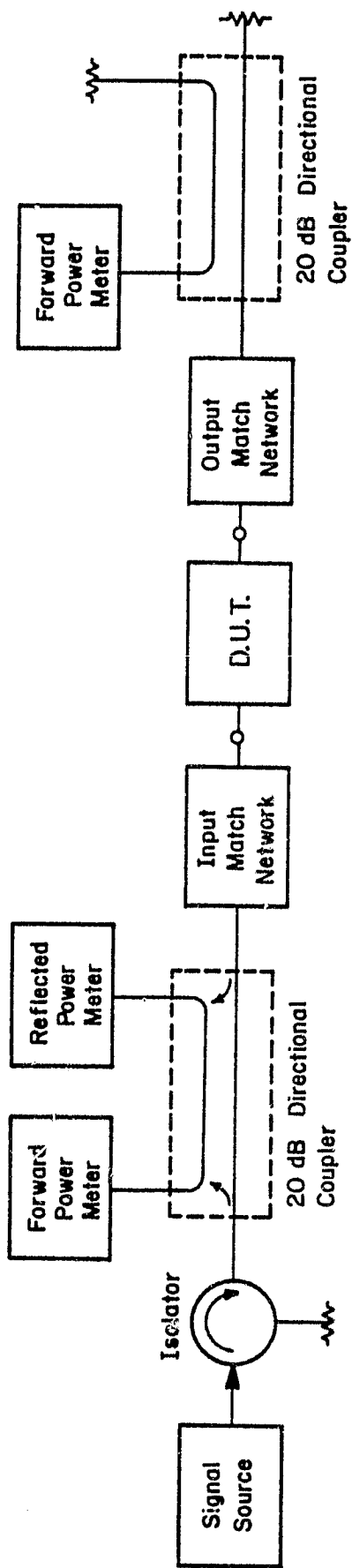


Figure II.3 Measurement method for input and output impedances measured at high power.

3R. 1

APPENDIX III. RIGID COAXIAL CABLE.

The rigid copper coaxial transmission lines of which so much of the Urbana Radar transmitter is constructed is meant to withstand the high voltages and currents associated with RF power transmission. Observed damage and a desire for completeness lend the reasoning behind this documentation of the limits of these transmission lines. The following nomographs have been taken from the 1973 Andrew Corp. Catalog. Figure III.1 gives the average power limitations for each size of the 50  $\Omega$  coax currently in use. Currently the Urbana Radar is near none of these limits. The derating factor for the average power with respect to load VSWR is

$$D.F. = \frac{VSWR^2 + 1}{2VSWR} + F' \left( \frac{VSWR^2 - 1}{2VSWR} \right)$$

where F' may be determined from Figure III.2. Figure III.3 shows the variation of permissible average power with the ambient temperature.

Of more concern to the Urbana Radar are the peak power limitations rather than average power limitations. The following formula may be used:

$$P_{pk} = \frac{(E_{rF})^2}{200 \cdot VSWR} \text{ watts}$$

where  $E_{rF} = .247 E_p$ , where  $E_p$  is the dc production test voltage given in Table III.1. Figure III.4 gives the variation in peak power with respect to the effects of pressurization. As a note of caution, please observe that the peak power limitation at VSWR = 1 for 3 1/8" lines is listed as 400 kw (unpressurized). These limits are easily exceeded in the Urbana Radar under high VSWR conditions, and arcover has been observed during tuning.

Figure III.5, III.6 and III.7 describe the line attenuation versus length, the effect of load VSWR on line attenuation, and the variation of

BR. 1

ORIGINAL PAGE IS  
OF POOR QUALITY

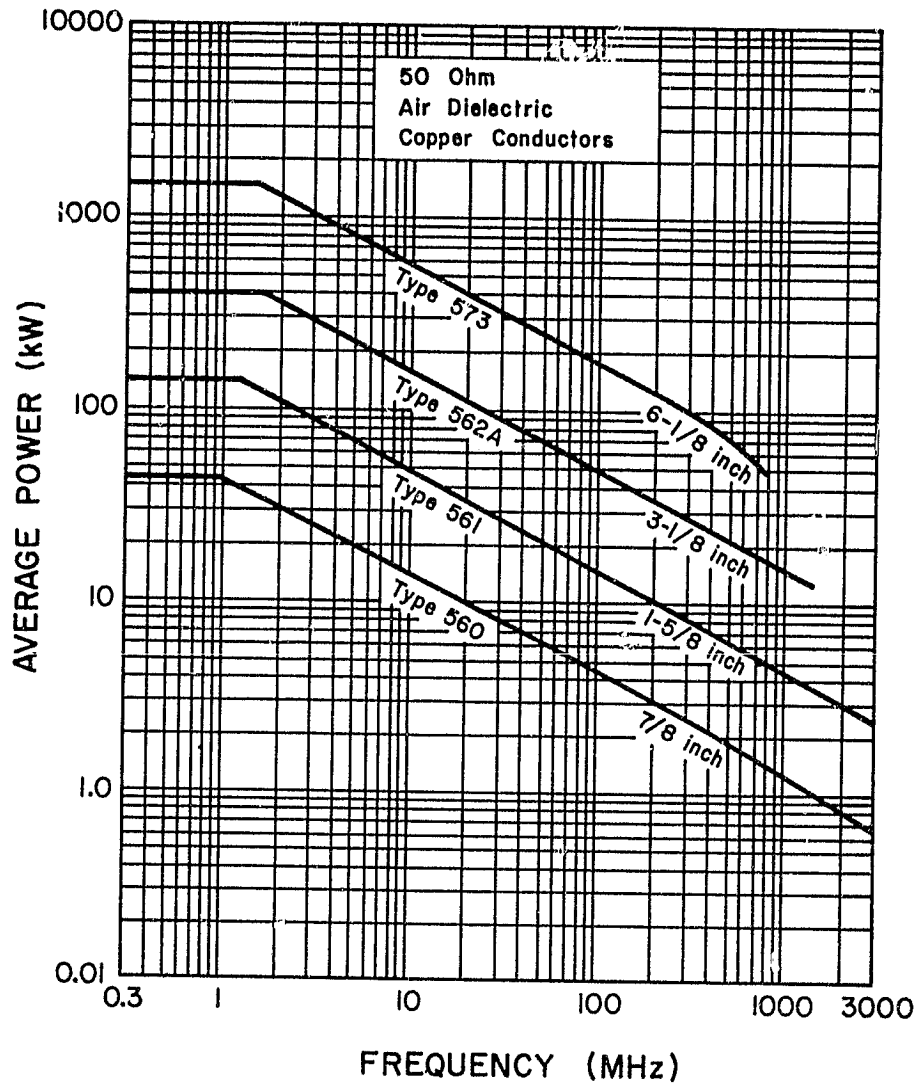


Figure III.1 Average power limitations versus frequency for the currently used types of rigid transmission lines.

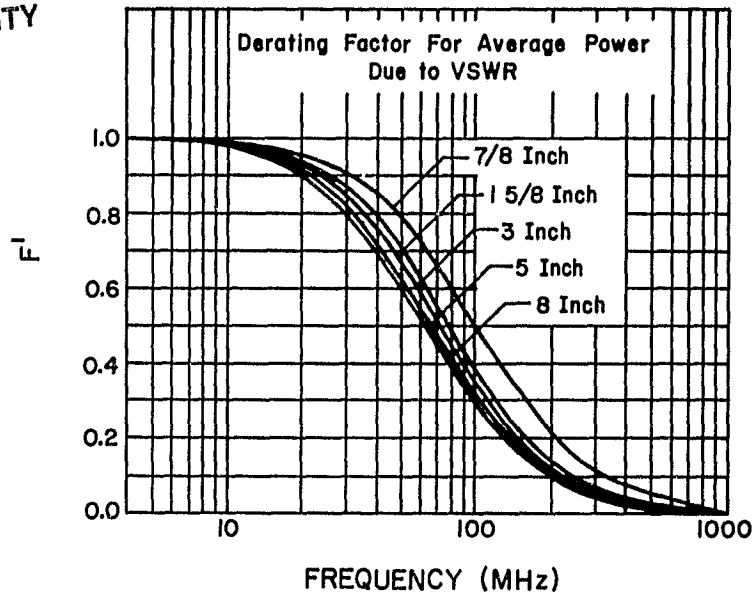


Figure III.2 Derating factor vs. frequency for rigid transmission line.

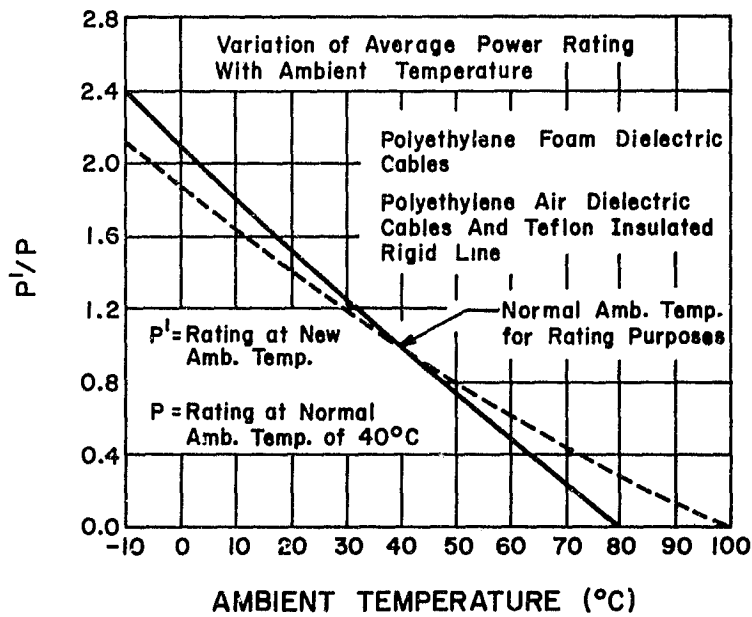


Figure III.3 Variation of permissible average power vs. temperature for rigid coaxial transmission line.

ORIGINAL PAGE IS  
OF POOR QUALITY

Table III.1 Production test voltage versus outer conductor diameter.

Outer Conductor OD, inches	7/8	1-5/8	3	3-1/8	5	6-1/8	8
Ep volts	6,000	11,000	16,000	19,000	25,000	35,000	35,000

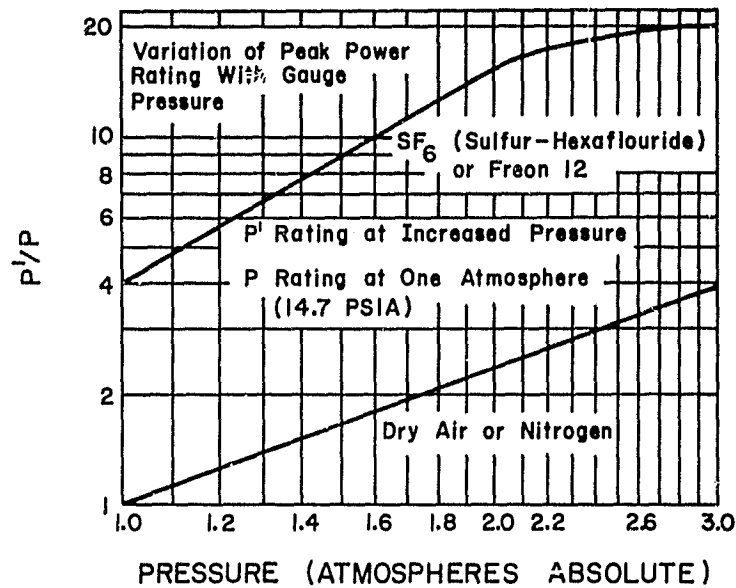


Figure III.4 Peak power limits vs. internal pressure for  $SF_6$  and dry air or nitrogen.

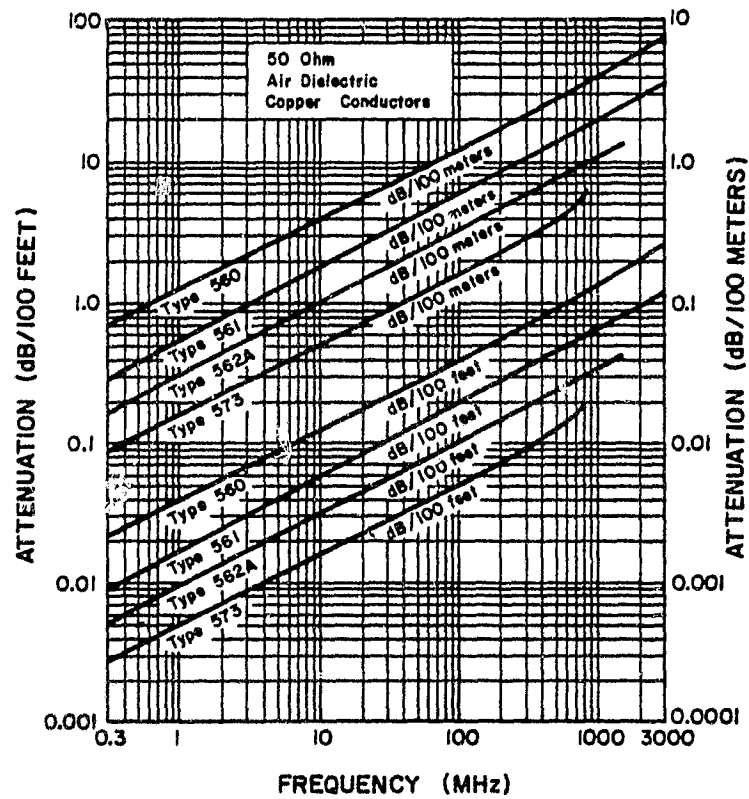
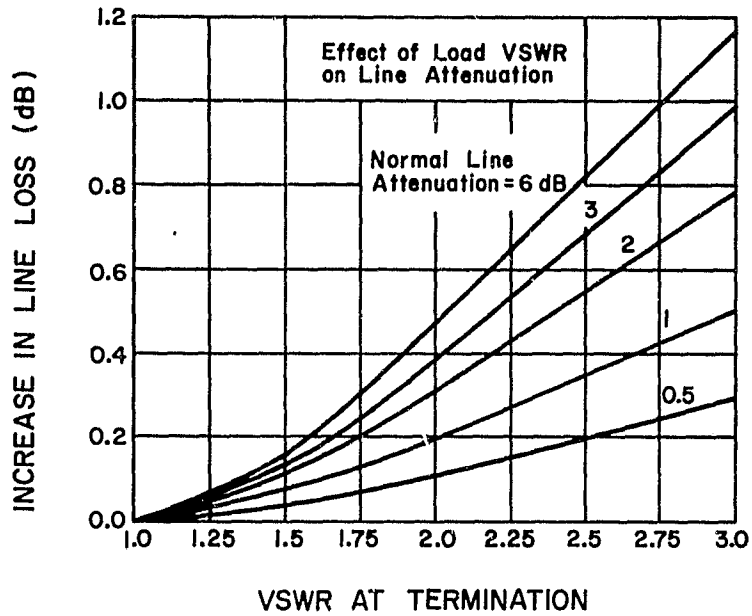


Figure III.5 Attenuation vs. frequency for rigid coaxial transmission line.

ORIGINAL PAGE IS  
OF POOR QUALITY



R. 1

Figure III.6 Attenuation vs. VSWR for rigid coaxial transmission line.

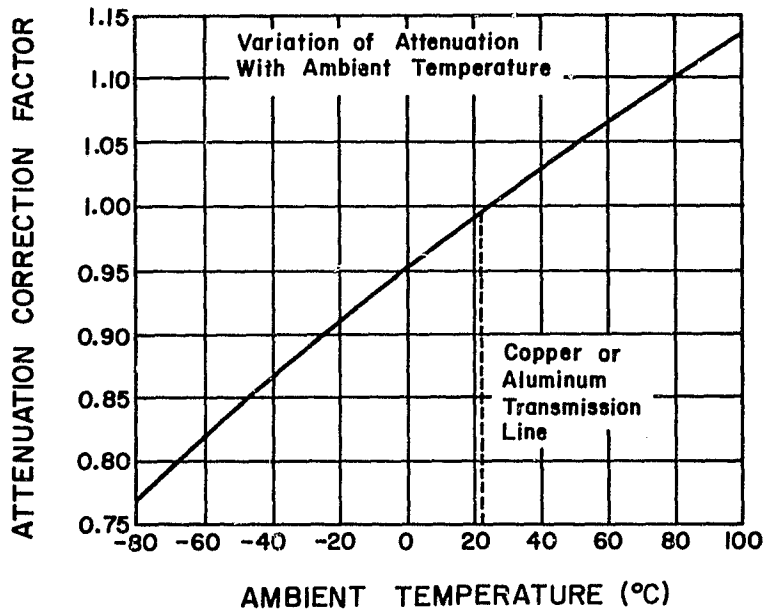


Figure III.7 Attenuation vs. temperature for rigid coaxial transmission line.

attenuation with temperature respectively.

Figure III.8 gives the inner conductor versus outer conductor temperature rise.

A few further comments are appropriate here, based on observations of past damage to the coaxial lines.

1. The lines should be periodically checked for accumulation of moisture. On one occasion the author removed two pints of water from the output network of unit 3.

2. Once arcover occurs in a line, the pits and catwhisker damage caused will permit it more easily the next time.

3. Parts of these coax lines are unpressurized. These parts should be evaluated and pressurized if needed.

In summary we simply note that the coaxial lines of the Urbana Radar are important to its operation; they deserve care and careful periodic maintenance.

ORIGINAL PAGE IS  
OF POOR QUALITY

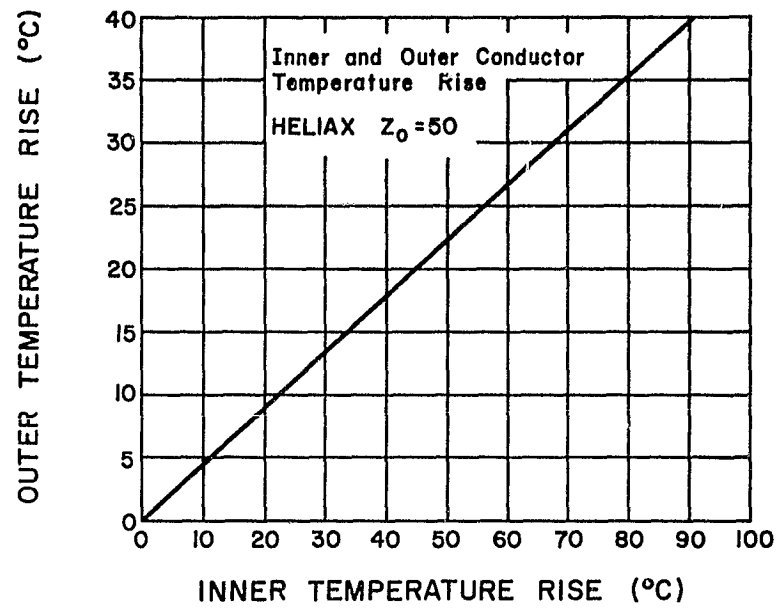


Figure III.8 Inner conductor vs. outer conductor temperature rise.

APPENDIX IV. PROGRAM LISTINGS AND DESCRIPTIONS

Program 1. "PA MATCH"

Description: This program generates data on the impedance matching capabilities of units 3 and 4. It contains a model of the three variable-length transmission line segments which form the output tuning networks of these units. For input it requires the load impedance seen by the final segment. These data are produced by the program "CAPAUG" which is listed hereafter. Further data on the tuned bandwidth of these units are provided graphically by the program "PA BANDWIDTH", also listed hereafter, using selected data from "PA MATCH" to compute from.

```

1 REM PA MATCH BY L.J.HERRINGTON
10 REM THIS PROGRAM IS INTENDED
    TO PROVIDE DATA FOR THE
    CONSTRUCTION
20 REM OF A TUNING NOMOGRAPH FOR
    UNITS 3 AND 4 OF THE URBANA
    RADAR
30 REM IT USES THE BRUTE FORCE
    APPROACH TO COMBINE T-LINE
    EQUATIONS
40 REM AND THE EFFECT OF ABRUPT
    JUNCTION CAPACITANCES TO
    COMPUTE POSSIBLE
50 REM REAL LOAD IMPEDANCES AS
    SEEN BY THE ML5682 TUBES.
60 REM IT SEARCHES FOR REAL IMPEDA
    NCES BY HOLDING L2 CONSTANT
    AND VARYING L1
80 INPUT "ENTER THE REAL PART OF
    THE LOAD IMPEDANCE."; V
90 INPUT "ENTER THE IMAGINARY PART
    OF THE LOAD IMPEDANCE.";
    W
100 DIM L1(22), L2(22), R(22), X(22)

110 FOR I = 1 TO 22
120 L2 = .044 + I*.002
130 L1 = 0
    : DLTA = .005
140 GOSUB 380
150 ROUT = R
    : XOUT = X
160 GOSUB 380
170 IF SGN (XOUT) < > SGN (X)
    GOTO 210
180 L1 = L1 + DLTA
190 IF L1 > .085 GOTO 350
200 GOTO 150
210 L1 = L1 - DLTA
220 DLTA = DLTA / 10
230 IF ABS (X) < 1 GOTO 250
240 GOTO 140
250 L1(I) = .201 - (L1 + L2)
260 L2(I) = L2
270 R(I) = R
280 X(I) = X
290 PRINT R
300 NEXT I
310 FOR I = 1 TO 22
320 PRINT "L1="; L1(I), "L2=";
    L2(I), "R="; R(I), "X=";
    X(I)
330 NEXT I
340 END
350 PRINT "NO MATCH AT L2="; L2
360 NEXT I
370 GOTO 310
380 RL = V
390 XL = W
400 Z0 = 52
410 A = L1*60.2832
420 GOSUB 590
430 GOSUB 630
440 B = B + 4.37E - 3
450 GOSUB 680
460 Z0 = 5.2
    : RL = R
    : XL = X
470 A = L2*60.2832
480 GOSUB 590
490 GOSUB 630
500 B = B + 5.14E - 3

```

ORIGINAL PAGE IS  
OF POOR QUALITY

135

```

510 GOSUB 680
520 Z0 = 82
: RL = R
: XL = X
530 A = 6.2832*(.201 - (L1 + L2))
540 GOSUB 590
550 GOSUB 630
560 B = B + 2.18E - 2
570 GOSUB 630
580 RETURN
590 D = (1 - XL / Z0* TAN (A))*2
+ (RL / Z0* TAN (A))*2
600 R = RL*(1 + TAN (A)*2) / D

610 X = (XL*(1 - TAN (A)*2) + Z0*
TAN (A)*(1 - (RL / Z0)*2
- (XL / Z0)*2)) / D
620 RETURN
630 BETA = - ATN (X / R)
640 MAG = SQR (X*2 + R*2)
650 G = 1 / MAG* COS (BETA)
660 B = 1 / MAG* SIN (BETA)
670 RETURN
680 BETA = - ATN (B / G)
690 MAG = SQR (G*2 + B*2)
700 R = 1 / MAG* COS (BETA)
710 X = 1 / MAG* SIN (BETA)
720 RETURN

```

]

Program 2. "CAPAUG"

Description: This program computes the load impedance seen by the tuning elements in units 3 and 4. It assumes a 50  $\Omega$  load. It requires as input the effective characteristic impedance of the blocking capacitor segments of units 3 and 4.

```

1 REM CAPAUG BY L.J.HERRINGTON
10 INPUT "ENTER Z0"; Z
20 Z0 = Z
100 FOR F = 3E7 TO 5E7 STEP 1E6
110 WAVL = 3E10 / F
120 A = 29.25 / WAVL
130 RL = 50
135 XL = 0
140 GOSUB 900
150 RL = R
160 XL = X - 3.183E8 / F
170 A = 58.5 / WAVL
180 GOSUB 900
190 RL = R
200 XL = X - 3.183E8 / F
210 A = 58.5 / WAVL
220 GOSUB 900
230 RL = R
240 XL = X - 3.183E8 / F
250 A = 29.25 / WAVL
260 GOSUB 900
270 RL = R
280 XL = X

290 A = 299.2 / WAVL
300 Z0 = 40
310 GOSUB 900
320 RL = R
330 XL = X
340 A = 267.3 / WAVL
350 Z0 = 56
360 GOSUB 900
370 Z0 = Z
375 PRINT "F="; F
380 PRINT "R="; R, "X="; X
385 PRINT
390 NEXT
400 END
900 D = (1 - XL / Z0* TAN (A))*2
+ (RL / Z0* TAN (A))*2
1000 R = RL*(1 + TAN (A)*2) / D
1100 X = (XL*(1 - TAN (A)*2) + Z0*
TAN (A)*(1 - (RL / Z0)*2
- (XL / Z0)*2)) / D
1200 RETURN

```

]

Program 3. "PA BANDWIDTH"

PA BANDWIDTH is a modeling program providing data to evaluate the bandwidth of the output matching networks of units 3 and 4. It requires as inputs the lengths of the tuning element of units 3 and 4, the resistance being matched, and the effective characteristic impedance of the blocking capacitor structures. Further it requires access to two binary files on floppy disk: "BANDWIDTH" which is essentially the blank graph paper on which the data will be graphed, and "SHAPE TABLE" which contains the + mark plotted at each data point. The program assumes a current source whose resistance is matched by the network. The transmission coefficient is plotted as a function of frequency. For typical results see Chapter 3.

```

1 REM PA BANDWIDTH BY L.J.HERRING
   TON
10 INPUT "ENTER Z0"; Z
20 INPUT "ENTER L1"; L1
30 INPUT "ENTER L2"; L2
32 INPUT "ENTER TUBE LOAD"; TL
35 B1 = 25
   : A1 = 17
   : XN = 3.6E7
   : YN = 0
   : YI = .1
   : XI = 1E6
40 HGR : POKE - 16302, 0
50 LET D$ = CHR$(4)
   : REM CTRL-D
60 HCOLOR= 3
   : HPLOT 0, 179
   : CALL 62454
70 HCOLOR= 0
   : SCALE= 1
   : ROT= 0
80 PRINT D$"BLOAD BANDWIDTH,A$2000"

95 PRINT D$"BLOAD SHAPE TABLE,A$400
   0"
96 POKE 232, 0
   : POKE 233, 64
100 Z0 = Z
110 FOR F = 3.6E7 TO 4.6E7 STEP 2E5
120   WAVL = 3E10 / F
130   A = 29.25 / WAVL
140   RL = 50
150   XL = 0
160   GOSUB 2000
170   RL = R
180   XL = X - 3.183E8 / F
190   A = 58.5 / WAVL
200   GOSUB 2000

210   RL = R
220   XL = X - 3.183E8 / F
230   A = 58.5 / WAVL
240   GOSUB 2000
250   RL = R
260   XL = X - 3.183E8 / F
270   A = 29.25 / WAVL
280   GOSUB 2000
290   RL = R
300   XL = X
310   A = 299.2 / WAVL
320   Z0 = 40
330   GOSUB 2000
340   RL = R
350   XL = X
360   A = 267.3 / WAVL
370   Z0 = 56
380   GOSUB 2000
410   RL = R
420   XL = X
430   A = (.201 - L1 - L2)*733.1
       / WAVL
440   Z0 = 52
450   GOSUB 2000
470   GOSUB 2090
480   B = B + 1.07E - 10*F
490   GOSUB 2040
500   RL = R
510   XL = X
520   Z0 = 5.2
530   A = L2*6.2832*733.1 / WAVL
540   GOSUB 2000
560   GOSUB 2090
570   B = B + 1.26E - 10*F
580   GOSUB 2040
590   RL = R
600   XL = X
610   Z0 = 82

```

```

620 REM A IS ANGLE IN RADIANS
630 REM WAVL IS WAVELENGTH IN
    CM.
640 A = L1*6.2832*733.1 / WAVL
650 GOSUB 2000
660 GOSUB 2090
670 B = B + 5.*4E - 10*F
680 GOSUB 2040
690 PRINT R, X
700 Z0 = Z
710 RHO = SQR ((R - TL)*2 + X*2)
    / SQR ((R + TL)*2 + X*2)
720 XC = F
730 YC = 1 - RHO*2
760 X9 = 29 + INT ((XC - XN)*B1
    / XI + .5)
770 Y9 = 174 - INT ((YC - YN)*A1
    / YI + .5)
780 DRAW 15 AT X9, Y9
785 NEXT
790 TEXT
800 INPUT "SAVE UNDER WHAT NAME?";

```

```

SN$
810 PRINT D$"BSAVE"SN$,A$2000,L$200
    0"
820 END
2000 D = (1 - XL / Z0* TAN (A))*2
    + (RL / Z0* TAN (A))*2
2010 R = RL*(1 + TAN (A)*2) / D
2020 X = (XL*(1 - TAN (A)*2) + Z0*
    TAN (A)*(1 - (RL / Z0)*2
    - (XL / Z0)*2)) / D
2030 RETURN
2040 BETA = - ATN (B / G)
2050 MAG = SQR (G*2 + B*2)
2060 R = 1 / MAG* COS (BETA)
2070 X = 1 / MAG* SIN (BETA)
2080 RETURN
2090 BETA = - ATN (X / R)
2100 MAG = SQR (R*2 + X*2)
2110 G = 1 / MAG* COS (BETA)
2120 B = 1 / MAG* SIN (BETA)
2130 RETURN

```

Program 4. "PA INPUT"

This program computes the input impedance and VSWR of the input match network in units 3 and 4. The load RL assumed in step 60 must be changed to correspond with the operating conditions of the ML-5682.

5L

```

10 REM PA INPUT BY L.J.HERRING@DN
20 PR# 1
30 FOR L = 3.3 TO 5.7 STEP .1
: REM DERIVED FROM WORK BY
    JAY GOOCH.
40 Z0 = 20
: REM VERIFIED VIA TIME DOMAIN
    REFLECTOMETER
50 A = .3267
: REM VERIFIED VIA T.D.R.
60 RL = 20
70 REM RL IN 60 DEPENDS ON
    TUBE OPERATING CONDITIONS
80 XL = 1 / (.26157468 - 1 / L)
90 G = 1 / RL
: B = 1 / XL
100 GOSUB 390
110 RL = R
: XL = X
120 GOSUB 300
130 PRINT
140 Z0 = 31
150 A = 1.615
160 RL = R
: XL = X
170 GOSUB 300
180 PRINT "L= "; L
190 MAG = SQR ((R - 50)*2 + X*2)
    / SQR ((R + 50)*2 + X*2)
200 ANG = (ATN (X / (R - 50))

```

```

- ATN (X / (R + 50)))*57.3
210 PRINT "THE REAL PART IS ";
    R
220 PRINT "THE IMAGINARY PART
    IS "; X
230 PRINT "RHO= "; MAG, "ANG=
    "; ANG
240 VSWR = (1 + MAG) / (1 - MAG)
250 PRINT "VSWR= "; VSWR
260 PRINT
270 NEXT
280 PR# 0
290 END
300 D = (1 - XL / Z0* TAN (A))*2
    + (RL / Z0* TAN (A))*2
310 R = RL*(1 + TAN (A)*2) / D
320 X = (XL*(1 - TAN (A)*2) + Z0*
    TAN (A)*(1 - (RL / Z0)*2
    - (XL / Z0)*2)) / D
330 RETURN
340 BETA = - ATN (X / R)
350 MAG = SQR (X*2 + R*2)
360 G = 1 / MAG* COS (BETA)
370 B = 1 / MAG* SIN (BETA)
380 RETURN
390 BETA = - ATN (B / G)
400 MAG = SQR (G*2 + B*2)
410 R = 1 / MAG* COS (BETA)
420 X = 1 / MAG* SIN (BETA)
430 RETURN

```

Program 5. "T-LINE CALCULATOR"

This is a utility program used to compute the input impedance of a transmission line with a complex load. It was frequently used and often modified for use in larger programs.

```

1 REM T-LINE CALCULATOR BY L.J.HERRINGTON
10 PRINT "THIS PROGRAM WILL COMPUTE THE INPUT IMPEDANCE OF A TRANSMISSION"
20 PRINT "LINE WITH A COMPLEX LOAD"
30 INPUT "ENTER THE LENGTH OF THE LINE IN WAVELENGTHS"; LA
40 A = LA*6.2832
50 INPUT "ENTER THE CHARACTERISTIC IMPEDANCE OF THE LINE"; ZO
60 INPUT "ENTER THE REAL PART OF THE LOAD IMPEDANCE"; RL
70 INPUT "ENTER THE IMAGINARY PART OF THE LOAD IMPEDANCE"; XL
80 GOSUB 120
90 PRINT "THE REAL PART OF THE INPUT IMPEDANCE IS "; R
100 PRINT "THE IMAGINARY PART OF THE INPUT IMPEDANCE IS "; X
110 END
120 D = (1 - XL / ZO* TAN (A))^2 + (RL / ZO* TAN (A))^2
130 R = RL*(1 + TAN (A)^2) / D
140 X = (XL*(1 - TAN (A)^2) + ZO* TAN (A)*(1 - (RL / ZO)^2 - (XL / ZO)^2)) / D
150 RETURN

```

1

Program 6. "T-MATCH"

The output of unit 3 includes a coaxial Tee as part of the power splitter used to drive unit 4. This program evaluates that match by computing and printing the reflection coefficient "seen" by unit 3.

```

1 REM T-MATCH BY L.J.HERRINGTON
10 REM THIS PROGRAM IS FOR EVALUATION OF THE T-MATCH
20 FOR F = 10E6 TO 80E6 STEP 1E6
30 A = 3.3E - 8*F
40 R1 = 50*(1 + (TAN (A))^2) / (.69444* TAN (A))^2
50 X1 = .5177* TAN (A) / (.69444* TAN (A))^2
60 B = 4.5E - 9*F
70 D = (1 - (X1 / 50)* TAN (B))^2 + ((R1 / 50)* TAN (B))^2
80 R2 = R1*(1 + (TAN (B))^2) / D
90 X2 = (X1*(1 - (TAN (B))^2) + (1 - (R1 / 50)^2 - (X1 / 50)^2)* TAN (B)) / D
100 RO = R2 / 2
110 XO = X2 / 2
120 MAG = SQR ((RO - 50)^2 + XO^2) / SQR ((RO + 50)^2 + XO^2)
130 ANG = (ATN (XO / (RO - 50)) - ATN (XO / (RO + 50))) * 57.3
140 PRINT "F="; F; "MAG="; MAG; "ANG="; ANG
145 PRINT "RO="; RO; "XO="; XO
150 NEXT
160 END

```

1

Programs 7 and 8. "CORRELATION" and "CORRESHORT"

The next two programs may be used to cross correlate binary codes, "CORRELATION" evaluates 8 times per interval while "CORRESHORT" evaluates only once. Further comments and instructions are contained in the remarks sections of the programs.

```

10 PRINT "THIS PROGRAM IS INTENDED
    TO PROVIDE CORRELATION CAPAB
    ILITIES FOR FINITE LENGTH
    BINARY CODES"
20 PRINT "IT DOES SIMPLE NUMERICAL
    CORRELATION BY FORMING ARRAY
    S, THEN CORRELATING THEM"
30 PRINT "
    "
40 PRINT "TO BEGIN, ENTER THE FIRST
    FUNCTION. LABEL IT A AND
    USE N AS THE INDEPENDENT
    VARIABLE. BEGIN AT 1000 AND
    END WITH RETURN."
50 PRINT " NEXT, ENTER THE SECOND
    FUNCTION THE SAME WAY, EXCEPT
    LABEL IT B AND USE M AS
    THE INDEPENDENT VARIABLE."
60 PRINT "THE PROGRAM CALLS THESE
    AS SUBROUTINES. TO RESTART
    THE PROGRAM ENTER RUN20."
70 END
80 INPUT "ENTER THE LENGTH OF THE
    FIRST FUNCTION IN UNITS
    --- "; L1
90 INPUT "ENTER THE LENGTH OF THE
    SECOND FUNCTION IN UNITS
    --- "; L2
100 Q = (L1 + L2)*8
110 DIM A(Q)
120 REM A IS THE NAME GIVEN TO
    THE FIRST ARRAY
130 DIM B(Q)
140 REM B IS THE NAME GIVEN TO
    THE SECOND ARRAY
150 DIM C(Q)
160 REM C IS THE NAME GIVEN TO
    THE OUTPUT ARRAY
170 FOR N = .0625 TO L1 - .0625
    STEP .125
180 GOSUB 1000
190 A(INT (N*8 + .5)) = A
200 NEXT
210 FOR M = .0625 TO L2 - .0625
    STEP .125
220 GOSUB 2000
230 B(INT (M*8 + .5) + L1*8) = B
240 NEXT
250 FOR J = 0 TO Q
260 FOR K = 0 TO J
270 A = A(K)*B(Q - J + K)
280 ACC = ACC + A
290 NEXT K
300 C(J) = ACC
310 PRINT J / 8, C(J) / 8
320 ACC = 0
330 NEXT J
340 END
1000 IF N = 0 THEN A = 1
1010 IF N > 0 AND N < 5 THEN A = 1

```

```

1020 IF N > = 5 AND N < 7 THEN A
    = - 1
1030 IF N > = 7 AND N < 9 THEN A
    = 1
1040 IF N > = 9 AND N < 10 THEN A
    = - 1
1050 IF N > = 10 AND N < 11 THEN A
    = 1
1060 IF N > = 11 AND N < 12 THEN A
    = - 1
1070 IF N > = 12 AND N < 13 THEN A
    = 1
1080 RETURN
2000 B = A(INT (M*8 + .5))
2010 RETURN
2015 IF M = 5 THEN B = 0
2020 IF M > 5 AND M < 7 THEN B =
    - 1
2025 IF M = 7 THEN B = 0
2030 IF M > 7 AND M < 9 THEN B = 1
2035 IF M = 9 THEN B = 0
2040 IF M > 9 AND M < 11 THEN B =
    - 1
2045 IF M = 10 THEN B = 0
2050 IF M > 10 AND M < 11 THEN B
    = 1
2055 IF M = 11 THEN B = 0
2060 IF M > 11 AND M < 12 THEN B
    = - 1
2065 IF M = 12 THEN B = 0
2070 IF M > 12 AND M < 13 THEN B
    = 1
2080 RETURN

```

```

1 REM CORRESHORT BY L.J.HERRINGTO
    N
10 PRINT "THIS PROGRAM IS INTENDED
    TO PROVIDE CORRELATION CAPAB
    ILITIES FOR FINITE LENGTH
    BINARY CODES"
20 PRINT "IT DOES SIMPLE NUMERICAL
    CORRELATION BY FORMING ARRAY
    S, THEN CORRELATING THEM"
30 PRINT "
    "
40 PRINT "TO BEGIN, ENTER THE FIRST
    FUNCTION. LABEL IT A AND
    USE N AS THE INDEPENDENT
    VARIABLE. BEGIN AT 1000 AND

```

```

END WITH RETURN."
50 PRINT " NEXT, ENTER THE SECOND
FUNCTION THE SAME WAY, EXCEPT
LABEL IT B AND USE M AS
THE INDEPENDENT VARIABLE."
60 PRINT "THE PROGRAM CALLS THESE
AS SUBROUTINES. TO RESTART
THE PROGRAM ENTER RUN2C."
70 END
80 INPUT "ENTER THE LENGTH OF THE
FIRST FUNCTION IN UNITS
--- "; L1
90 INPUT "ENTER THE LENGTH OF THE
SECOND FUNCTION IN UNITS
--- "; L2
100 Q = L1 + L2
110 DIM A(Q)
120 REM A IS THE NAME GIVEN TO
THE FIRST ARRAY
130 DIM B(Q)
140 REM B IS THE NAME GIVEN TO
THE SECOND ARRAY
150 DIM C(Q)
160 REM C IS THE NAME GIVEN TO
THE OUTPUT ARRAY
170 FOR N = .5 TO L1 - .5
180 GOSUB 1000
190 A(N) = A
200 NEXT
210 FOR M = .5 TO L2 - .5
220 GOSUB 2000
230 B(M + L1) = B
240 NEXT
250 FOR J = 0 TO Q
260 FOR K = 0 TO J
270 A = A(K)*B(Q - J + K)
280 ACC = ACC + A
290 NEXT K
300 C(J) = ACC
310 ACC = 0
320 NEXT J
330 FOR T = 0 TO Q
340 PRINT T, C(T)
350 NEXT
360 END
1000 IF N >= 0 AND N < 3 THEN A
= 1
1010 IF N >= 3 AND N < 6 THEN A
= - 1
1020 IF N >= 6 AND N < 7 THEN A
= 1
1030 IF N >= 7 AND N < 9 THEN A
= - 1
1040 IF N >= 9 AND N < 10 THEN A
= 1
1050 IF N >= 10 AND N < 11 THEN A
= - 1
1060 RETURN
2000 B = A(M)
2010 RETURN
]

```

Program 9. "MACHLETT POWER TUBE CALCULATOR"

This program automates the worksheet of the Machlett Power Tube Calculator. It requires an operator who already knows how to use the "calculator" to input the data on power tube operating conditions and to enter the data read from the cosine scale. The program then does the routine calculations and prints the results or stores to floppy disk if requested for later printing.

```

1 REM MACHLETT POWER TUBE CALCULA
TOR BY L.J.HERRINGTON
10 PRINT "THIS PROGRAM AUTOMATES
THE WORKSHEET"
20 PRINT "OF THE MACHLETT POWER
TUBE CALCULATOR"
30 PRINT
40 PRINT "DO YOU WANT HELP? (Y
OR N)"
50 INPUT A$
60 IF ASC (A$) = 89 THEN GOSUB 1670
70 DIM IB(6), G1(6), G2(6)
80 PRINT
90 PRINT "IS THIS A COMMON CATHODE
OR COMMON GRID"
100 INPUT "CIRCUIT (CC OR CG)";
A$
110 PRINT A$
120 PRINT
130 INPUT "TETRODE OR TRIODE?";
B$
140 IF BS = "TETRODE" OR B$ = "TRIODE

```

```

E" THEN 180
150 PRINT
160 PRINT "MUST BE A TETRODE OR
      A TRIODE."
170 GOTO 1470
180 PRINT
190 INPUT "ENTER THE DC PLATE VOLTAGE"; EB
200 PRINT
210 INPUT "ENTER THE MINIMUM PLATE
      VOLTAGE"; EM
220 PRINT
230 INPUT "ENTER THE DC BIAS VOLTAGE"; BIAS
240 PRINT
250 INPUT "ENTER THE PEAK GRID VOLTAGE"; EP
260 PRINT
270 IF B$ = "TRIODE" THEN 290
280 INPUT "ENTER THE SCREEN VOLTAGE"; E2
290 PRINT
300 FOR I = 0 TO 90 STEP 15
310 PRINT "ENTER THE INSTANTANEOUS
      PLATE CURRENT"
320 PRINT "AT "; I; " DEGREES"
330 INPUT IB(I / 15)
340 PRINT
350 PRINT "ENTER THE INSTANTANEOUS
      GRID CURRENT"
360 PRINT "AT "I" DEGREES"
370 INPUT G1(I / 15)
380 PRINT
390 IF B$ = "TRIODE" THEN 430
400 PRINT "ENTER THE INSTANTANEOUS
      SCREEN CURRENT"
410 PRINT "AT "; I; " DEGREES"
420 INPUT G2(I / 15)
430 NEXT
440 PRINT
450 INPUT "DO YOU WANT TO CHANGE
      ANY OF THE INSTANTANEOUS
      VALUES? (Y OR N)"; L$
460 IF L$ = "Y" THEN 1520
470 AVIB = (IB(0) / 2 + IB(1) + IB(2)
      + IB(3) + IB(4) + IB(5))
      / 12
480 FIB = (IB(0) + IB(1)*1.93 + IB(2)
      *1.73 + IB(3)*1.41 + IB(4)
      + IB(5)*.52) / 12
490 A1 = (G1(0) / 2 + G1(1) + G1(2)
      + G1(3) + G1(4) + G1(5))
      / 12
500 FG1 = (G1(0) + G1(1)*1.93 + G1(2)
      *1.73 + G1(3)*1.41 + G1(4)
      + G1(5)*.52) / 12
510 IF B$ = "TRIODE" THEN 530
520 A2 = (G2(0) / 2 + G2(1) + G2(2)
      + G2(3) + G2(4) + G2(5))
      / 12
530 IF A$ = "CG" THEN 580
540 PO = (EB - EM)*FIB / 2
550 PD = (EP - BIAS)*FG1 / 2
560 RL = (EB - EM) / FIB
570 GOTO 610
580 PO = (EB - EM + EP - BIAS)*FIB
      / 2
590 PD = (EP - BIAS)*(FG1 + FIB)
      / 2

```

```

600 RL = (EB - EM + EP - BIAS) / FIB
610 PIN = EB*AVIB
620 PP = PIN - PO
630 EFF = PO / PIN
640 GAIN = PO / PD
650 PC = -BIAS*A1
660 P1 = PD - PC
670 PRINT
680 INPUT "IS PROTECTIVE BIAS USED?
      (Y OR N)"; G$
690 IF G$ = "Y" THEN 730
700 PRINT
710 RC = -BIAS / A1
720 GOMD 770
730 PRINT
740 INPUT "ENTER THE PROTECTIVE
      BIAS VOLTAGE"; ECC
750 PRINT
760 RC = (ABS(BIAS) - ABS(ECC))
      / A1
770 IF B$ = "TRIODE" THEN 790
780 P2 = E2*A2
790 INPUT "IS A PRINTER IN USE?
      (Y OR N)"; H$
800 IF H$ = "N" GOTO 1240
810 PRINT
      : INVERSE
820 PRINT "ALIGN THE PAGE IN THE
      PRINTER."
830 NORMAL
840 PRINT
850 INPUT "WANT A FULL PRINTOUT
      OR A SHORT ONE? (F OR S)";
      J$
860 IF J$ = "F" THEN 900
870 PR# 1
880 PRINT
890 GOTO 1240
900 IF J$ = "S" THEN 1240
      : PRINT
910 INPUT "WHAT TUBE TYPE?"; C$
920 PRINT
930 INPUT "WHAT IS THE DATE?"; D$
940 PRINT
950 INPUT "WHAT CLASS OF SERVICE?";
      E$
960 PRINT
970 INPUT "PERSON PERFORMING ANALYSIS?";
      F$
980 PRINT
990 PR# 1
1000 PRINT
1010 PRINT "TUBE TYPE"; TAB(20);
      C$
1020 PRINT
1030 PRINT "DATE"; TAB(25); D$
1040 PRINT
1050 PRINT "CLASS OF SERVICE"; TAB(13);
      E$
1060 PRINT
1070 PRINT "BY"; TAB(27); F$
1080 PRINT
1090 PRINT "EB = "; EB, "EC1 = ";
      BIAS, "EC2 = "; E2
1100 PRINT
1110 PRINT "EM = "; EM, "EPG = ";
      EP

```

```

1120 PRINT "      -----"
1130 PRINT "EP = "; (EB - EM), "EG
      = "; (EP - RIAS)
1140 PRINT
1150 HTAB (10)
      : PRINT "PLATE";
      : HTAB (20)
      : PRINT "GRID";
      : HTAB (30)
      : PRINT "SCREEN"
1160 HTAB (10)
      : PRINT "CURRENT";
      : HTAB (20)
      : PRINT "CURRENT";
      : HTAB (30)
      : PRINT "CURRENT"
1170 PRINT
1180 PRINT "ANGLE"
1190 FOR I = 0 TO 6
1200 PRINT I*15;
      : HTAB (10)
      : PRINT INT (IB(I)*10 + .5)
        / 10;
      : HTAB (20)
      : PRINT INT (G1(I)*10 + .5)
        / 10;
      : HTAB (30)
      : PRINT INT (G2(I)*10 + .5)
        / 10
1210 PRINT
1220 NEXT
1230 PRINT
      : PRINT
1240 PRINT
1260 PRINT " IB = "; INT (AVIB*10
      + .5) / 10;
      : HTAB (14)
      : PRINT "IC1 = "; INT (A1*180
      + .5) / 100;
      : HTAB (26)
      : PRINT "IC2 = "; INT (A2*180
      + .5) / 100
1270 PRINT
1280 PRINT " IP = "; INT (FIB*10
      + .5) / 10;
      : HTAB (14)
      : PRINT "IG1 = " INT (FG1*180
      + .5) / 100
1290 PRINT
      : PRINT
1300 PRINT " PO = "; INT (PO / 100
      + .5) / 10; "KW";
      : HTAB (20)
      : PRINT "PD = "; INT (PD*10 + .5)
        / 10
1310 PRINT
1320 PRINT " PIN = "; INT (PIN / 100
      + .5) / 10; "KW";
      : HTAB (20)
      : PRINT "PC = "; INT (PC*10 + .5)
        / 10
1330 PRINT
1340 PRINT " PP = "; INT (PP / 100
      + .5) / 10; "KW";
      : HTAB (19)
      : PRINT "PG1 = "; INT (P1*10 + .5)
        / 10
1350 PRINT
1360 PRINT " RL = "; INT (RL*10
      + .5) / 10;
      : HTAB (20)
      : PRINT "RC = "; INT (RC*10 + .5)
        / 10
1370 PRINT
1380 PRINT " EFF = "; INT (PO / PIN*1
      00 + .5) / 100;
      : HTAB (19)
      : PRINT "PG2 = "; INT (P2*10 + .5)
        / 10
1390 PRINT
1400 PRINT "GAIN = "; INT (GAIN*10
      + .5) / 10;
      : HTAB (19)
      : PRINT "ECC = "; ECC
1410 PRINT
      : PRINT
      : PRINT
      : PRINT
1420 HTAB (18)
      : PRINT "DONE"
1430 PR# 0
1435 INPUT "DO YOU WANT TO WRITE
      TO DISK FOR LATER PRINTING?
      (Y OR N) "; P1$
1440 IF P1$ = "Y" THEN GOSUB 1750
1450 IF H$ = "N" THEN 1510
1460 PRINT
1470 INPUT "WANT ANOTHER COPY?";
      K$
1480 IF K$ = "N" THEN 1510
1490 IF K$ = "Y" AND J$ = "F" THEN 99
      0
1500 PR# 1: GOTO 1240
1510 END
1520 INPUT "WANT TO CHANGE PLATE,
      GRID, OR SCREEN VALUES?
      (P, G, OR S)"; M$
1530 PRINT
1540 INPUT "WHAT ANGLE IN DEGREES?";
      X
1550 PRINT
1560 INPUT "WHAT IS THE NEW VALUE?";
      Y
1570 IF M$ = "P" THEN 1610
1580 IF M$ = "G" THEN 1630
1590 IF M$ = "S" THEN 1650
1600 GOTO 440
1610 IB(X / 15) = Y
1620 GOTO 440
1630 G1(X / 15) = Y
1640 GOTO 440
1650 G2(X / 15) = Y
1660 GOTO 440
1670 PRINT "THIS PROGRAM INTERACTS
      WITH AN OPERATOR TO ANALYZE
      THE PERFORMANCE OF TRIODES
      AND TETRODES IN COMMON CATHO
      DE AND COMMON GRID CONFIGURAT
      IONS."
1680 PRINT
1690 PRINT "THE OPERATOR MUST FIRST
      HAVE A COSINE SCALE AND
      THE TUBE'S CONSTANT CURRENT
      CHARACTERISTICS IN HIS/HER
      POSSESSION AND KNOW HOW TO
      USE THEM."
1700 PRINT
1710 PRINT "TO OBTAIN THIS INFORMATIO

```

```

N THE USER IS REFERRED TO
THE ARTICLE:THE MACHLETT
POWER TUBE CALCULATOR: FOUND
IN THE MACHLETT CATHODE
PRESS VOL.22,NO. 4,1965;SIMI
LAR DATA MAY BE FOUND IN
:REFERENCE DATA FOR RADIO
ENGINEERS:"
1720 PRINT
1730 PRINT "THE OPERATOR MUST DRAW
HIS OWN LOAD LINE AND PROVID
E THE REQUESTED INFORMATION.
THE PROGRAM THEN DOES THE
ANALYSIS AND PRINTS THE
RESULTS."
1740 END
1750 INPUT "WHAT TUBE TYPE?"; C$
1760 PRINT
1770 INPUT "WHAT IS THE DATE?"; D$
1780 PRINT
1790 INPUT "WHAT CLASS OF SERVICE?";
E$
1800 PRINT
1810 INPUT "PERSON PERFORMING ANALYSI
S?"; F$
1820 PRINT
1830 GOTO 1840
1840 REM MAKE POWER TUBE DATA
1850 T$ = "[D]"
: REM C7TL-D
1860 INPUT "WHICH FILE NUMBER?";
J
1870 PRINT T$; "OPEN POWER TUBE DATA"
; J
1880 PRINT T$; "WRITE POWER TUBE
DATA"; J
1890 PRINT A$
: PRINT B$
: PRINT C$
: PRINT D$
1900 PRINT E$
: PRINT F$
: PRINT G$
1910 PRINT EB
: PRINT EM
: PRINT BLAS
: PRINT EP
1920 PRINT E2
1930 FOR I = 0 TO 6
1940 PRINT IB(I)
: PRINT GI(I)
: PRINT G2(I)
1950 NEXT I
1960 PRINT AVIB
: PRINT FIB
1970 PRINT AI
: PRINT FGI
1980 PRINT A2
1990 PRINT PO
: PRINT PD
: PRINT RL
2000 PRINT PIN
: PRINT PP
: PRINT EFF
2010 PRINT GAIN
: PRINT PC
: PRINT P1
2020 PRINT RC
: PRINT EGC
: PRINT P2
2030 PRINT T$; "CLOSE POWER TUBE
DATA"; J
2040 PRINT
2050 PRINT "DONE"
2060 RETURN

```

1

Program 10. "MACHPRINT"

This program will print the data stored on disk when that option is used in Program 9.

```

1 REM MACHPRINT BY L.J.HERRINGTON
10 REM THIS PROGRAM WILL PRINT
THE DATA RECORD CREATED
BY MACHLETT CALC/DISC STORAG
E
20 INVERSE
30 PRINT "ALIGN THE PAGE IN THE
PRINTER"
40 NORMAL
: PRINT
: PRINT
50 PRINT "HIT ANY KEY TO CONTINUE"
60 PRINT
70 GET Z$
80 GOTO 660
90 PRINT
100 PR# 1
110 PRINT
120 PRINT "TUBE TYPE"; TAB(20);
C$
130 PRINT
140 PRINT "DATE"; TAB(25); D$
150 PRINT
160 PRINT "CLASS OF SERVICE"; TAB(13
); E$

```

```

170 PRINT
180 PRINT "BY"; TAB(27); F$
190 PRINT
200 PRINT "EB = "; EB, "EC1 = ";
    BIAS, "EC2 = "; E2
210 PRINT
220 PRINT "EM = "; EM, "EPG = ";
    EP
230 PRINT "
    _____"
240 PRINT "EP = "; (EB - EM), "EG
    = "; (EP - BIAS)
250 PRINT
260 HTAB (10)
    : PRINT "PLATE";
    : HTAB (20)
    : PRINT "GRID";
    : HTAB (30)
    : PRINT "SCREEN"
270 HTAB (10)
    : PRINT "CURRENT";
    : HTAB (20)
    : PRINT "CURRENT";
    : HTAB (30)
    : PRINT "CURRENT"
280 PRINT
290 PRINT "ANGLE"
300 FOR I = 0 TO 6
310 PRINT I*15;
    : HTAB (10)
    : PRINT INT (IB(I)*10 + .5)
    : / 10;
    : HTAB (20)
    : PRINT INT (G1(I)*10 + .5)
    : / 10;
    : HTAB (30)
    : PRINT INT (G2(I)*10 + .5)
    : / 10
320 PRINT
330 NEXT
340 PRINT
    : PRINT
350 PRINT
360 PRINT " IB = "; INT (AVIB*10
    + .5) / 10;
    : HTAB (14)
    : PRINT "IC1 = "; INT (A1*10 + .5)
    : / 100;
    : HTAB (26)
    : PRINT "IC2 = "; INT (A2*10 + .5)
    : / 100
370 PRINT
380 PRINT " IP = "; INT (FIB*10
    + .5) / 10;
    : HTAB (14)
    : PRINT "IG1 = " INT (FG1*10 + .5)
    : / 100
390 PRINT
    : PRINT
400 PRINT " PO = "; INT (PO / 100
    + .5) / 10; "KW";
    : HTAB (20)
    : PRINT "PD = "; INT (PD*10 + .5)
    : / 10
410 PRINT
420 PRINT " PIN = "; INT (PIN / 100
    + .5) / 10; "KW";
    : HTAB (20)
    : PRINT "PC = "; INT (PC*10 + .5)
    : / 10
430 PRINT
440 PRINT " PP = "; INT (PP / 100
    + .5) / 10; "KW";
    : HTAB (19)
    : PRINT "PG1 = "; INT (P1*10 + .5)
    : / 10
450 PRINT
460 PRINT " RL = "; INT (RL*10
    + .5) / 10;
    : HTAB (20)
    : PRINT "RC = "; INT (RC*10 + .5)
    : / 10
470 PRINT
480 PRINT " EFF = "; INT (PO / PIN*1
    0 + .5) / 100;
    : HTAB (19)
    : PRINT "PG2 = "; INT (P2*10 + .5)
    : / 10
490 PRINT
500 PRINT "GAIN = "; INT (GAIN*10
    + .5) / 10;
    : HTAB (19)
    : PRINT "ECC = "; ECC
510 PRINT
    : PRINT
    : PRINT
    : PRINT
520 HTAB (18)
    : PRINT "DONE"
530 PR# 0
540 IF H$ = "N" THEN 610
550 PRINT
560 INPUT "WANT ANOTHER COPY?";
    K$
570 IF K$ = "N" THEN 610
580 IF K$ = "Y" THEN 100
590 PR# 1: GOTO 350
600 PRINT
610 INPUT "DO YOU WANT TO DELETE
    THE FILE JUST PRINTED? (Y
    OR N)"; Q$
620 IF Q$ = "Y" THEN 640
630 END
640 PRINT T$; "DELETE POWER TUBE
    DATA"; J
650 END
660 REM PRINT POWER TUBE DATA
670 T$ = "[D]"
    : REM CTRL-D
680 INPUT "WHICH FILE NUMBER?";
    J
690 PRINT T$; "OPEN POWER TUBE DATA"
    ; J
700 PRINT T$; "READ POWER TUBE DATA"
    ; J
710 INPUT A$
    : INPUT F$
    : INPUT G$
    : INPUT D$
720 INPUT E$
    : INPUT F$
    : INPUT G$
730 INPUT EB
    : INPUT EM
    : INPUT BIAS
    : INPUT EP
740 INPUT E2
750 FOR I = 0 TO 6
760 INPUT IB(I)
    : INPUT G1(I)
    : INPUT G2(I)

```

```
770 NEXT I
780 INPUT AVIB
: INPUT FIB
790 INPUT AI
: INPUT FG1
800 INPUT A2
: INPUT FO
810 INPUT ED
: INPUT RL
820 INPUT PIN
: INPUT PP
: INPUT EFF
830 INPUT GAIN
: INPUT PC
: INPUT P1
840 INPUT RC
: INPUT ECC
: INPUT P2
850 PRINT T$; "CLOSE POWER TUBE
DATA"; J
860 PRINT
870 GOTO 90
```

1

Program 11. "GRAPH MAKER"

GR. 1

This program interacts with the user to create graphs. It will plot either linear or log scale along either axis. The user may enter any header and limits desired for either axis. The program will then create and label the desired graph. The user is practically limited to about 15 divisions vertically and 20 horizontally in linear mode, or 3 decades vertically and 4 horizontally in the logarithmic mode.

The program requires access to two binary files: "ALPHANUMERICS" in which character information is stored for the headers, and "SHAPE TABLE" which is a shape table of the numerals and plotting symbols used.

After the graph is created the user has 3 options: 1) store it to disk for use elsewhere, 2) plot points on it manually by entering the coordinates desired, or 3) print the graph using a Silentype printer.

An additional note is required concerning "ALPHANUMERICS". This compact labeling system used in the headers is not based on the shape table functions of the Apple Computer, but is instead based on the byte structure of the graphics memory as deciphered by Professor Gernot Metze.

```

1 REM GRAPH MAKER BY L.J.HERRINGT
  ON
10 LOMEM: 18432
20 PRINT
30 INPUT "LEFT LIMIT ON X AXIS?
"; XN
: PRINT
40 INPUT "RIGHT LIMIT ON X AXIS?
"; XM
: PRINT
50 INPUT "DO YOU WANT A LINEAR
OR A LOG PLOT ALONG THE
X AXIS? (LIN OR LOG)
"; HL$
: PRINT
60 IF HL$ = "LIN" THEN 90
70 IF HL$ = "LOG" THEN 130
80 GOTO 50
90 INPUT "HORIZONTAL INTERVAL?
"; XI
: PRINT
100 B = (XM - XN) / XI
110 IF B <= 25 GOTO 130
120 PRINT "DECREASE THE SEPARATION
BETWEEN XMAX AND XMIN OR
INCREASE THE INTERVAL"
: PRINT
: GOTO 30
130 INPUT "X AXIS HEADER?"; XA$
: PRINT
140 XI = LEN (XA$)
150 IF XI > 39 THEN PRINT "TOO LONG"

: PRINT
: GOTO 130
160 INPUT "LOWER LIMIT ON Y AXIS?
"; YN
: PRINT
170 INPUT "UPPER LIMIT ON Y AXIS?
"; YM
: PRINT
180 INPUT "DO YOU WANT A LINEAR
OR A LOG PLOT ALONG THE
Y AXIS? (LIN OR LOG)
"; VL$
: PRINT
190 IF VL$ = "LIN" THEN 220
200 IF VL$ = "LOG" THEN 260
210 GOTO 180
220 INPUT "VERTICAL INTERVAL? ";
YI
: PRINT
230 A = (YM - YN) / YI
240 IF A <= 20 GOTO 260
250 PRINT "DECREASE THE SEPARATION
BETWEEN YMAX AND YMIN OR
INCREASE THE INTERVAL"
: PRINT
: GOTO 160
260 INPUT "Y AXIS HEADER?"; YA$
: PRINT
270 Y1 = LEN (YA$)
280 IF Y1 > 31 THEN PRINT "TOO LONG"

: PRINT
: GOTO 260
290 INPUT "LINE DENSITY? "; LD
: PRINT
300 HCOLOR= 3
: SCALE= 1
: HGR
: POKE - 16302, 0
: HPLOT 20, 180
: CALL 62454
: HCOLOR= 0
310 D$ = "[D]"
: REM CTRL-D
320 PRINT D$"BLOAD ALPHANUMERICS,A$4
000"
330 X4 = INT ((40 - X1) / 2)
340 FOR LINE = 1 TO 7
350 FOR I = 1 TO X1
360 X1$ = RIGHT$ (XA$, X1 - I
+ 1)
370 X2 = (ASC (X1$) - 32)*7
+ 16687
380 ADR = 9168 + LINE*1024 + X4
+ I
390 X3 = PEEK (X2 + LINE)
400 POKE ADR, X3
410 NEXT I
420 NEXT LINE
430 YU = 95 - INT (Y1*3)
440 FOR I = 1 TO Y1
450 Y1$ = RIGHT$ (YA$, Y1 + 1
- I)
460 Y2 = (ASC (Y1$) - 32)*5 + 1638
4
470 FOR J = 1 TO 5
480 Y3 = PEEK (Y2 + J - 1)
490 Y4 = YU + I*6 + J
500 K1 = INT (Y4 / 64)
: J1 = INT ((Y4 - K1*64) / 8)
: I1 = Y4 - K1*64 - J1*8
510 N = 8192 + 1024*I1 + 128*J1
+ 40*K1
520 POKE N, Y3
530 NEXT J
540 NEXT I
550 PRINT D$; "BLOAD SHAPE TABLE,A$4
000"
560 POKE 232, 0
: POKE 233, 64
: ROT= 0
: SCALE= 1
570 IF HL$ = "LOG" THEN GOSUB 1000
580 IF HL$ = "LIN" THEN GOSUB 3000
590 IF VL$ = "LOG" THEN GOSUB 2000
600 IF VL$ = "LIN" THEN GOSUB 3500
610 FOR I = 1 TO 4000
: NEXT
: REM PAUSE
620 TEXT
630 INPUT "WANT TO PLOT SOME POINTS?
(Y OR N) "; PL$
: PRINT
640 IF PL$ = "Y" THEN GOSUB 5010
650 INPUT "WANT TO PRINT GRAPH ON
SILENTYPE? (Y OR N) ";
PG$
: PRINT
660 PH$ = "[Q]"
: REM CTRL-Q:PI$=":REM CTRL-H
670 IF PG$ = "Y" THEN PRINT
: POKE - 12529, 255
: POKE - 12528, 7
: POKE - 12527, 18
: PR# 1
: PRINT PH$
680 PR# 0
690 PRINT "WANT TO SAVE GRAPH ON
DISK? (Y OR N)"

```

ORIGINAL PAGE IS  
OF POOR QUALITY

147

```

: PRINT
700 INPUT SG$
710 IF SG$ = "N" THEN 770
720 INPUT "NAME OF GRAPH?"; GN$
: PRINT
730 PRINT D$"BSAVE"; GN$; ",A$2000,L
    $2000"
740 HTAB (12)
: PRINT "GRAPH NOW ON DISK"
: PRINT
770 END
1000 UO = LOG (10)
: LN = LOG (XN) / UO
: LM = LOG (XM) / UO
: U1 = INT (LN)
: U2 = INT (LM)
1010 IF U2 < > LM THEN U8 = 0
: GOTO 1030
1020 U8 = 1
1030 HIN = INT (250 / (LM - LN))
1040 FOR X = U1 TO U2 + U8
1050 U3 = 29 + INT ((X - LN)*HIN
    + .5)
1060 U4 = INT (EXP (UO*X)*1000
    + .5) / 1000
1070 U6 = U3
1080 IF X < LN GOTO 1110
1090 IF X > LM GOTO 1210
1100 GOSUB 1290
1110 IF X + .30103 < INT (LN*1E8
    + .5) / 1E8 GOTO 1160
1120 IF X + .30103 > LM GOTO 1210
1130 U4 = INT (EXP (UO*(X + .30103)
    )*1000 + .5) / 1000
1140 U6 = U3 + INT ((.30103*HIN)
    + .5)
1150 GOSUB 1290
1160 IF X + .69897 < INT (LN*1E8
    + .5) / 1E8 GOTO 1210
1170 IF X + .69897 > LM GOTO 1210
1180 U4 = INT (EXP (UO*(X + .69897)
    )*1000 + .5) / 1000
1190 U6 = U3 + INT ((.69897*HIN)
    + .5)
1200 GOSUB 1290
1210 NEXT X
1220 U4 = XN
1230 U6 = 29
1240 GOSUB 1290
1250 U4 = XM
1260 U6 = 29 + HIN*(LM - LN)
1270 GOSUB 1290
1280 RETURN
1290 FOR I = 0 TO 174 STEP LD
: H PLOT U6, I
: NEXT
1300 IF U6 > 268 THEN RETURN
1310 S$ = STR$ (U4)
1320 AN = U4
1330 IF U4 > = 1000 THEN GOSUB 4500
1340 IF U4 < = .001 THEN GOSUB 4500
1350 S3 = LEN (S$)
1360 S2 = 183
1370 FOR J = 1 TO S3
1380 S1 = U6 - (S3 - 1)*2 + (J
    - 1)*4
1390 GOSUB 4000
1400 NEXT J
1410 RETURN
2000 UO = LOG (10)
: LN = LOG (YN) / UO
: LM = LOG (YM) / UO
: U1 = INT (LN)
: U2 = INT (LM)
2010 IF U2 < > LM THEN U8 = 0
: GOTO 2030
2020 U8 = 1
2030 VIN = INT (174 / (LM - LN))
2040 FOR Y = U1 TO U2 + U8
2050 U3 = 174 - INT ((Y - LN)*VIN
    + .5)
2060 U4 = INT (EXP (UO*Y)*10000
    + .5) / 10000
2070 U6 = U3
2080 IF Y < LM GOTO 2110
2090 IF Y > LM GOTO 2210
2100 GOSUB 2290
2110 IF Y + .30103 < INT (LN*1E8
    + .5) / 1E8 GOTO 2160
2120 IF Y + .30103 > LM GOTO 2210
2130 U4 = INT (EXP (UO*(Y + .30103)
    )*10000 + .5) / 10000
2140 U6 = U3 - INT ((.30103*VIN)
    + .5)
2150 GOSUB 2290
2160 IF Y + .69897 < INT (LN*1E8
    + .5) / 1E8 GOTO 2210
2170 IF Y + .69897 > LM GOTO 2210
2180 U4 = INT (EXP (UO*(Y + .69897)
    )*10000 + .5) / 10000
2190 U6 = U3 - INT ((.69897*VIN)
    + .5)
2200 GOSUB 2290
2210 NEXT Y
2220 U4 = YN
2230 U6 = 174
2240 GOSUB 2290
2250 U4 = YM
2260 U6 = 174 - VIN*(LM - LN)
2270 GOSUB 2290
2280 RETURN
2290 FOR I = 29 TO 279 STEP LD
: H PLOT I, U6
: NEXT
2300 IF U6 < 8 GOTO 2410
2310 S$ = STR$ (U4)
2320 AN = U4
2330 IF AN > = 1000 THEN GOSUB 4500
2340 IF AN < = .001 THEN GOSUB 4500
2350 S3 = LEN (S$)
2360 FOR J = 1 TO S3
2370 S1 = 15 - (S3 - 1)*2 + (J
    - 1)*4
2380 S2 = U6
2390 GOSUB 4000
2400 NEXT J
2410 RETURN
3000 B1 = INT (250 / B)
3010 FOR X = 0 TO 250 / B1 STEP
    SGN (B1)
3020 FOR I = 0 TO 174 STEP LD
: H PLOT 29 + B1*X, I
: NEXT I
3030 IF 29 + X*B1 > 260 GOTO 3120
3040 AN = XN + X*XI
3050 S$ = STR$ (AN)
3051 IF AN = 0 THEN GOTO 3060
3052 IF AN < = .001 THEN GOSUB 4500
3054 IF AN > = 1000 THEN GOSUB 4500
3060 S3 = LEN (S$)
3070 FOR J = 1 TO S3

```

```

3080 S1 = 29 + X*B1 + (J - 1)*4
      - (S3 - 1)*2
3090 S2 = 183
3100 GOSUB 4000
3110 NEXT J
3120 NEXT X
3130 RETURN
3500 A1 = INT (174 / A)
3510 FOR Y = 0 TO 174 / A1 STEP
      SGN (A1)
3520 FOR I = 29 TO 279 STEP LD
      : H PLOT I, 174 - A1*Y
      : NEXT
3530 AN = YN + Y*YI
3540 S$ = STR$ (AN)
3542 IF AN = 0 THEN GOTO 3550
3544 IF AN < = .001 THEN GOSUB 4500

3546 IF AN > = 1000 THEN GOSUB 4500

3550 S3 = LEN (S$)
3560 FOR J = 1 TO S3
3570 S1 = 15 + J*4 - S3*2
3580 S2 = 174 - A1*Y
3590 GOSUB 4000
3600 NEXT J
3610 NEXT Y
3620 RETURN
4000 REM THIS SBR NUMBERS LINES
4010 S1$ = RIGHT$ (LEFT$ (S$, J),
      1)
4020 IF S1$ = "." THEN DRAW 11 AT S1,
      S2
      : GOTO 4070
4030 IF S1$ = "0" THEN DRAW 10 AT S1,
      S2
      : GOTO 4070
4040 IF S1$ = "E" THEN DRAW 13 AT S1,
      S2
      : GOTO 4070
4050 IF S1$ = "-" THEN DRAW 14 AT S1,
      S2
      : GOTO 4070
4060 DRAW VAL (S1$) AT S1, S2
4070 RETURN
4500 REM THIS SBR CONVERTS TO EXP
      NOTATION
4510 E = LOG (AN) / LOG (10)
4520 E1 = INT (E)
4530 AM = INT (AN / 10*(E1 - 2) + .5)
      / 100
4540 S$ = LEFT$ (STR$ (AM), 4) + "E"
      + STR$ (E1)
4550 RETURN
5000 REM THIS SBR PROVIDES MANUAL
      GRAPH CAPABILITIES
5010 INPUT "HOW MANY POINTS?"; PN
      : PRINT
5020 POKE - 16301, 0
      : POKE - 16304, 0
5030 IF HL$ = "LOG" THEN XO = LOG (XN
      ) / UO
5040 IF VL$ = "LOG" THEN YO = LOG (YN
      ) / UO
5050 FOR I = 1 TO PN
5060 PRINT "ENTER X,Y COORDS OF
      POINT #"; I
      : PRINT
5070 INPUT XC, YC
5080 IF HL$ = "LOG" THEN X9 = 29
      + INT ((LOG (XC) / UO
      - XO)*HIN + .5)
      : GOTO 5100
5090 X9 = 29 + INT ((XC - XN)*B1
      / XI + .5)
5100 IF VL$ = "LOG" THEN Y9 = 174
      - INT ((LOG (YC) / UO
      - YO)*VIN + .5)
      : GOTO 5160
5110 Y9 = 174 - INT ((YC - YN)*A1
      / YI + .5)
5120 IF X9 < 29 THEN PRINT "X COORD
      TOO SMALL"
      : GOTO 5060
5130 IF X9 > 279 THEN PRINT "X
      COORD TOO LARGE"
      : GOTO 5060
5140 IF Y9 < 0 THEN PRINT "Y COORD
      TOO LARGE"
      : GOTO 5060
5150 IF Y9 > 174 THEN PRINT "Y
      COORD TOO SMALL"
      : GOTO 5060
5160 DRAW 15 AT X9, Y9
5170 NEXT I
5180 POKE - 16302, 0
      : FOR I = 1 TO 4000
      : NEXT
5190 TEXT
5200 RETURN

```

1

Program 12. "GRAPH DISPLAYER"

This short program permits the user to view any graph previously stored to disk.

```

1 REM GRAPH DISPLAYER BY L.J.HERR
      INGTON
10 INPUT "WHICH DISPLAY?"; A$
20 HGR : POKE - 16302, 0
30 D$ = "[D]"
      : REM CTRL-D
40 HCOLOR= 3
      : H PLOT 0, 179
      : CALL 62454
50 HCOLOR= 0
60 PRINT D$; "BLOAD"A$; ",A$2000"
70 END

```

1

## Program 13. "SHAPE DISPLAYER"

This program permits the user to examine the shapes on file in the shape table.

```

1 REM SHAPE DISPLAYER BY L.J.HERR
  INGTON
10 SCALE= 1
20 ROT= 0
30 HCOLOR= 3
40 D$ = "[D]"
: REM CTRL-D
50 PRINT D$; "BLOAD SHAPE TABLE,A$4
  000"
60 POKE 232, 00
: POKE 233, 64
70 HGR
80 FOR I = 1 TO PEEK (16384) STEP 1
  0
85   FOR J = 0 TO 9
89     IF I + J > PEEK (16384)
        THEN GOTO 95
90     DRAW I + J AT J*27, I + 20
95   NEXT J
100 NEXT I
110 END

```

## Program 14. "MEMORY EXAMINER"

This program uses the Spinwriter and prints the HEX version of the contents of a range of memory as seen through use of the Apple monitor. It was written because for some unexplained reason it was not possible to use the regular monitor commands to dump onto the Spinwriter.

```

1 REM MEMORY EXAMINER BY L.J.HERR
  INGTON
10 INPUT "ADDRESSES IN HEX OR DECIM
AL? "; A$
: PRINT
20 IF A$ = "HEX" THEN GOTO 400
30 INPUT "STARTING ADDRESS? ";
  ST
40 INPUT "ENDING ADDRESS? "; SP
50 PR# 1
60 PRINT
70 FOR I = ST TO 8 + SP STEP 8
80   IF A$ = "HEX" THEN GOTO 330
90   PRINT I;
:   HTAB (10)
100  FOR J = 0 TO 7
110   A1 = INT (PEEK (I + J) / 16)
120   A2 = PEEK (I + J) - A1*16
130   IF A1 = 10 THEN PRINT "A";
:   GOTO 200
140   IF A1 = 11 THEN PRINT "B";
:   GOTO 200
150   IF A1 = 12 THEN PRINT "C";
:   GOTO 200
160   IF A1 = 13 THEN PRINT "D";
:   GOTO 200
170   IF A1 = 14 THEN PRINT "E";
:   GOTO 200
180   IF A1 = 15 THEN PRINT "F";
:   GOTO 200
:   PRINT A1;

```

```

200 IF A2 = 10 THEN PRINT "A";
: GOTO 270
210 IF A2 = 11 THEN PRINT "B";
: GOTO 270
220 IF A2 = 12 THEN PRINT "C";
: GOTO 270
230 IF A2 = 13 THEN PRINT "D";
: GOTO 270
240 IF A2 = 14 THEN PRINT "E";
: GOTO 270
250 IF A2 = 15 THEN PRINT "F";
: GOTO 270
260 PRINT A2;
270 PRINT " ";
280 NEXT J
: PRINT
290 PRINT
300 NEXT I
: PRINT
310 PR# 0
320 END
330 B1 = INT (I / 4096)
340 B2 = INT ((I - B1*4096) / 256)
350 B3 = INT ((I - B1*4096 - B2*256)
/ 16)
360 B4 = INT (I - B1*4096 - B2*256
- B3*16)
370 GOTO 710
380 PRINT B1$; B2$; B3$; B4$;
: HTAB (10)
390 GOTO 100
400 INPUT "ENTER HEX STARTING ADDRESS
S "; ST$
410 PRINT
420 INPUT "ENTER HEX END ADDRESS
"; SP$
430 PRINT
440 H1$ = ST$
: GOSUB 490
450 ST = G6
460 H1$ = SP$
: GOSUB 490
470 SP = G6
480 GOTO 50
490 H2$ = RIGHT$ (LEFT$ (H1$, 1),
1)
500 H3$ = RIGHT$ (LEFT$ (H1$, 2),
1)
510 H4$ = RIGHT$ (LEFT$ (H1$, 3),
1)
520 H5$ = RIGHT$ (LEFT$ (H1$, 4),
1)
530 G$ = H2$
: GOSUB 630
540 G2 = G*4096
550 G$ = H3$
: GOSUB 630
560 G3 = G*256
570 G$ = H4$
: GOSUB 630
580 G4 = G*16
590 G$ = H5$
: GOSUB 630
600 G5 = G
610 G6 = G2 + G3 + G4 + G5
620 RETURN
630 IF G$ = "A" THEN G = 10
: RETURN
640 IF G$ = "B" THEN G = 11
: RETURN
650 IF G$ = "C" THEN G = 12
: RETURN
660 IF G$ = "D" THEN G = 13
: RETURN
670 IF G$ = "E" THEN G = 14
: RETURN
680 IF G$ = "F" THEN G = 15
: RETURN
690 G = VAL (G$)
700 RETURN
710 B1$ = STR$ (B1)
720 B2$ = STR$ (B2)
730 B3$ = STR$ (B3)
740 B4$ = STR$ (B4)
750 C$ = B1$
: GOSUB 840
760 B1$ = C$
770 C$ = B2$
: GOSUB 840
780 B2$ = C$
790 C$ = B3$
: GOSUB 840
800 B3$ = C$
810 C$ = B4$
: GOSUB 840
820 B4$ = C$
830 GOTO 380
840 IF C$ = "10" THEN C$ = "A"
850 IF C$ = "11" THEN C$ = "B"
860 IF C$ = "12" THEN C$ = "C"
870 IF C$ = "13" THEN C$ = "D"
880 IF C$ = "14" THEN C$ = "E"
890 IF C$ = "15" THEN C$ = "F"
900 RETURN

```

Program 15. "SPINPLOTTER"

This program was written by Professor Gernot Metze and is included here for completeness. It permits the literal transcription of page 1 of the Apple graphic memory using the Spinwriter. Hence the user can load a

graphics display using "GRAPH DISPLAYER", then run "SPINPLOTTER" to make a hard copy.

```

10 REM SPINPLOTTER BY G.A.METZE
20 LOMEM: 16384
30 DIM R$(127)
40 PR# 1
50 PRINT CHR$(13); CHR$(27);
  CHR$(30); CHR$(3); CHR$(2
  7); CHR$(31); CHR$(6);

60 FOR A = 0 TO 1
  : FOR B = 0 TO 1
  :   FOR C = 0 TO 1
  :     FOR D = 0 TO 1
  :       FOR E = 0 TO 1
  :         FOR F = 0 TO 1
  :           FOR G = 0 TO 1
70             R$(64*A + 32*B
                + 16*C + 8*D
                + 4*E + 2*F
                + G) = CHR$(46
                - 14*G) +
                CHR$(46 - 14*F
                ) + CHR$(46
                - 14*E) +
                CHR$(46 - 14*D
                ) + CHR$(46
                - 14*C) +
                CHR$(46 - 14*B
                ) + CHR$(46
                - 14*A)
80           NEXT
  :         NEXT
  :       NEXT
  :     NEXT
  :   NEXT
  : NEXT
90 FOR K = 0 TO 2
100 FOR J = 0 TO 7
110 FOR I = 0 TO 7
120   N = 8192 + 1024*I + 128*J
      + 40*K
130   FOR L = 0 TO 39
140     B = PEEK(N + L)
150     IF B > 127 THEN B = B
      - 128
160     PRINT R$(B);
170   NEXT
180 PRINT
190 NEXT
200 NEXT
210 NEXT
220 PR# 0
230 PRINT CHR$(7); CHR$(7); CHR$(
  7);
240 END

```

Program 16. "SHAPE TABLE"

This is a binary listed shape table in the standard Apple format for such. It contains the numerics plus plotting shapes for use in "GRAPH MAKER".

16384	0F 00 20 00 28 00 30 00	16456	2D 24 F7 24 2C 3D 00 00
16392	38 00 40 00 48 00 50 00	16464	21 64 3C 27 00 00 00 00
16400	58 00 62 00 69 00 70 00	16472	24 24 2D 36 3F 2D 36 3F
16408	73 00 78 00 80 00 88 00	16480	05 00 09 24 24 3F 36 2D
16416	50 50 24 24 06 00 00 00	16488	00 2D 24 24 3F 36 36 00
16424	2D DC 2C 25 3C 2F 00 00	16496	05 00 00 2A 38 00 00 00
16432	2D 24 2F 24 3F 05 00 00	16504	2D 3F 64 FD 24 2D 96 00
16440	09 24 24 1F 36 2D 00 00	16512	C8 28 2D 07 00 00 00 00
16448	2D 24 3F 24 2D 07 00 00	16520	0C 16 1F 0C 1C 0E 00 FF

Program 17. "ALPHANUMERICS"

This binary file contains two coded versions of all the ASC characters. The characters for the vertical header are listed first with 5 bytes per character. Then the characters for the horizontal header are listed with 7 bytes per character. The total, 12 bytes/character, still represents a considerable savings over a shape table of similar content, but cannot be easily plotted anywhere on the graph except in the header locations.

16384	FF FF FF FF FF FF 82	16584	80 F7 F7 F7 80 FF BE 80
16392	FF FF FF 8F FF 8F FF EB	16592	BE FF FD FE FE FE C1 80
16400	80 EB 80 EB ED D5 80 D5	16600	F7 EB DB BE 80 FE FE FE
16408	DB 9D 9B F7 EC DC C9 B6	16608	FE 80 DF E7 DF 80 80 EF
16416	CA FD FA FF FF 8F FF FF	16616	F7 FB 80 C1 BE BE BE C1
16424	FF E3 DD BE FF FF BE DD	16624	80 B7 B7 B7 CF C1 BE BA
16432	E3 FF DD EB 80 EB DD F7	16632	BD C2 80 B7 B3 B5 CE CD
16440	F7 C1 F7 F7 FF FE FD FF	16640	B6 B6 B6 D9 BF BF 80 BF
16448	FF F7 F7 F7 F7 F7 FF FF	16648	BF 81 FE FE FE 81 83 FD
16456	FE FF FF FD FB F7 EF DF	16656	FE FD 83 80 FD F3 FD 80
16464	C1 BA B6 AE C1 FF DE 80	16664	9C EB F7 EB 9C 9F EF F0
16472	FE FF DC BA B6 B6 CE BD	16672	EF 9F BC BA B6 AE 9E 00
16480	BE B6 A6 99 F3 EB DB 80	16680	00 00 00 00 FF FF FF FF
16488	FB 8D AE AE AE B1 E1 D6	16688	FF FF FF FF FF FF FF F7
16496	B6 B6 B9 BF B8 B7 AF 9F	16696	F7 F7 F7 F7 FF F7 EB EB
16504	C9 B6 B6 B6 C9 CE B6 B6	16704	EB FF FF FF FF EB EB C1
16512	B5 C3 FF FF EB FF FF FF	16712	EB C1 EB EB F7 C3 F5 E3
16520	FE E9 FF FF F7 EB DD BE	16720	D7 E1 F7 FC DC EF F7 FB
16528	FF EB EB EB EB EB FF BE	16728	CD CF FB F5 F5 FB D5 ED
16536	DD EB F7 DF BF B2 AF DF	16736	D3 F7 F7 F7 FF FF FF FF
16544	C1 BE A2 F2 C5 E0 DB BB	16744	DF EF F7 F7 F7 EF DF FD
16552	DB E0 80 B6 B6 B6 C9 C1	16752	FB F7 F7 F7 FB FD F7 D5
16560	BE BE BE CD 80 BE BE BE	16760	E3 F7 E3 D5 F7 FF F7 F7
16568	C1 80 B6 B6 B6 BE 80 B7	16768	C1 F7 F7 FF FF FF FF FF
16576	B7 B7 BF C1 BE BE BA B8	16776	FF F7 FB FF FF FF C1 FF

iR. |

16784 FF FF FF FF FF FF FF FF  
16792 F7 FF DF EF F7 FB PD FF  
16800 E3 DD CD D5 D9 DD F3 F7  
16808 F3 F7 F7 F7 F7 F3 E3 DD  
16816 DF E7 FB FD C1 C1 DF EF  
16824 E7 DF DD E3 EF E7 EB ED  
16832 C1 EF EF C1 FD E1 DF DF  
16840 DD E3 C7 FB FD E1 DD DD  
16848 E3 C1 DF EF F7 FB FB FB  
16856 E3 DD DD E3 DD DD E3 E3  
16864 DD DD C3 DF EF F1 FF FF  
16872 F7 FF F7 FF FF FF FF F7  
16880 FF F7 F7 FB DF EF F7 FB  
16888 F7 EF DF FF FF C1 FF C1  
16896 FF FF FD FB F7 EF F7 FB  
16904 FD E3 DD EF F7 F7 FF F7  
16912 E3 DD D5 C5 E5 FD C3 F7  
16920 EB DD DD C1 DD DD E1 DD  
16928 DD E1 DD DD E1 E3 DD DD  
16936 FD FD DD E3 E1 DD DD DD  
16944 DD DD E1 C1 FD FD E1 FD

16952 FD C1 C1 FD FD E1 FD FD  
16960 FD C3 FD FD FD CD DD C3  
16968 DD DD DD C1 DD DD DD E3  
16976 F7 F7 F7 F7 F7 E3 DF DF  
16984 DF DF DF DD E3 DD ED F5  
16992 F9 F5 ED DD FD FD FD FD  
17000 FD FD C1 DD C9 D5 D5 DD  
17008 DD DD DD DD D9 D5 CD DD  
17016 DD E3 DD DD DD DD DD E3  
17024 E1 DD DD E1 FD FD FD E3  
17032 DD DD DD D5 ED D3 E1 DD  
17040 DD E1 F5 ED DD E3 DD FD  
17048 E3 DF DD E3 C1 F7 F7 F7  
17056 F7 F7 F7 DD DD DD DD DD  
17064 DD E3 DD DD DD DD DD EB  
17072 F7 DD DD DD D5 D5 C9 DD  
17080 DD DD EB F7 EB DD DD DD  
17088 DD EB F7 F7 F7 F7 C1 DF  
17096 EF F7 FB FD C1 00 00 FF  
17104 FF FF FF FF FF FF FF FF

## REFERENCES

- Allman, M. E. and S. A. Bowhill (1976), Feed system design for the Urbana incoherent-scatter radar antenna, Aeron. Rep. No. 71, Aeron. Lab., Dept. Elec. Eng., Univ. of Ill., Urbana-Champaign.
- Andrew General Issue Catalog, August 1973
- Bloodgood, Peter (1965), The Machlett power tube calculator, Machlett Cathode Press, 22, 30-37.
- Brown, G. H. and H. C. Morrison (1949), Method of multiple operation of transmitter tubes particularly adapted for television, RCA Review, June 1949, 161-172.
- Bruene, W. B. (1956), Linear power amplifier design, Proc. of IRE, 1754-1759.
- Burwasser, A. J. (1981), Wideband monofilar autotransformers Part 1, R.F. Design, January/February 1981, 38-44.
- Burwasser, A. J. (1981), Wideband monofilar autotransformers Part 2, R.F. Design, March/April 1981, 20-29.
- Clarke, K. K. and D. T. Hess (1971), Communication Circuits: Analysis and Design, (Addison Wesley).
- Countryman, I. D. and S. A. Bowhill (1979), Wind and wave observations in the mesosphere using coherent-scatter radar, Aeron. Rep. 68, Aeron. Lab., Dept. Elec. Eng., Univ. of Ill., Urbana-Champaign.
- Davis, A. W. and P. J. Kahn (1971), Coaxial bandpass filter design, IEEE Trans. Micro. Theory and Tech., MTT-19, 373-380.
- Dicke, R. H., Object Detection System, U.S. Patent No. 2,624,876 issued January 6, 1953.

- Doolittle, H. D. (1964), Vacuum power tubes for pulse modulation, Machlett Pulse Tubes, Machlett Laboratories Inc.
- Evans, J. V. (1969), Theory and practice of ionosphere study by Thompson scatter radar, Proc.IEEE, 57 #4, 496-530.
- Fair-Rite Products Corp (1977), Use of ferrites for wideband transformers, Fair-Rite Ferrite Cores and Assemblies for the Electronics Industry, Wallkill, New York.
- Frey, G. D. (1977), VMOS power amplifiers - this broadband circuit outputs 8W with a 15 dB gain, EDN, Sept. 5, 1977, 83-85.
- Golay, Marcel J. E. (1961) Complementary series, IRE Trans. Inform. Theory, IT-7, 82-87.
- Gray, R. W. and D. T. Farley (1973), Theory of incoherent-scatter measurements using compressed pulses, Radio Sci., 8, 123-131.
- Granberg, H. (1975), Broadband transformers and power combining techniques for RF, Motorola Application Note, AN-749.
- Hess, G. C. and M. A. Geller (1976), The Urbana meteor-radar system: design, development and first observations, Aeron. Rep. No. 74, Aeron. Lab., Dept. Elec. Eng., Univ. of Ill., Urbana-Champaign.
- Ioannidis, G. and D. T. Farley (1972), Incoherent scatter observations at Arecibo using compressed pulses, Radio Sci., 7, 763-766.
- Key, E. L., E. N. Fowle and R. D. Haggarty (1959), A method of sidelobe suppression in phase coded pulse compression systems, Tech. Rep. No. 209, Lincoln Laboratory, Mass. Inst. of Technology, Lexington, Mass.
- Killpatrick, W. K. (1957), Criterion for vacuum sparking designed to include both RF and dc, Rev. Sci. Inst., 824-826.
- Lefferson, P. (1971), Twisted magnet wire transmission line, IEEE Trans. on Parts, Hybr., and Pack., PHP-7, No. 4, 148-154.

- Leighton, L. and E. Oxner (1980), HF power amplifier design using VMOS power FETs, R.F. Design, January 1980, 32-37.
- Lindner, J. (1975), Binary sequences up to length 40 with best possible autocorrelation function, Electronic Letters, 11, 507.
- Machlett Laboratories, Inc. (1964), Machlett Power Tubes.
- Martin-Vegue, C. A. (1961), A 16 megawatt 100 microsecond pulse modulator, Machlett Cathode Press, 18, No. 1, 16-19.
- McDonald, R. S. (1982), Low cost wideband dual directional coupler, R.F. Design, 5 #3, 34-36.
- Motorola Semiconductor Products Inc. (1972), Mounting stripline-opposed-emitter (SOE) transistors, Motorola Application Note, AN-555.
- Nagle, J. (1976), Use wideband autotransformers in RF systems, Electronic Design, 3, February 2, 1976, 64-70.
- Oxner, E. (1976), Try MOSPOWER FETs in your next broadband driver, Siliconix, Inc., Tech. Article, TA76-1.
- Perna, Vincent F, Jr. (1979), The RF Capacitor Handbook, American Tech. Ceramics, Inc., Huntington Station, New York.
- Pitzalis, O., Jr. and T. P. M. Couse (1968), Broadband transformer design for RF power amplifiers, Proc., 1968 Elec. Comp. Conf., 207-216.
- Rastogi, P. K. and S. A. Bowhill (1976b), Scattering of radio waves from the mesosphere-2. Evidence for intermittent mesospheric turbulence, J. Atmos. Terr. Phys., 38, 449-462.
- Ruthroff, C. L. (1959), Some broadband transformers, Proc. of IRE, Aug., 1959, 1337-1342.
- Sartori, E. F. (1968), Hybrid transformers, IEEE Trans. on Parts, Material, and Packaging, PMP-4, 59-66.

- Skolnik, M. I. (1980), Introduction to Radar Systems, 2nd ed.
- Snelling, E. C. (1969), Soft Ferrites, Chemical Rubber Company.
- Somlo, P. I. (1967), The computation of coaxial line step capacitances,  
IEEE Trans. Micro. Theory and Tech., MTT-15, 48-53.
- Tseng, C. C. and C. H. Liu (1972), Complementary sets of sequences, IEEE  
Trans. Infor. Theory, IT-18, No. 5, 644-652.
- Turyn, R. (1968), Sequences with small correlation, Error Correcting  
Codes, ed. H. Mann, Wiley, New York, 195-228.
- Whinnery, J. R. and H. W. Jamieson (1944), Equivalent circuits for dis-  
continuities in transmission lines, Proc. of IRE, 33, 98-114.